Skaningowa mikrowiązka protonowa w iThemba LABS (Afryka Południowa) – wybrane zastosowania

Wojciech Przybyłowicz

Katedra Zastosowań Fizyki Jądrowej, Zespół Fizyki Środowiska

E-mail: przybylowicz@fis.agh.edu.pl

Nuclear (proton) microprobe

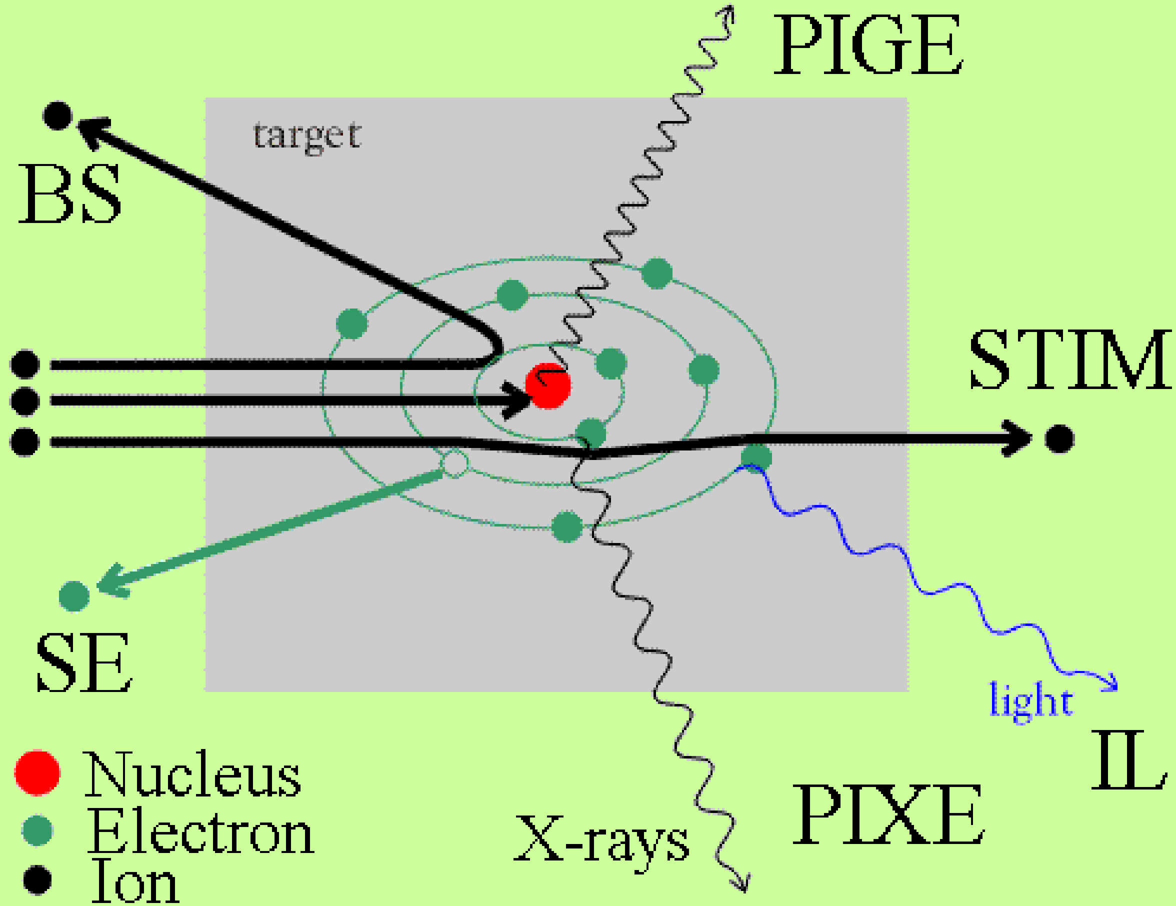

Protons **(energies of few MeV)**
excite characteristic X-rays in a measured material

Techniques using focused beam:

Combination PIXE-RBS results in complementary information

PIXE – very easy identification of elements Na – U down to ppm level, but limited depth information

(R)BS - very good depth information;
identification of the layer thickness,
limited to major and minor elements;
identification of light elements (C, O, N);
best material: high Z layer on low Z substrate

ERDA - Hydrogen analyses in materials at lateral resolution down to 30-50 micrometers

NRA - selective analysis of light elements and their isotopes (e.g. B, Li, F), depth profiling
DETECTOR BASED ON PIN DIODES

PIGE - sensitive for F (down to tens of ppm); also B, Li

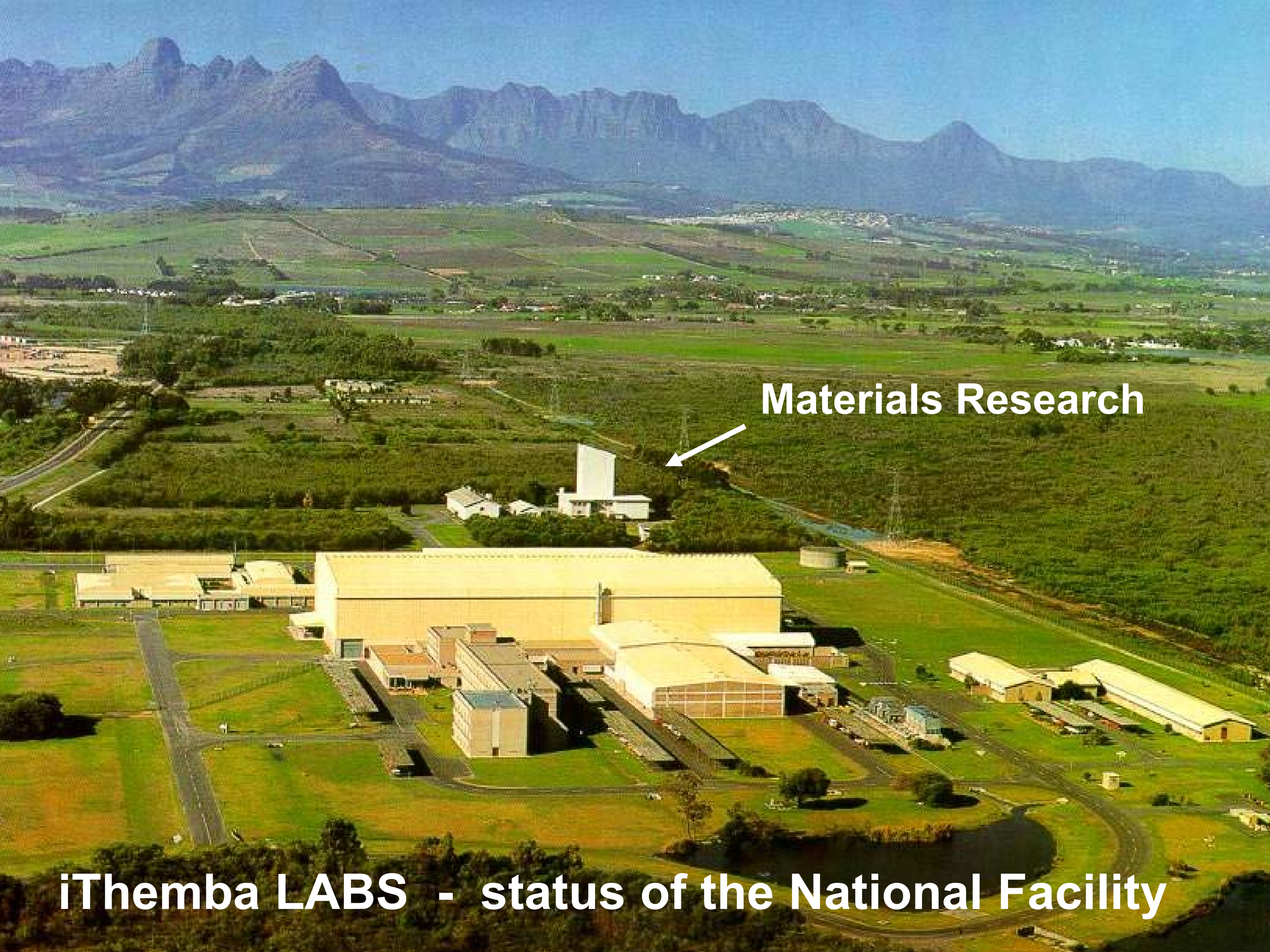
Materials Research
iThemba LABS - status of the National Facility

Accelerators – Overview

iThemba LABS provides accelerator and auxiliary facilities that are used for research and training in nuclear and accelerator physics, radiation biophysics, radiochemical and material sciences and radionuclide productions.

Proton beams are accelerated to a maximum energy of 200 MeV (megaelectron volt) in the **K=200 separated sector cyclotron (SSC), pre-accelerated with a K=8 solid-pole injector cyclotron (SPC1)**, for use in the production of radionuclides.

Radionuclides produced at iThemba LABS are used in research and industry, various radio-pharmaceuticals are prepared for diagnostic imaging at nuclear medicine centers.

Beam is delivered to the different users for 24 hours per day and seven days per week. The beam schedule is semi-rigid, with the Radionuclide Productions Department taking the beam on Monday and Tuesday.

The rest of the beamtime is reserved for subatomic physics experiments scheduled via the Program Advisory Committee (PAC). Beams of light and heavy ions as well as polarized protons, pre-accelerated in a second solid-pole injector cyclotron (SPC2), are used for nuclear physics experiments.

The proton beam that is used for the **production of radionuclides** and **neutron therapy**, is pre-accelerated in the first solid-pole injector cyclotron (SPC1) to an energy of 3.14 MeV and then finally in the separated-sector cyclotron (SSC) to an energy of 66 MeV at an RF frequency of 16.37 MHz

Radionuclides

Short-lived SPECT radiopharmaceuticals such as **123I**-related products and **67Ga** to over 25 nuclear medicine departments in South Africa.

In 2006, our first commercial PET radiopharmaceutical, **18F-FDG**, and in 2008 our first commercial **68Ge/68G**a generator was produced.

Positron emission tomography *with 2-deoxy-2-[fluorine-18]fluoro- D-glucose integrated with* ***computed tomography*** *(**18 F-FDG PET/CT**) has emerged as a powerful imaging tool for the detection of various cancers ...*

All iThemba LABS radiopharmaceuticals are mainly used for diagnostic purposes and/or therapeutic purposes in nuclear medicine.

Since the late 1990's, the supply of long-lived radionuclides focused mainly around the export of **22Na** and **22Na positron sources** and unprocessed radionuclides (irradiated targets) such as **73As**, **68Ge** and **82Sr** to over 60 clients worldwide.

Today, we still remain **the only supplier in the world** of **22Na** positron sources.

Supply and / or distribution agreements with reputable international companies / agencies such as Nordion (Canada), Department of Energy (USA), IDB-Holland, QT Instruments and others have ensured sustained annual income for iThemba LABS.

6 MV CN Van de Graaff Accelerator

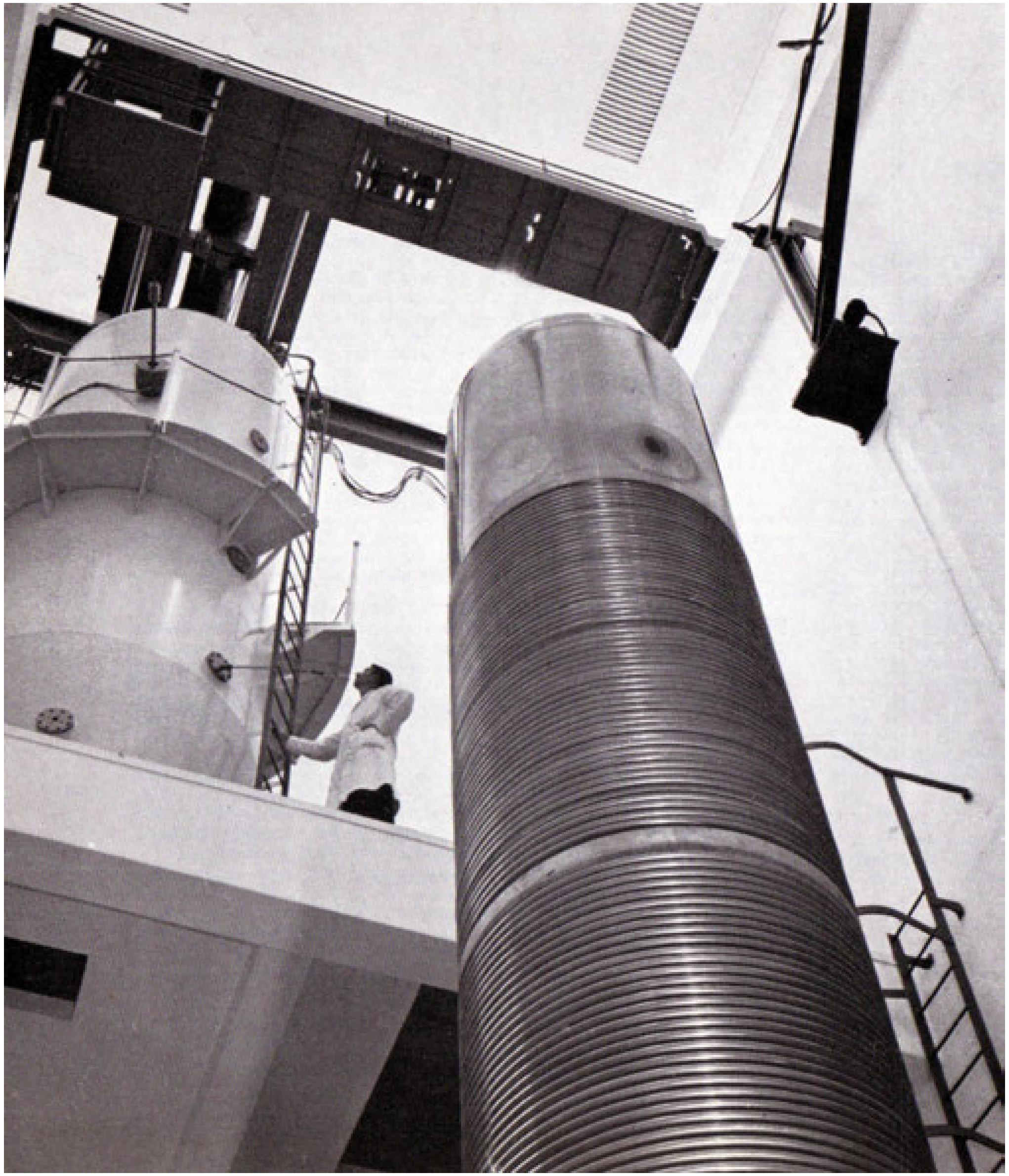

The high-voltage terminal with the dome removed

Wien-Filter

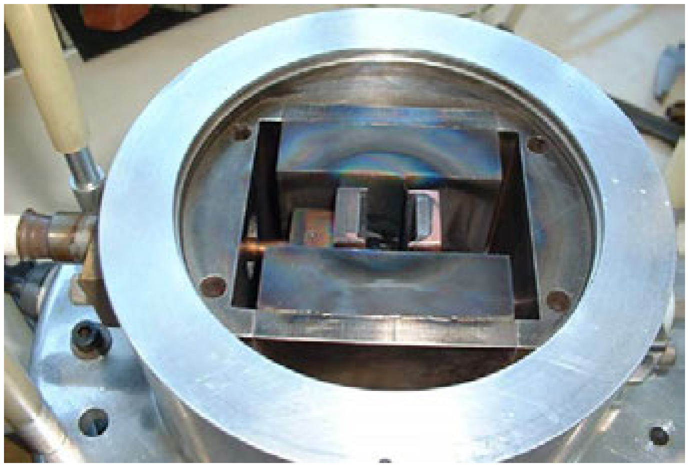

Gap lens

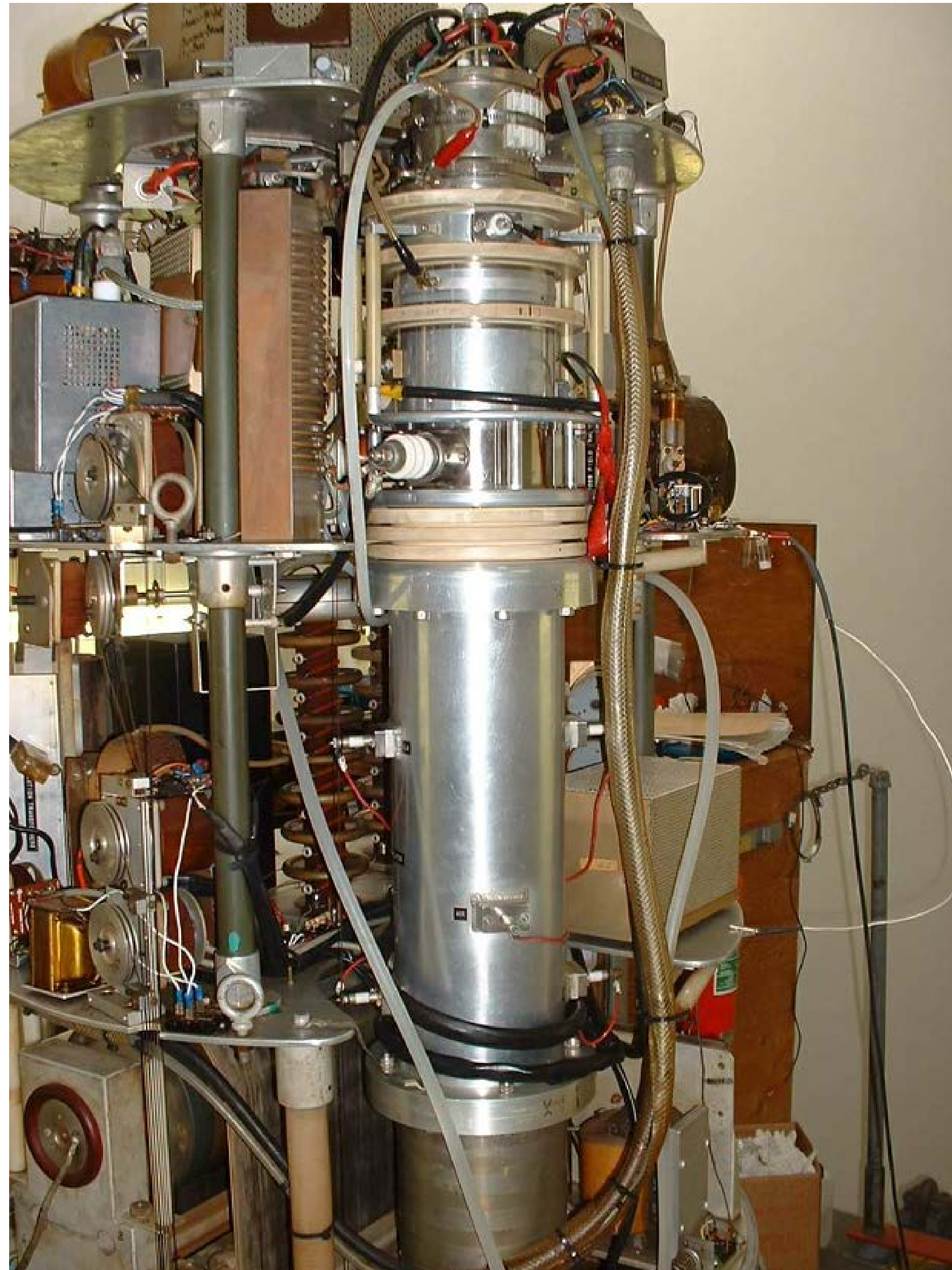

6 MV CN Van de Graaff Accelerator

- Manufactured by High Voltage Engineering – USA.
- Installed in 1963
- Vertical machine, Voltage range: 0.6 to 6 MV
- Tank 18 ton. Pressure: 16 Bar, Gas: N_2=80% and CO_2=20%
- Gas compressor, dryer and storage tank.
- Opening cycle 27 hours
- Current: DC 20 uA max. 1.5 nS, Pulsed @ 2 MHz 5 uA
- Drive motor 10 kW 60 Hz 1700 RPM, Belt speed 60 km/h
- Terminal generator 115 V 400 Hz 2 kW max
- Column/accelerating tube: 2 tubes with 132 insulated rings in total, with a resistor chain of 10^{11} ohm

Since 1991

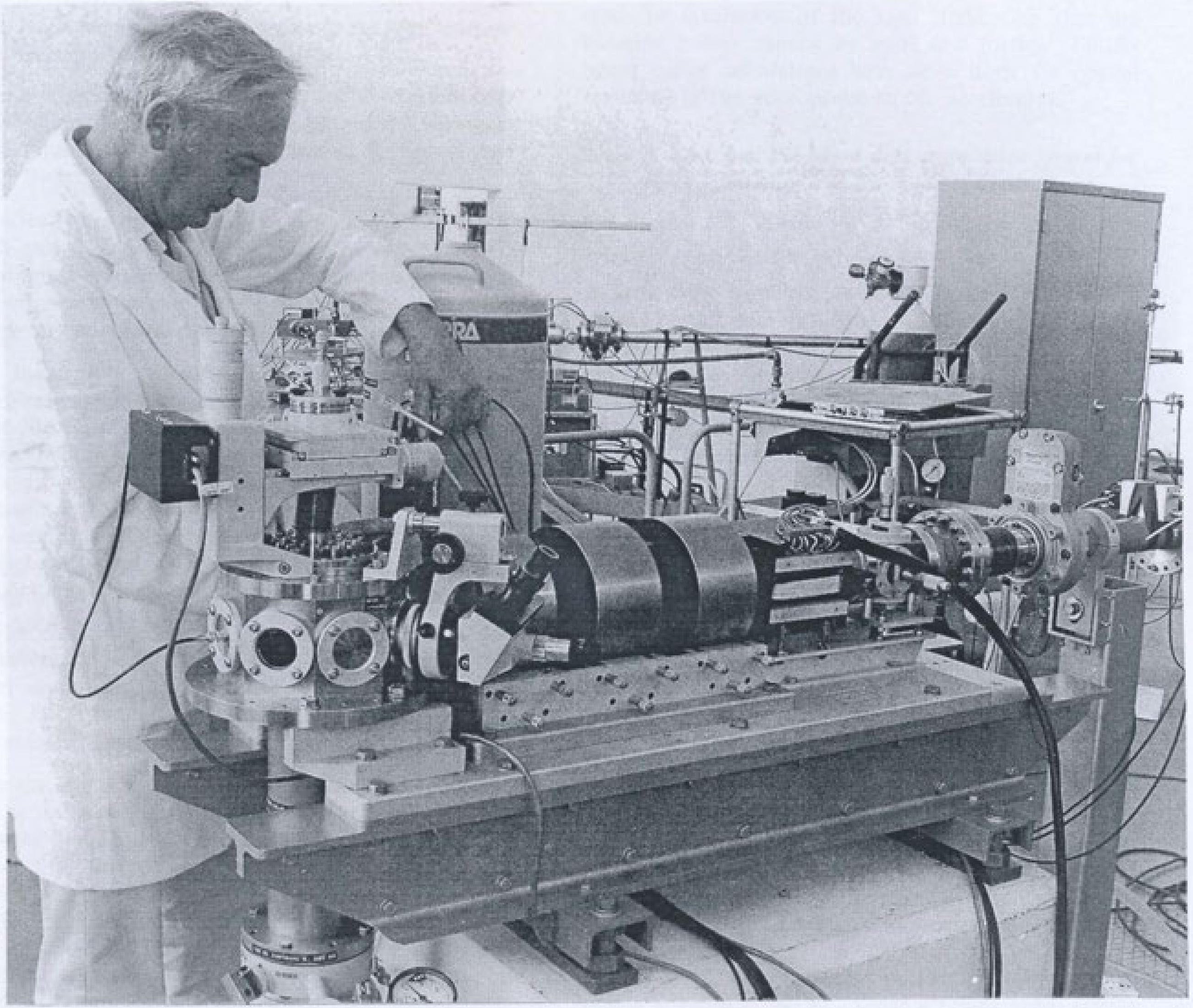

Figure 9.16 Photograph of the new scanning proton microprobe. The proton beam travels from right to left.

WHY?

Scanned ion beams, focused down to ca. 1 micrometer size, brought “a new life” to the Ion Beam Analysis field in every laboratory, where they were installed

Installation of a **nuclear microprobe** was a natural way to expand the analytical capabilities of **this laboratory**

BEAM LINES OF THE 6 MV CN VAN DE GRAAFF ACCELERATOR

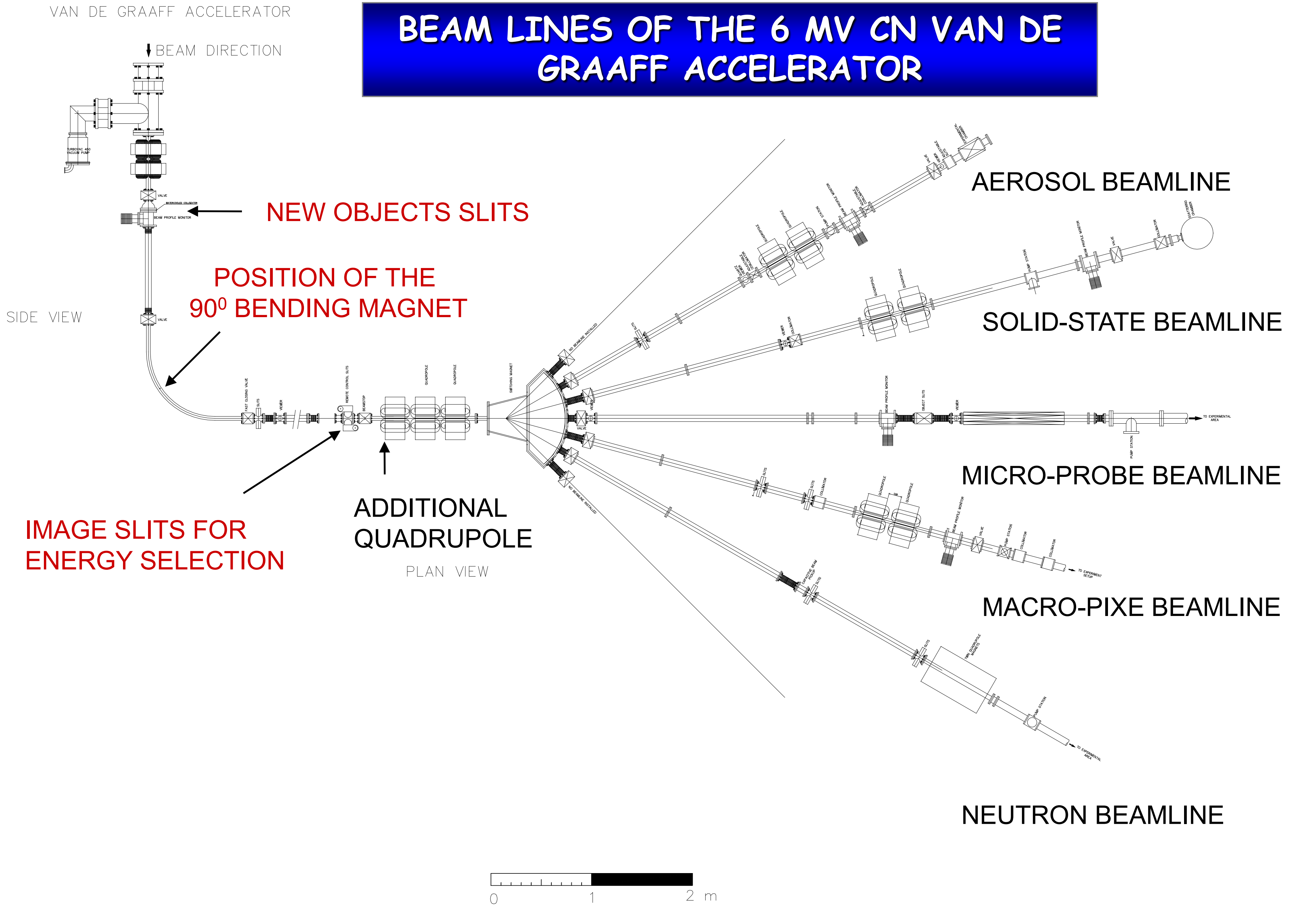

IBA team – on 10 December 2015

High-current techniques (current > 100 pA)

PIXE particle induced x-ray emission – **routinely used**

(R)BS backscattering spectrometry – **routinely used**
(Rutherford, non-Rutherford)

ERDA elastic recoil detection analysis – **used in 1 project**

NRA nuclear reaction analysis – **very seldom**

PIGE particle induced gamma emission – **seldom**

IBIL ion beam induced luminescence – **never used**

Low-current techniques (few fA or single ions)

Very dificult or impossible with the old Van de Graaff

STIM Scanning Transmission Ion Microscopy– **seldom**

IBIC ion beam induced current – **used in 1 project**

Single ion machining
Single event upsets
Single ion irradiation

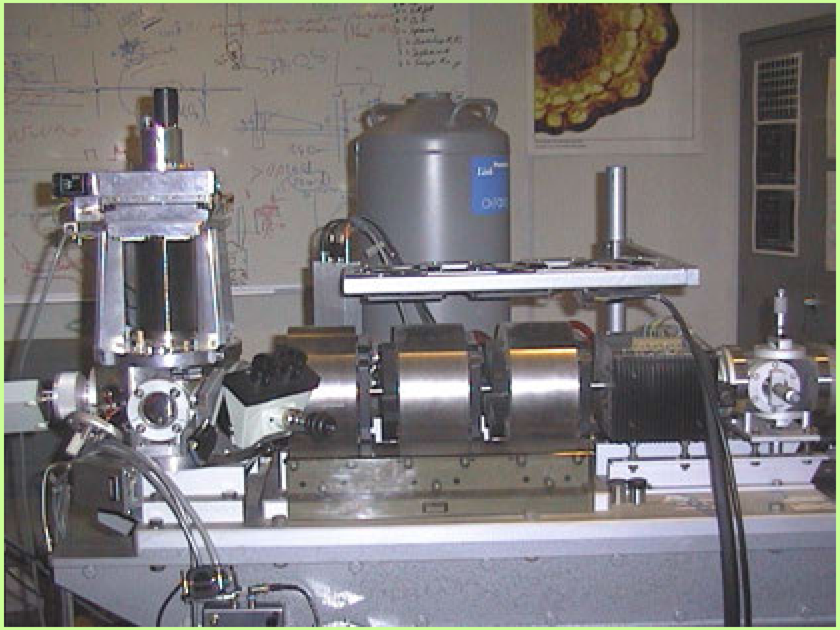

Features:

•OM150 Triplet and scanning system (Oxford Microbeams) Best beam spot at 100 pA

X – 1.6 μm ; Y – 0.6 μm

Typical sizes used X – 3 μm ; Y – 3 μm

•Chamber modified on-site with stepper motors for automated specimen movement;

• permanently mounted set of standards: 44 pure metals, 53 minerals, fused glasses

•On-demand beam deflection system (loop time ca. 900 ns)

Inside the NMP chamber:

•Si(Li) detector 30 mm^2 or HPGe detector 100 mm^2 and wheel with absorbers

•Annular Si surface –barrier detector for backscattering analysis (BS, RBS)

•Microscope (specimen viewed at 45^0)

•Faraday cup and PIN diode for on/off axis STIM

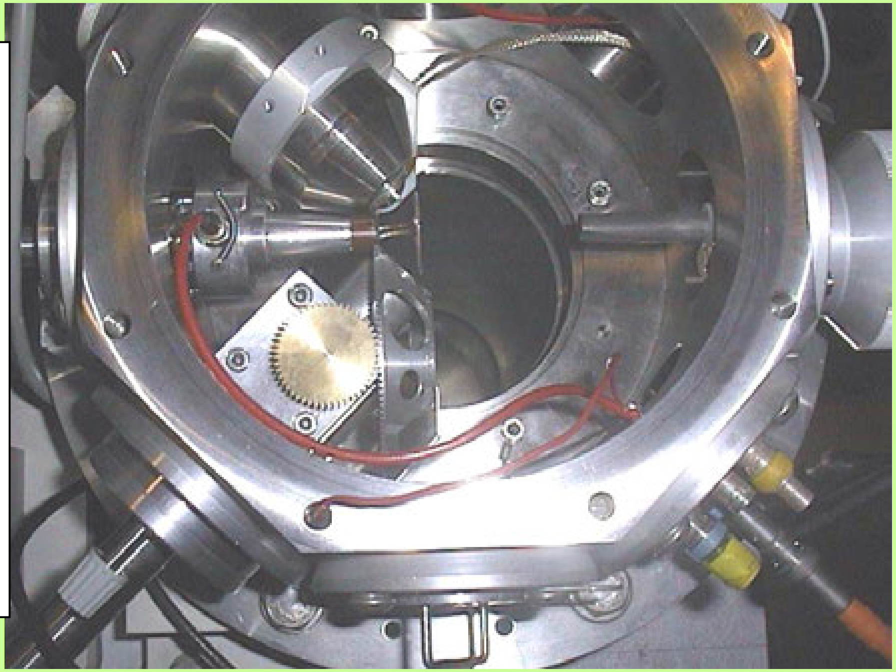

http://www.syd.dem.csiro.au/research/hydrothermal/chris/

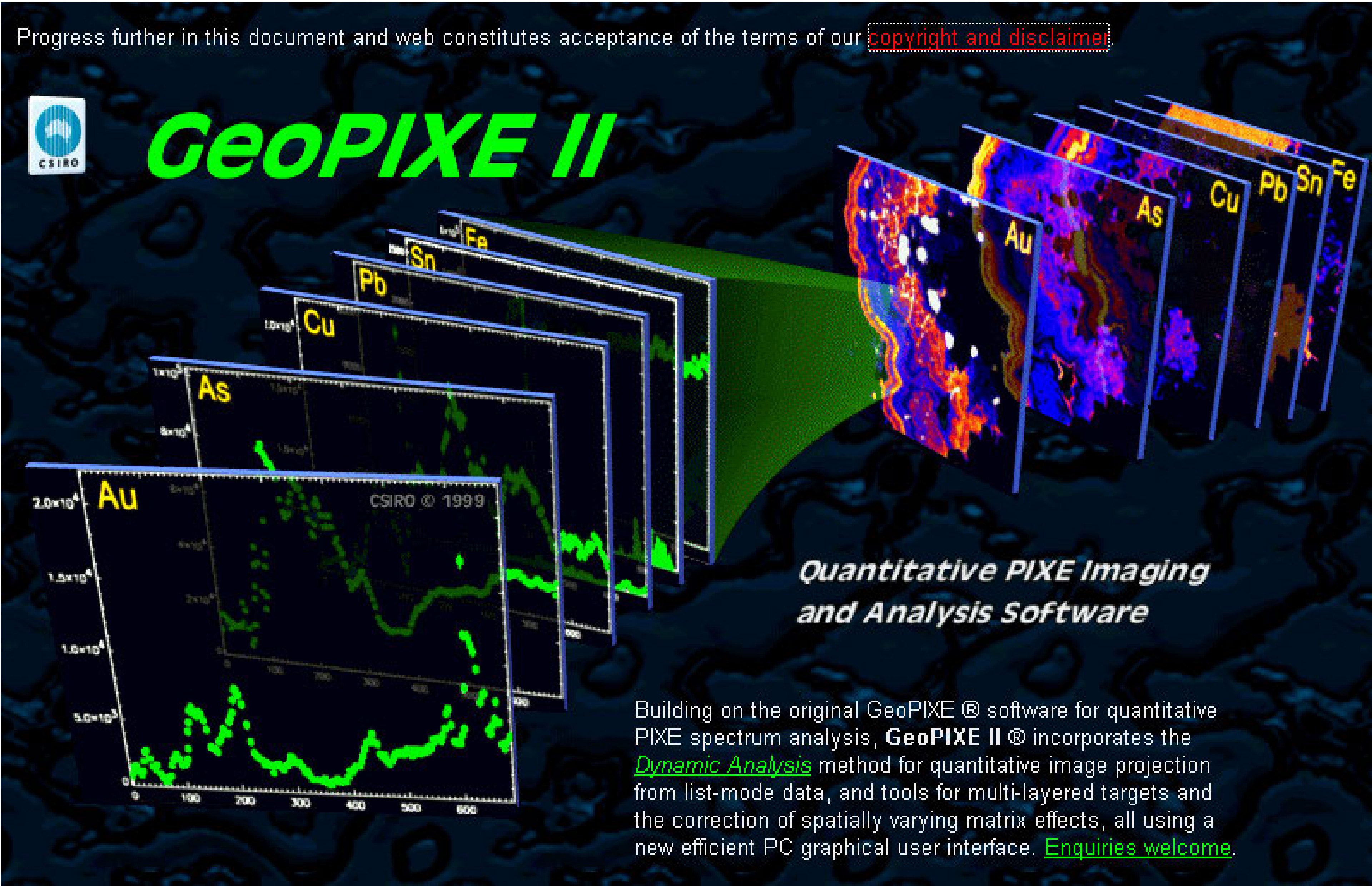

Some features:

Data sorting from all detectors (not only PIXE but PIXE+BS+PIGE+…)

Spectrum fit generates Dynamic Analysis transform matrix

Projection of EVT data onto quantitative elemental images

- **resolves element overlaps**
- **rejects artefacts from overlapping elements, detector response effects (escape peaks, tails)**
- **subtracts background**

- **treatment of pileups:**
  - **using spectrum**
  - **using images (the only software with this option?)**

Extraction of concentration data from selected “regions”

Basic requirements to reach disciplines other than physics and to make accelerator-based techniques competitive:

Reliable accelerator operation

-Operators (maintenance + standby availability)

-Long-term stability, small terminal voltage ripple

Proper equipment

-Permanent setup (electronic modules, measurement geometry)

-Data acquisition suitable for the needs (flexible but easy to use)

-Best available software for data processing

Dedicated, experienced scientist (analyst)

These requirements are very different from a "single experiment" approach

Competition:

- **Bulk analysis techniques**
  AAS, ICP-AES, ICP-MS, XRF, NAA, etc…
- **Microprobe techniques**
  EPMA, SIMS, μ(SR)XRF, LA-ICP-MS, etc…

Suggestion:

- **Rather complement than compete**

- **Concentrate on applications which cannot be done by other means**

Facility available free of charge:

This big advantage can be lost if no true interest in collaboration exists on both sides

How to make interdisciplinary research productive:

-project proposals and initial discussions

-collaborators from other disciplines present and active during measurements

-very strong emphasis on data evaluation and reporting (discussions, conference presentations, publications)

-Try to identify needs

- -Research seminars at users' work place
- -Pilot experiments
- -Advisory Committee

Nuclear microprobe uses ~ 70% of accelerator time

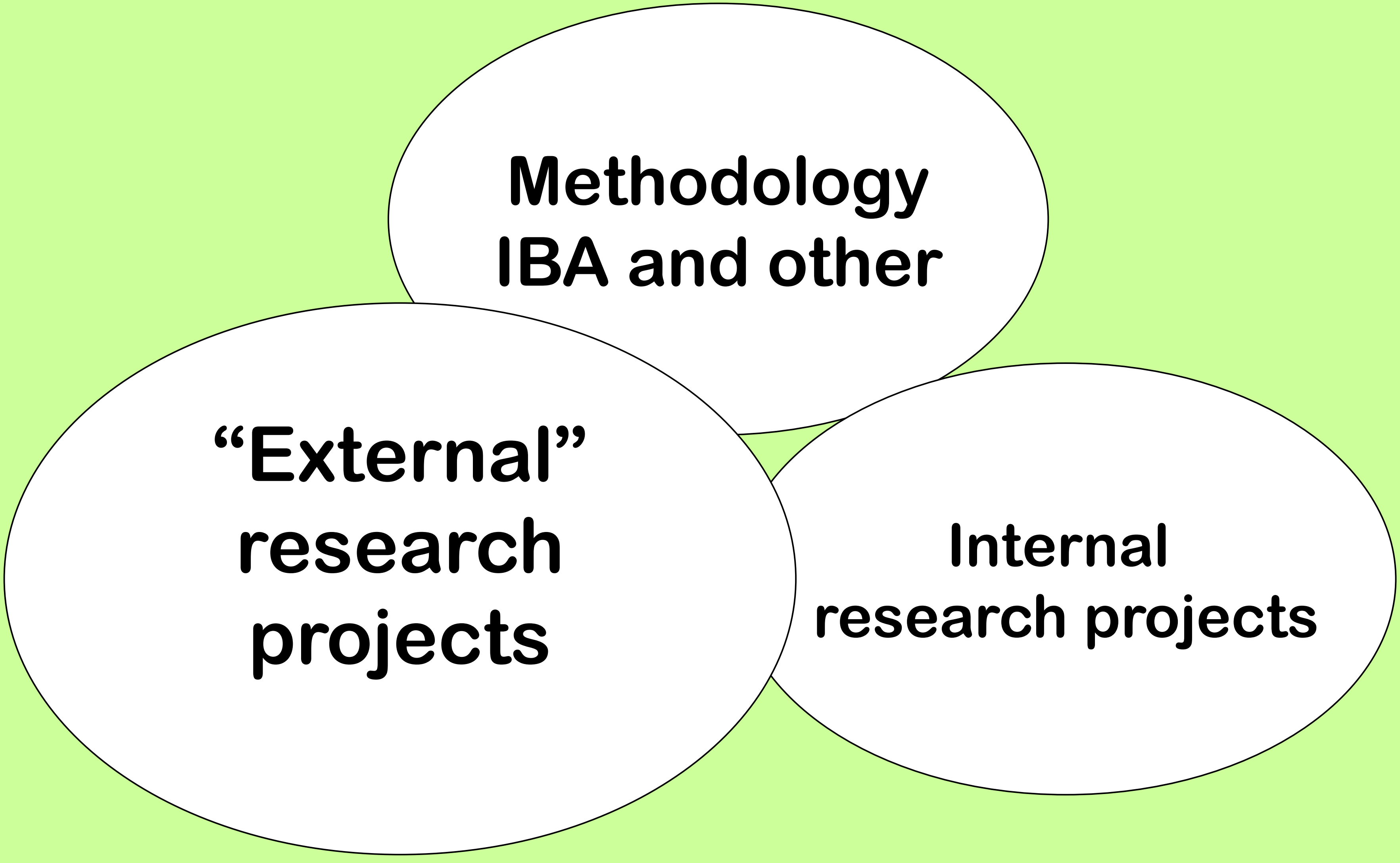

Geology and Ore Processing

Initially (1992-1995) the microprobe (PIXE) was tailored towards these applications.

Few years later a steady development of LA-ICP-MS facilities somehow reduced the number of geological applications (worldwide trend)

At present: nuclear microprobe is and should be used in combination with other microanalytical techniques, available to geologists

Geology, mineralogy

Sequence of microanalysis

1	2	3
SEM-EDS SEM-WDS	Micro-PIXE Micro-BS	LA-ICP-MS

Concentric pyrite from a Ventersdorp Contact Reef, South Africa.

This sample contains a wide range of different pyrite types.

True elemental maps were obtained using GeoPIXE software and dynamic analysis method of mapping

W.U. Reimold, W.J. Przybylowicz, and R.L. Gibson
X-Ray Spectrometry 33(2004)189.

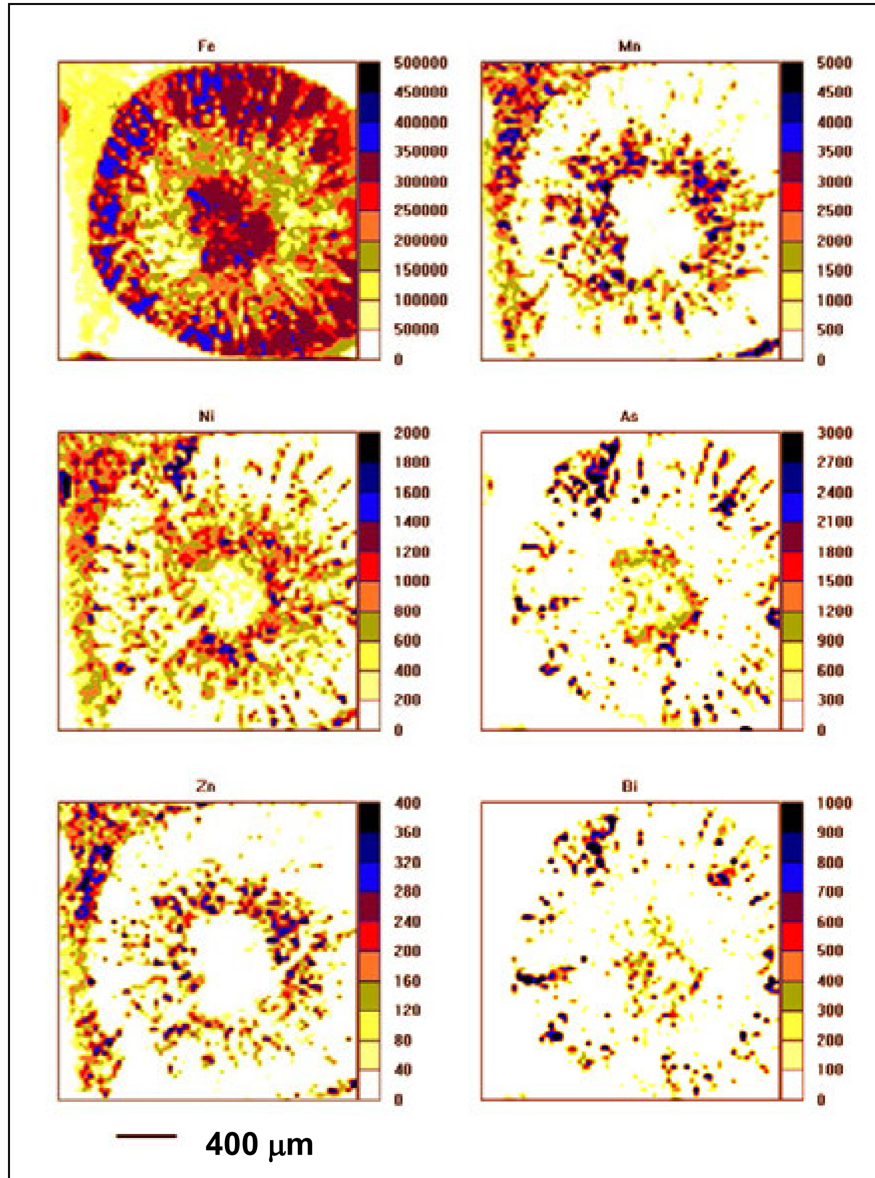

Studies of progressive leaching in single mineral Pb/Pb dating

PIXE mapping was used to study the behaviour of U, Th and Pb during the leaching in comparison with the main elements in titanite.

Technically: resolving many overlapping L-lines gave average concentrations of U-Th-Pb.

Age calculated using concentrations extracted from selected regions within maps is fully consistent with the isotope dating method.

PIXE age:	999 +- 80 Ma
Bulk U-Pb titanite age	999 +- 7 Ma

Frei et al. Geochim. Cosmochim. Acta 61 No 2 (1997) 393-414.
Frei et al. Nucl. Instr. and Meth. B130 (1997) 676-681.

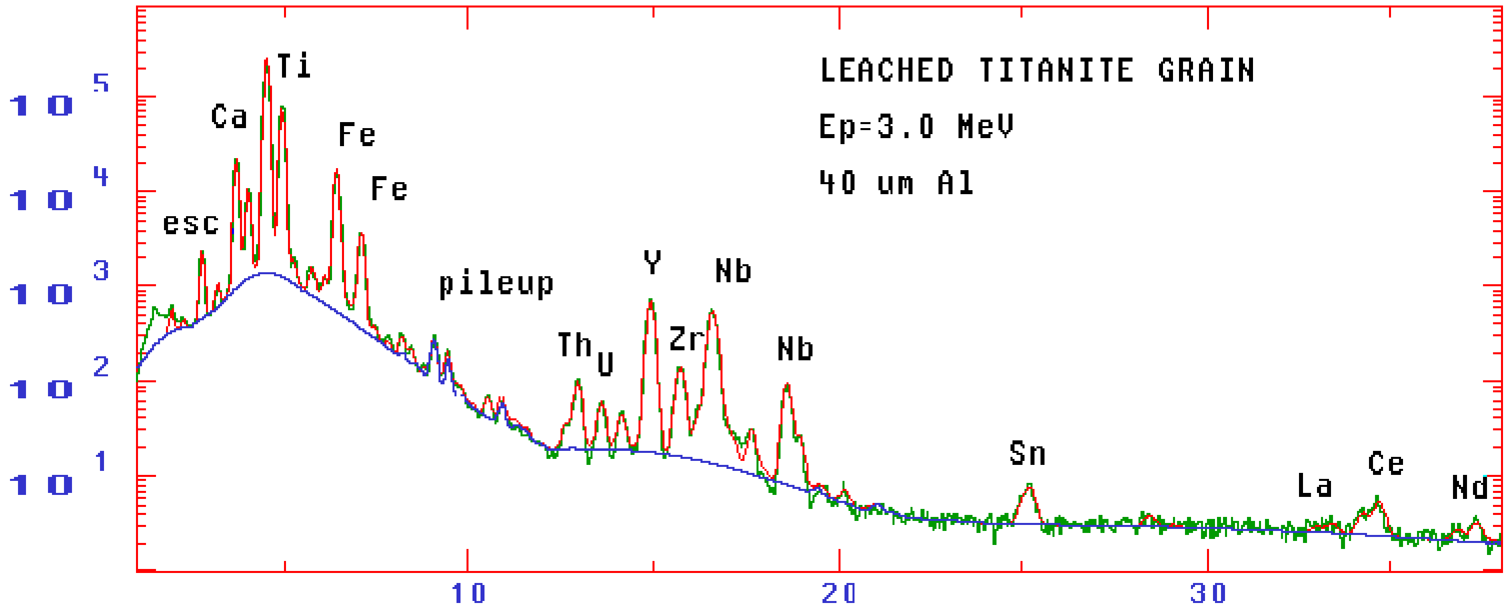

PIXE spectrum from a 150 x 150 μm^2 area in a severly leached portion of a gem quality titanite grain from Otter Lake, Canada.

Proton energy 3 MeV, total accumulated charge 30 μC.
Si(Li) detector shielded with 40 μm Al filter.

True elemental maps of leached titanite grain

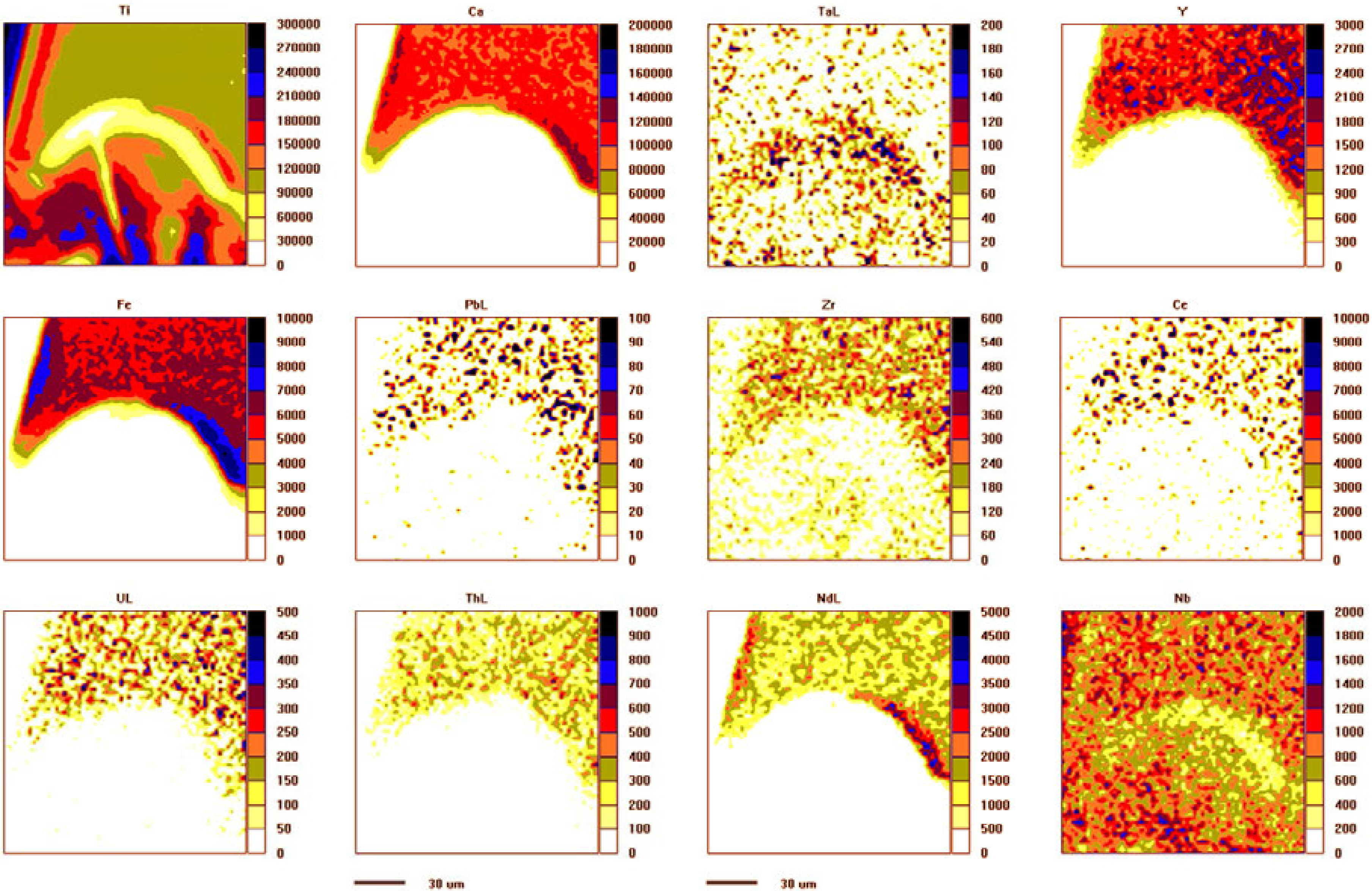

Gold preferentially accumulates on the cathode, i.e. under oxidizing conditions.

Galvanic cells simulate conditions occurring at surfaces of chemically inhomogeneous single crystals (zonated).

Sulphide minerals show either n- or p- type conductivity. Visible gold is accumulated on individual domains of sulphide surfaces that act as cathodes, i.e. p-type conductors in n-p junctions.

Arsenic is the most important element in establishing p-type conductivity of pyrite and arsenopyrite.

This explains why As is such a powerful pathfinder in gold exploration.

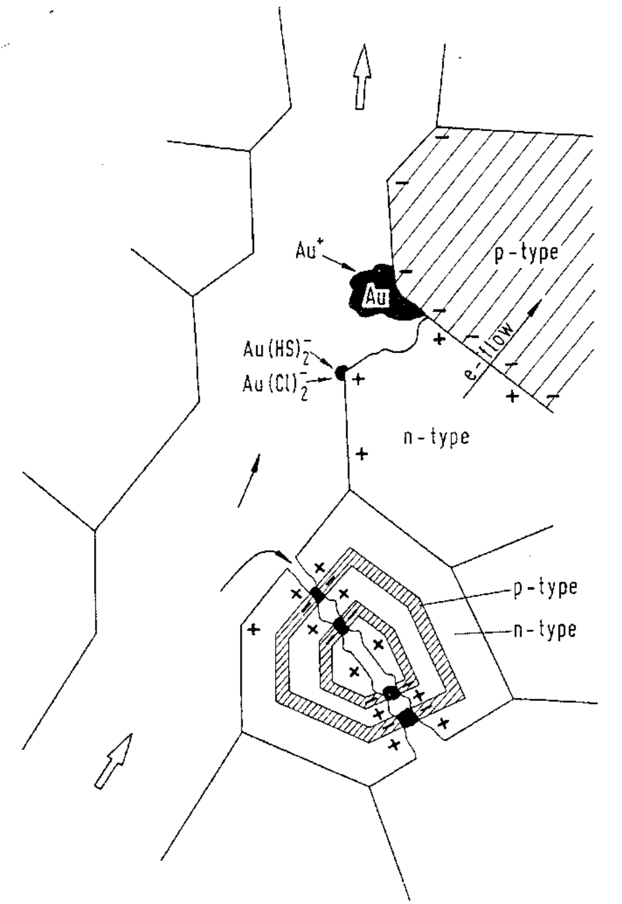

Fig. 10. Electrochemical reactions of a gold-bearing fluid moving along a pore made up of n-type and p-type sulfides as well as fractured n- and p-type zoned crystals.

W.J. Przybylowicz et al. Nucl. Instr. and Meth. B104 (1995) 450.

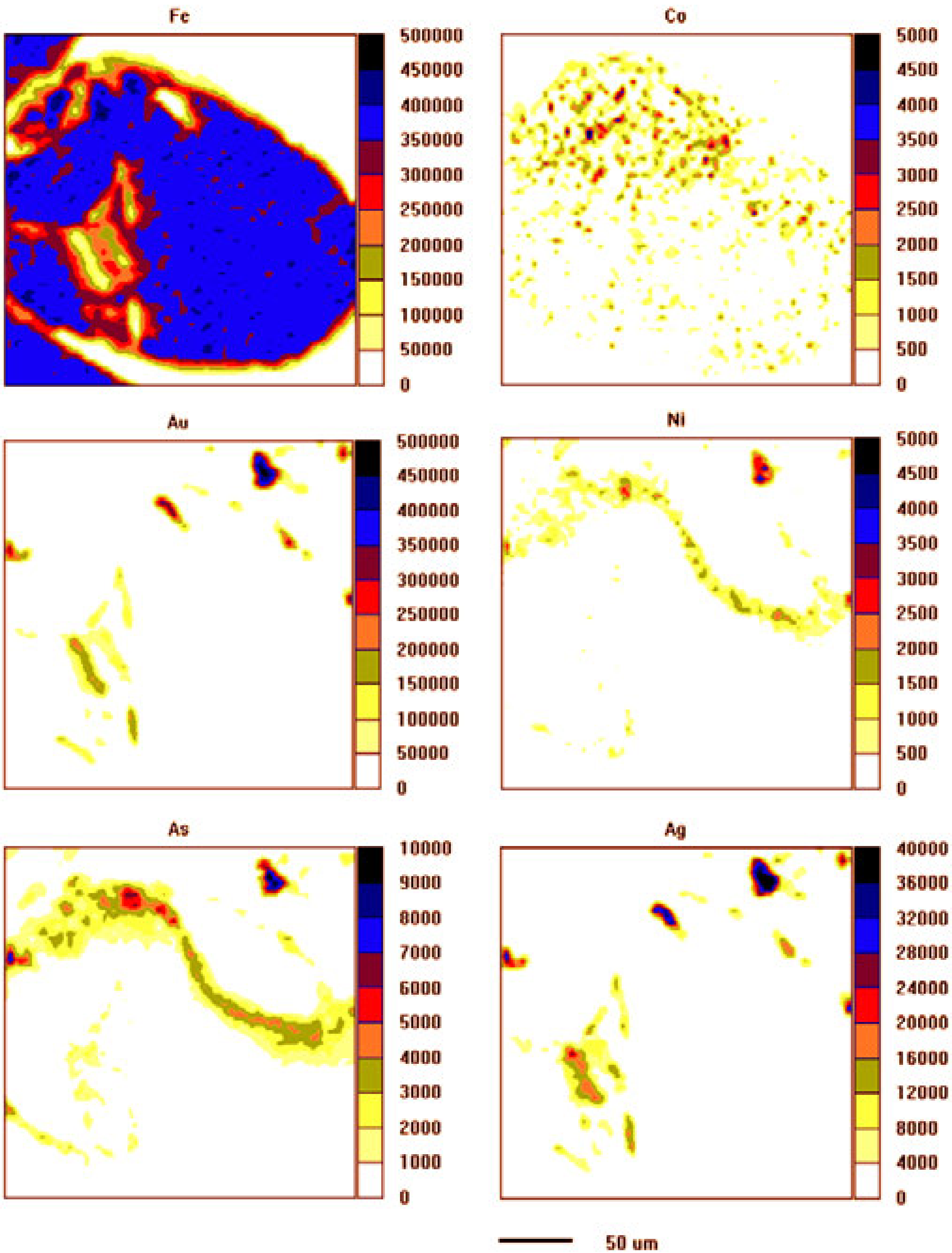

Quantitative elemental maps, non-destructive

Here: pyrites, research related to gold ore formation

Still the strong point

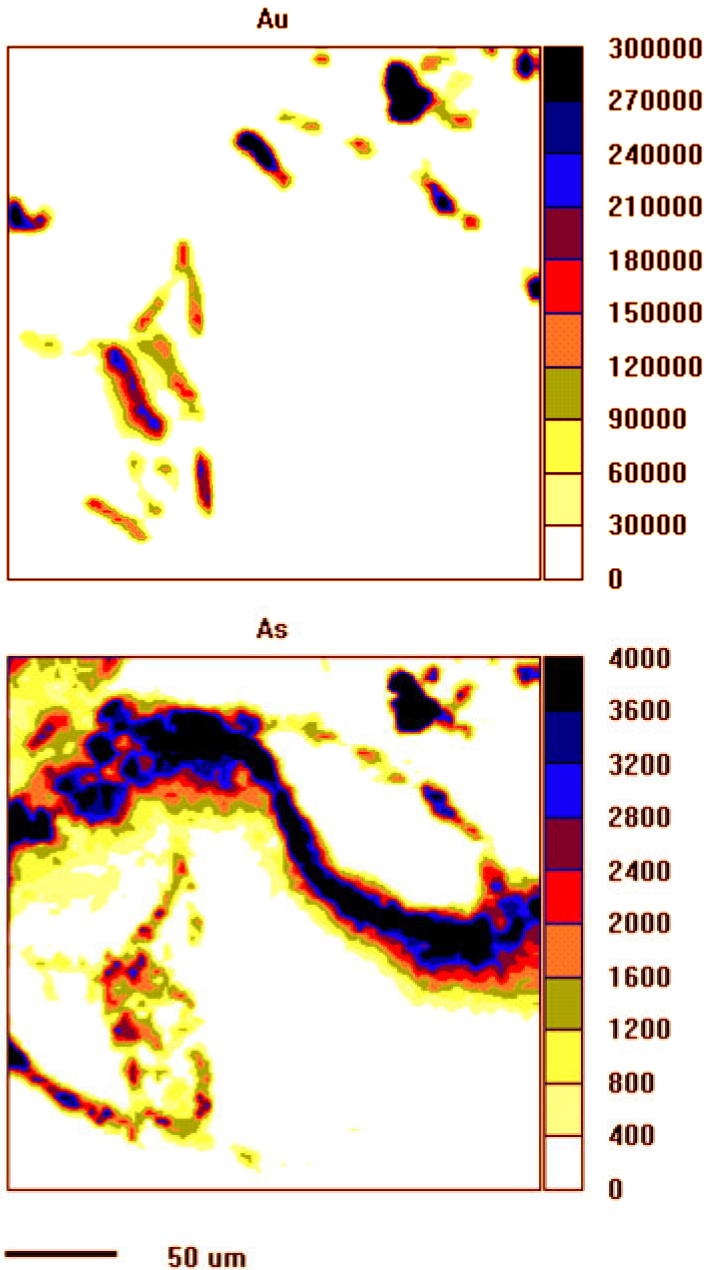

True elemental maps.

Au - As relation.

Reduced scale of concentration.

W.J. Przybylowicz et al. Nucl. Instr. and Meth. B104 (1995) 450-455.

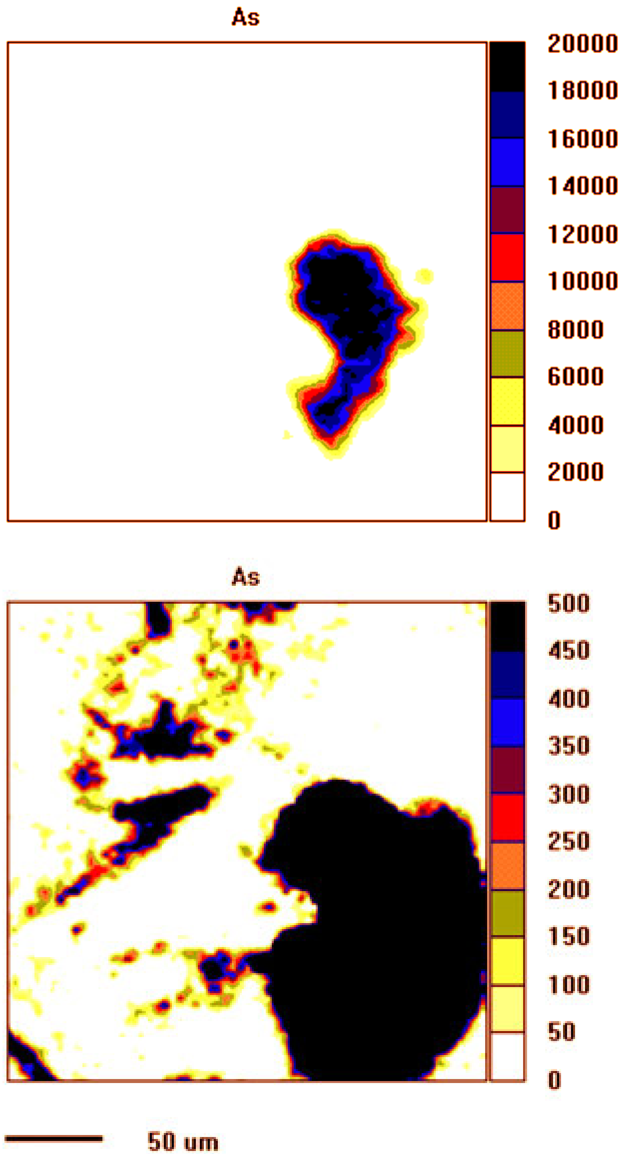

True elemental maps of As zonation in two round, compact pyrite grains from Witwatersrand reef.

Additional details can be distinguished after reduction of the concentration scale from 20000 ppm to 500 ppm.

W.J. Przybylowicz et al. Nucl. Instr. and Meth. B104 (1995) 450-455.

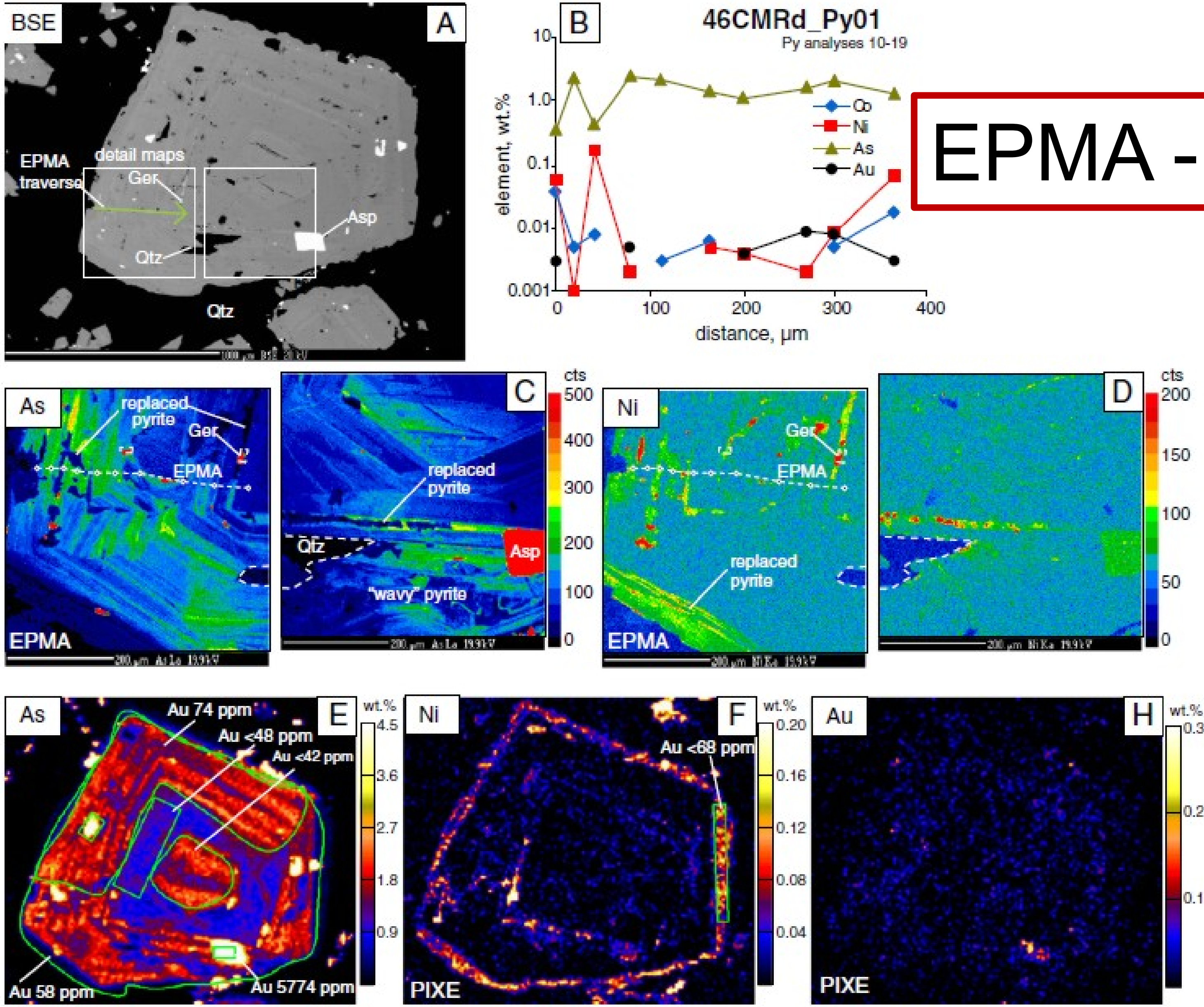

EPMA - PIXE

A. Agangi et al. Ore Geology Reviews 56 (2014) 94

Can LA-ICP-MS fail?

G. Stevens, W. Przybylowicz, L. Martin
X-ray Spectrometry 33 (2004) 216.

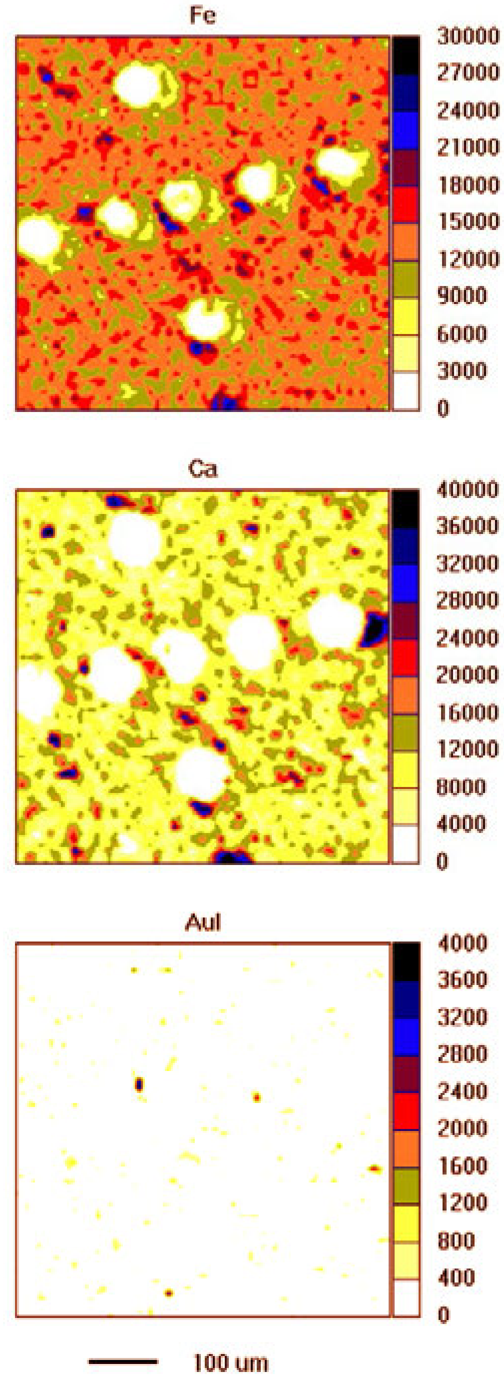

Studies of gold transport in granitoid and silica-undersaturated magmas

Initial analyses of the samples using LA-ICP-MS indicated that gold was dissolved within all of the glasses analysed. However, due to the <u>destructive cratering</u> of the technique (figure), the gold content is either diluted (by silicate and oxide presence) or concentrated
(where gold crystals are incorporated).

The true required Au content is that within the melt alone.

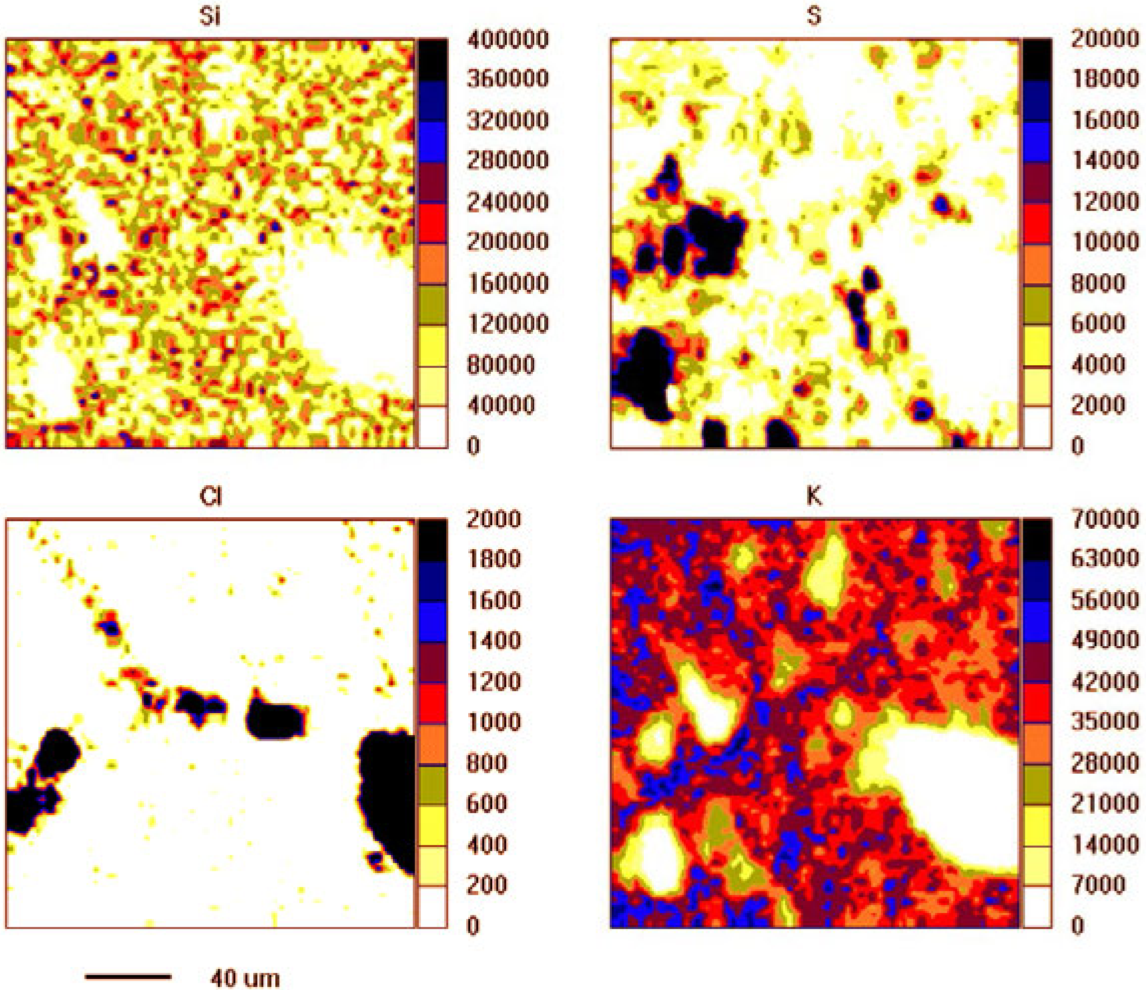

Example of reconnaissance maps to facilitate the location of melt and crystalline phases.

S-rich domains: Both glass and silicate minerals
K-rich areas: glass (the only K-rich phase)
Cl-rich domains: laser ablation pits
S-rich areas: pyrhotite

G. Stevens, W. Przybylowicz, L. Martin, X-ray Spectrometry 33(2004)216.

Elemental imaging of organic matter and metal associations in ore deposits using micro-PIXE and micro-EBS

S. Fuchs[1] and W.J. Przybylowicz[2]

[1]Earth and Planetary Science, McGill University, Montreal, H3A 2A7, Canada; e-mail: sebastian.fuchs@mail.mcgill.ca

[2]Materials Research Department, iThemba LABS, National Research Foundation, PO Box 722, Somerset West 7129, South Africa; e-mail: przybylowicz@tlabs.ac.za

Outline: Organic matter in mineral deposits

Basin-type deposits **Au-U-(REE)**
✧ **Witwatersrand (South Africa)**

Mississippi Valley-type deposits: **Cu-Zn-Pb**
✧ **Pine Point (Canada)**

Organic Matter in Ore Deposits

Hydrothermal Sinter/Spring deposits: **Au-Ag-Hg-Sn**
✧ **Californian Coastal Ranges (USA)**

Polymetallic (Black-) Shale deposits **Cu-Zn-Pb-PGE-Au**
✧ **Kupferschiefer (Poland)**

Objectives: Role of Organic Matter

- What is the role and impact of organic matter in ore deposits?
- Finding the right path for investigation:

Structure/Texture

SEM / TEM

Chemical

~~LA-ICP-MS~~

Micro-PIXE

Organo-Chemistry

No in-situ methods developed for non extractable micro-size samples

Why LA-ICP-MS not usable? standardization problem+very destructive

Micro-PIXE:

- non-destructive, standardless, in-situ analyses of micro-sized bitumen in veins
- quantitative mapping of trace element distribution in and around bitumens

Hydrocarbons in the Witwatersrand

- ✧ Largest known Au and U resource on earth
- ✧ Genesis - one of the most controversial debates in geology for 50 years
- ✧ Gold and/or Uranium are concentrated in the deposit as:

Detrital placer

Hydrothermal Precipitates

> 40% Gold and > 95% Uranium is associated with OM

Table: Au concentrations in carbon seams (Hallbauer, 1986)

Reef	Au g/t
Carbon Leader	1500
Carbon Leader	3600
Carbon Leader	8000
Basal Reef	1500
Basal Reef	29300
Vaal Reef	29900

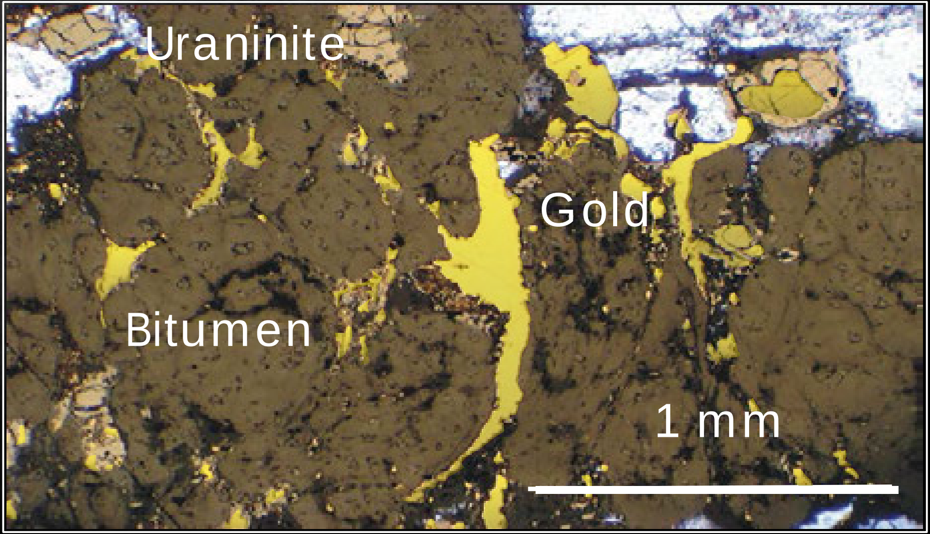

Hallbauer, 1986

Genetic Models

detrital, placer gold

Gold was concentrated together with other heavy minerals by hydraulic (fluvial/marine) processes, with a minimum of post-depositional changes on the detrital ore minerals.

hydrothermal gold

Hydrothermal fluids transport gold up into bedding-parallel structures during regional metamophism

Modified paleo placer model

> aspects of both hydrothermal & "placerist" genetic processes

> hydrothermal remobilization (mm to cm) of primary detrital gold

How to fit the hydrocarbons in the model?

detrital: not, in older publication it is explained as physical trap,
detrital uranium-minerals solidified bitumen by radiolytic polymerisation

hydrothermal: as reductant for Au-precipitation

Organic Matter in the Witwatersrand

Carbon Leader Reef

Single carbon nodules connected with veins (pearl-chain style)

In the alteration zones

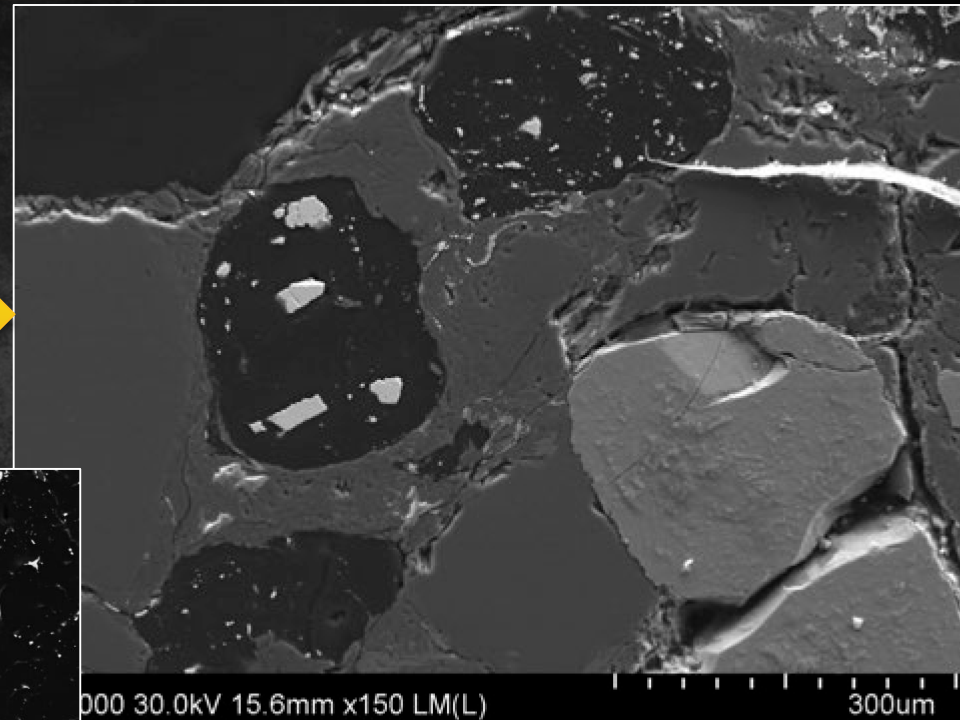

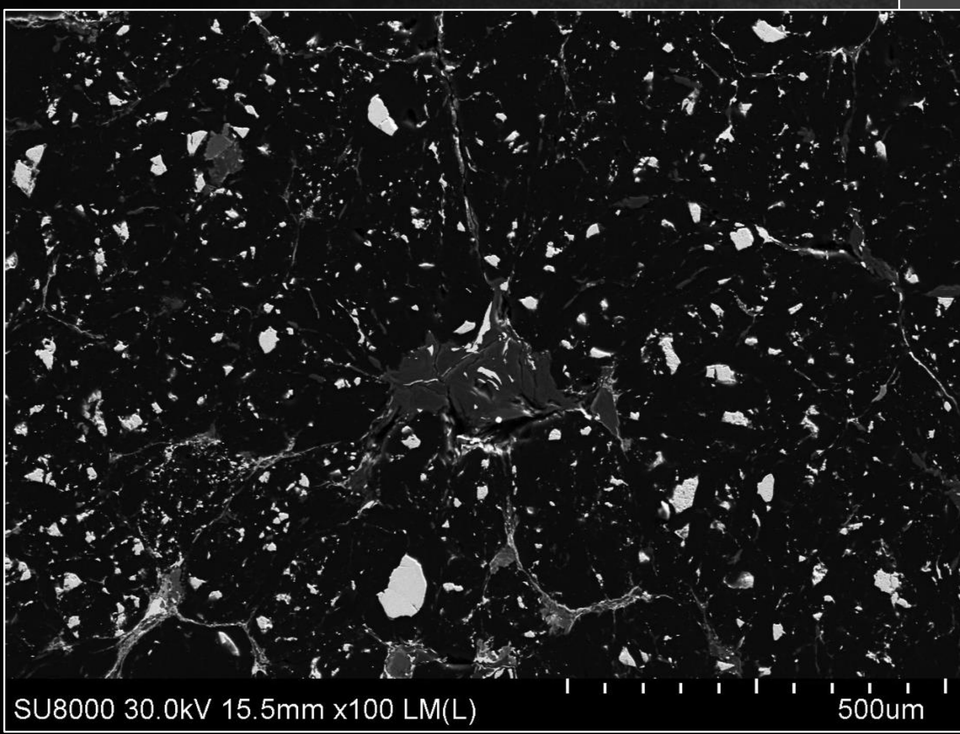

Carbon seams/veins – stack of rounded carbon nodules

Silicates in interstitial veins and small veinlets in “spongy” nodules

Selected area for analyses

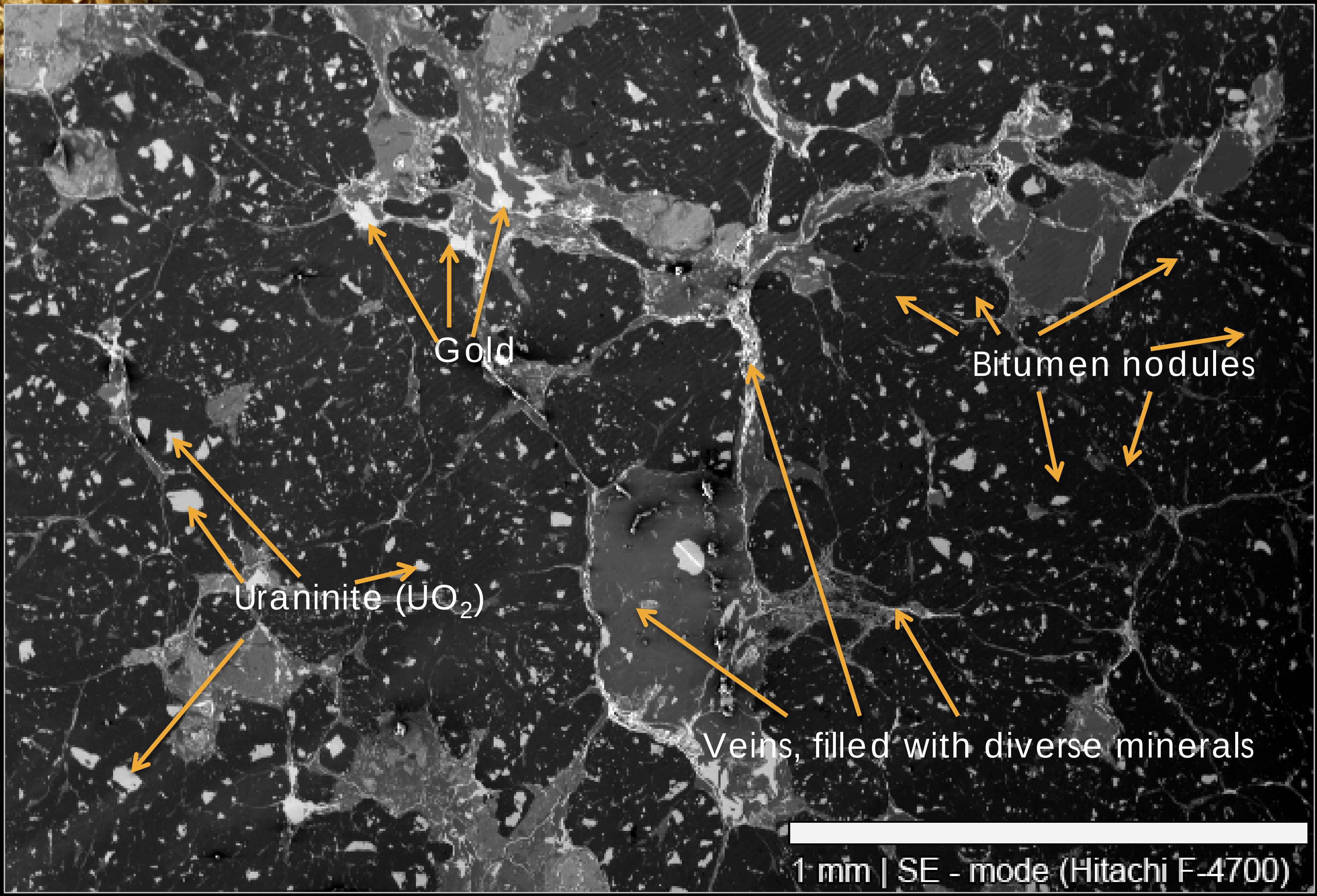

Micro-PIXE and micro-EBS

Nuclear microprobe:

6MV single-ended Van de Graaff, Oxford magnetic quadrupole triplet

3 MeV proton beam current focused to a 5 x 5 μm^2 spot;
square or rectangular scan patterns of variable sizes
(up to 2.5 mm x 2.5 mm); variable number of pixels (up to 128 x 128)

PIXE: Si(Li) detector (30 mm^2 active area, working distance 24 mm);
take-off angle 35°; E resolution 155-160 eV

Two measurements of the same areas:

higher absorption (150 µm Al); energy range 4-42 keV, current ~2 nA

lower absorption (125 µm Be), energy range 1-42 keV,
mainly for low-energy X-rays (between 1-5 keV), current ~500 pA

EBS (Proton elastic backscattering):
annular Si surface barrier detector (100 µm thick), E resolution 25 keV

Dynamic Analysis method:

- - resolves element overlaps
- - rejects artifacts from overlapping elements, detector response effects (escape peaks, tails)
- - subtracts background
- - groups of lines (K, L, M) are used for construction of images rather than individual lines
- - treatment of pileups:
- using spectrum
- using images (correction for spatial variation of pile-up components)

High complexity of PIXE spectra-I

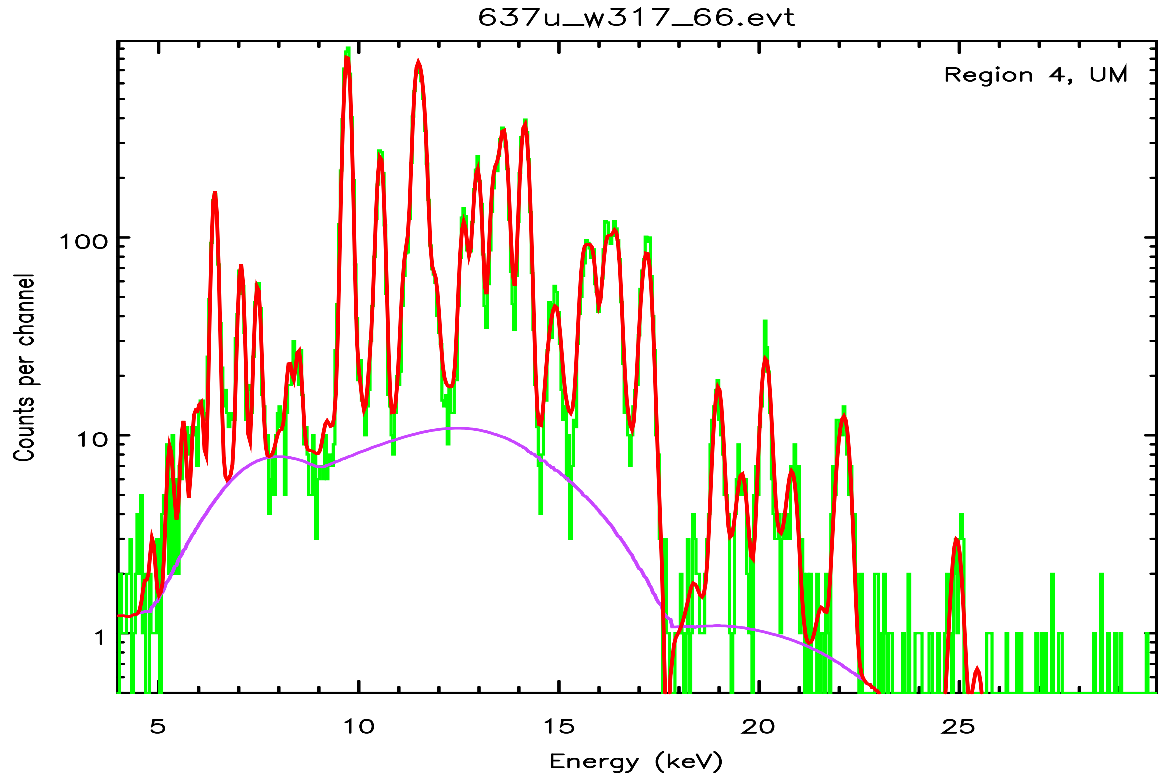

X-ray lines used to fit PIXE spectra recorded with the thicker X-ray absorber (150 µm Al) referred to as PIXE-I:

Cr(K), Fe(K), Co(K), Ni(K), Cu(K), Zn(K), As(K), Sr(K), Y(K), Ag(K), Sb(K), Cd(K), Ba(K), Ce(K), Nd(K), Au(L), Hg(L), Pb(L), Th(L), U(L)

High complexity of PIXE spectra -II

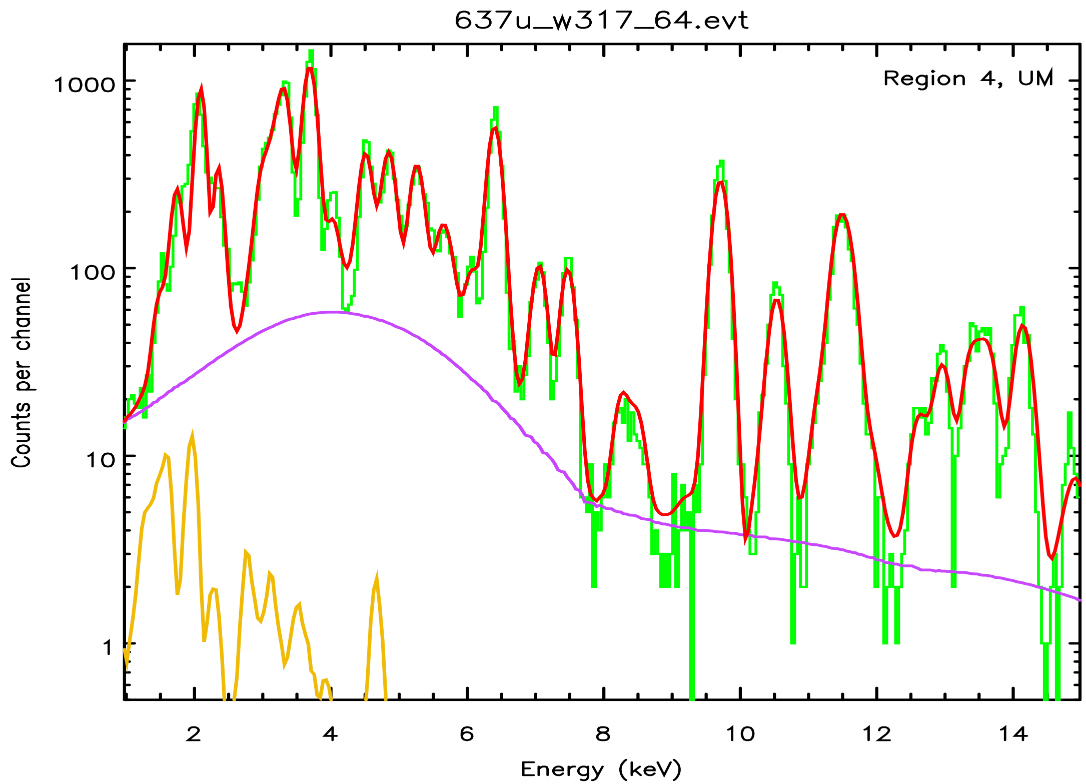

X-ray lines used to fit PIXE spectra recorded with smaller absorption (125 µm Be absorber), referred to as PIXE-II: Al(K), Si(K), S(K), K(K), Ca(K), Ti(K), Cr(K), Fe(K), Co(K), Ni(K), Cu(K), Zn(K), As(K), Sr(K), Y(K), Ag(K), Cd(K), Ba (K, L), Ce(K, L), Nd(K, L), Au(L, M), Hg(L, M), Pb(L, M), Th(L, M), U(L, M).

- **PIXE elemental maps are here shown without concentrations (due to tremendous local variation of matrix composition these concentrations are not reliable)**
- **Many small areas with very distinct changes of elemental composition were selected on the basis of maps (various mineral phases were identified)**
- **PIXE spectra from these areas were fitted individually, using matrix matching the identified minerals**

Vein-related mineralization

Pixe maps show different elemental distributions:

a) In interstitial veins
b) on hydrocarbon interfaces (as rimmings)
c) within the in hydrocarbons

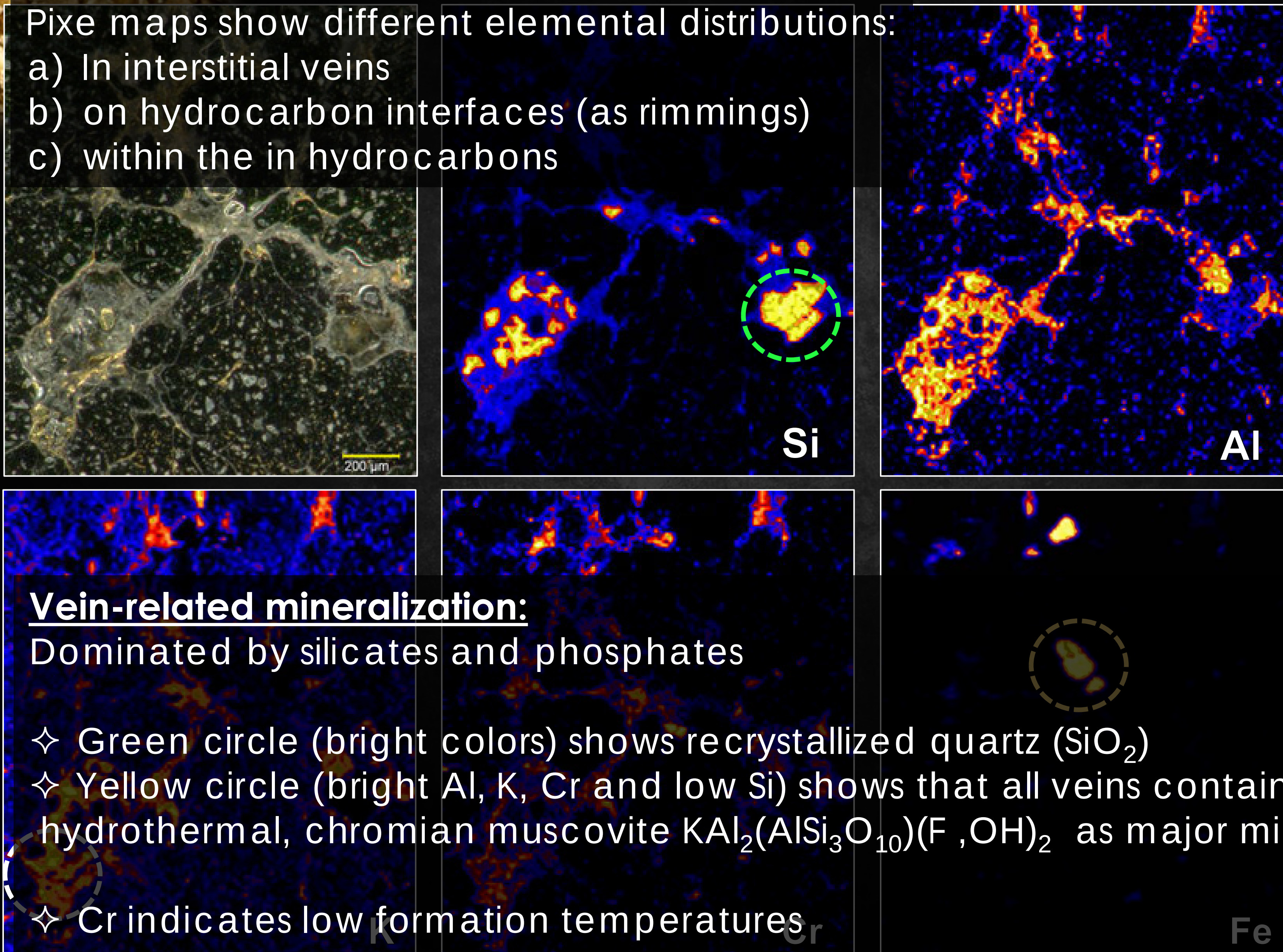

Vein-related mineralization:

Dominated by silicates and phosphates

✧ Green circle (bright colors) shows recrystallized quartz (SiO_2)

✧ Yellow circle (bright Al, K, Cr and low Si) shows that all veins contain hydrothermal, chromian muscovite $KAl_2(AlSi_3O_{10})(F,OH)_2$ as major minerals

✧ Cr indicates low formation temperatures

Vein-related mineralization

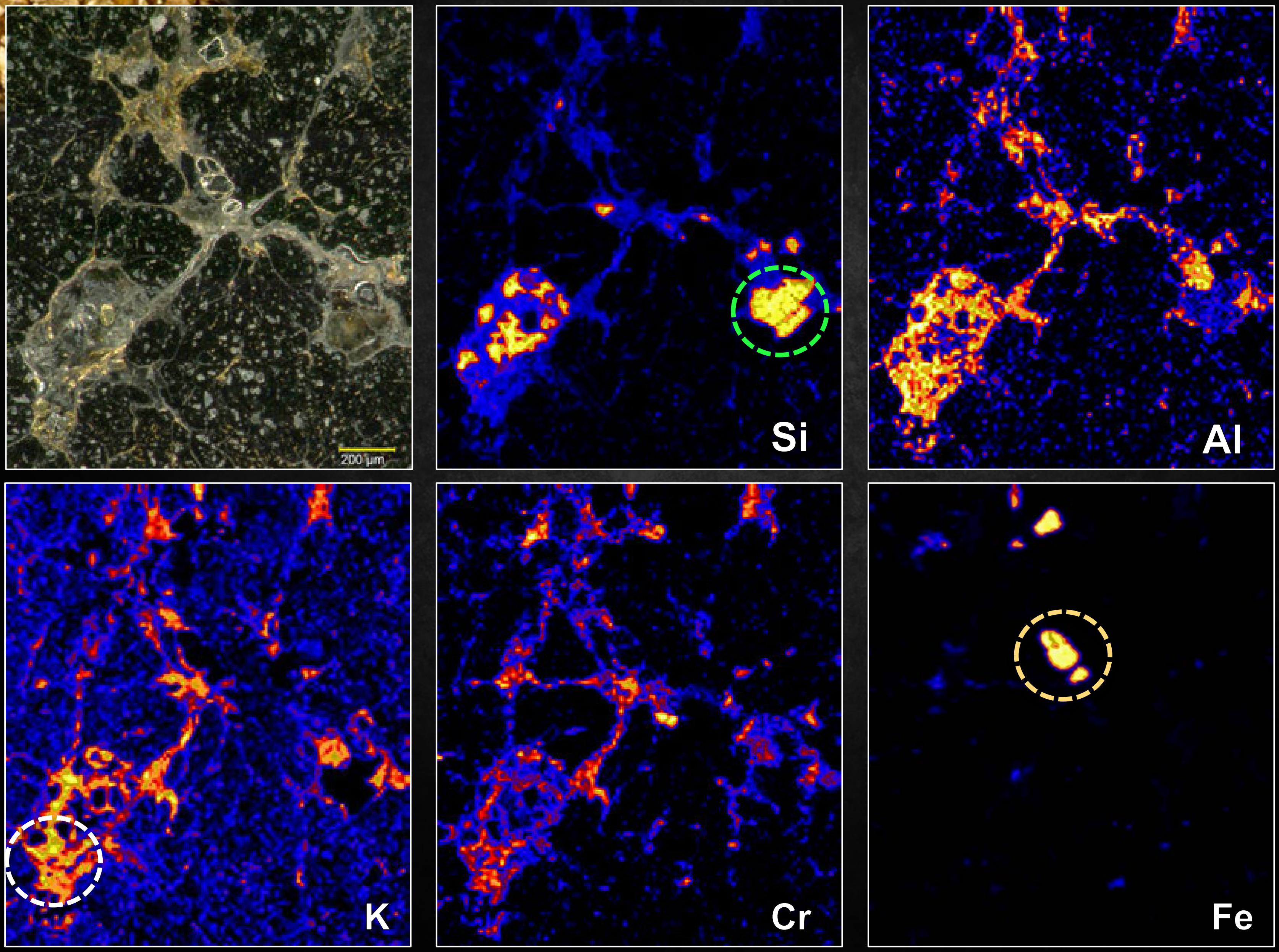

Mineralization within the Hydrocarbons

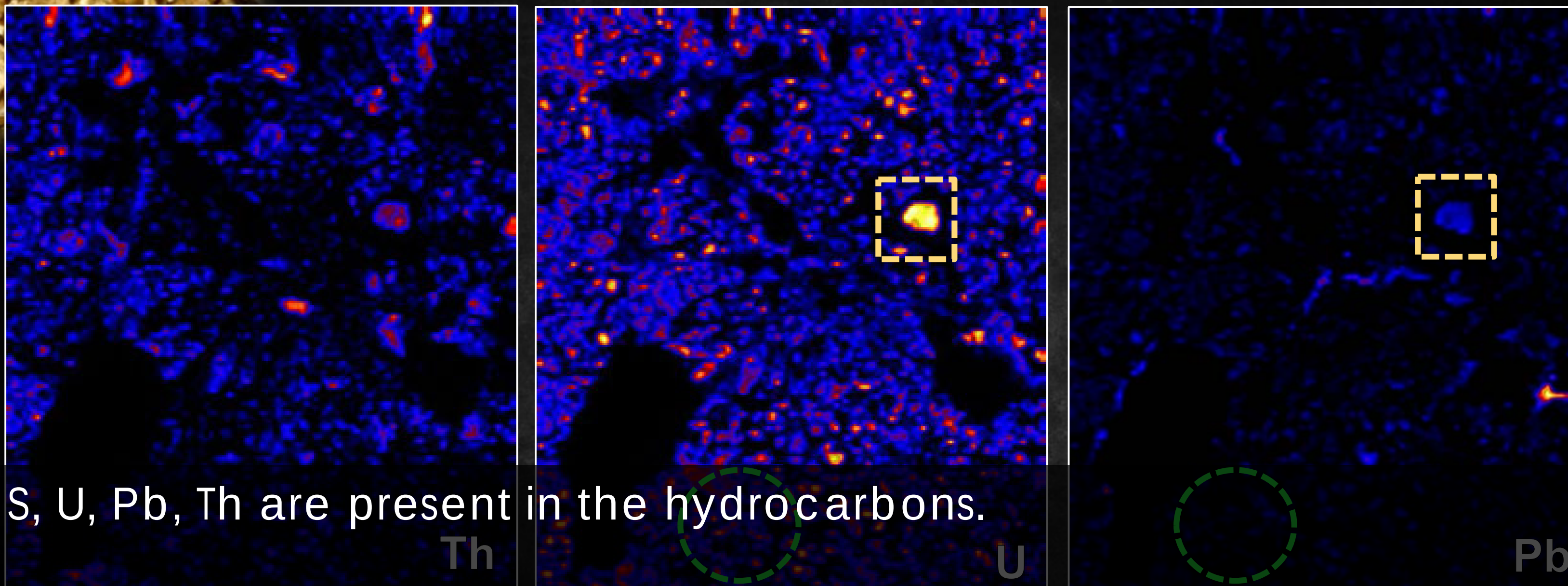

S, U, Pb, Th are present in the hydrocarbons.

- ✧ The uniform distribution of S (blue) in the hydrocarbon nodules accounts for the presence of complex insoluble hydrocarbon, such as asphaltenes

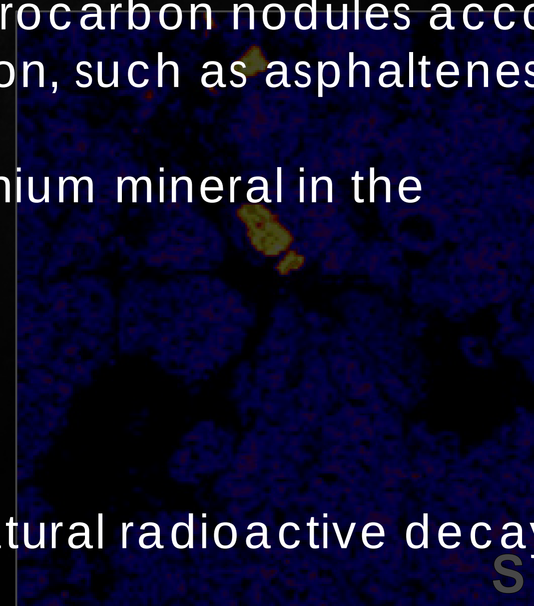

- ✧ U is present in Uraninite (UO_2), the major Uranium mineral in the Witwatersrand

  We can distinguish 2 different species:

  a) uraninite with Pb

  b) secondary uraninite without Pb

- ✧ Th is trace element in Uraninite – from the natural radioactive decay of U

Mineralization within the Hydrocarbons

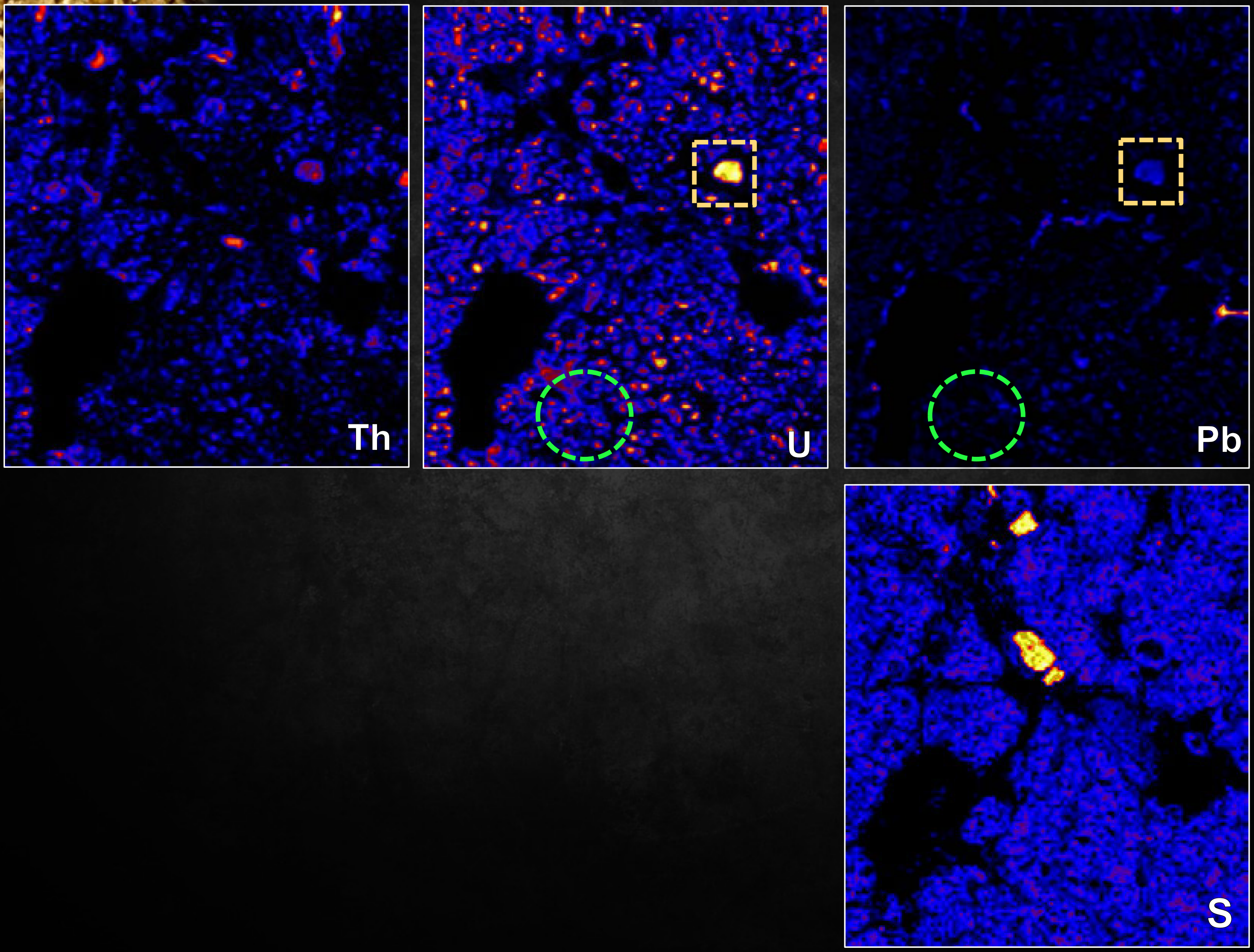

Rimmings and Veins

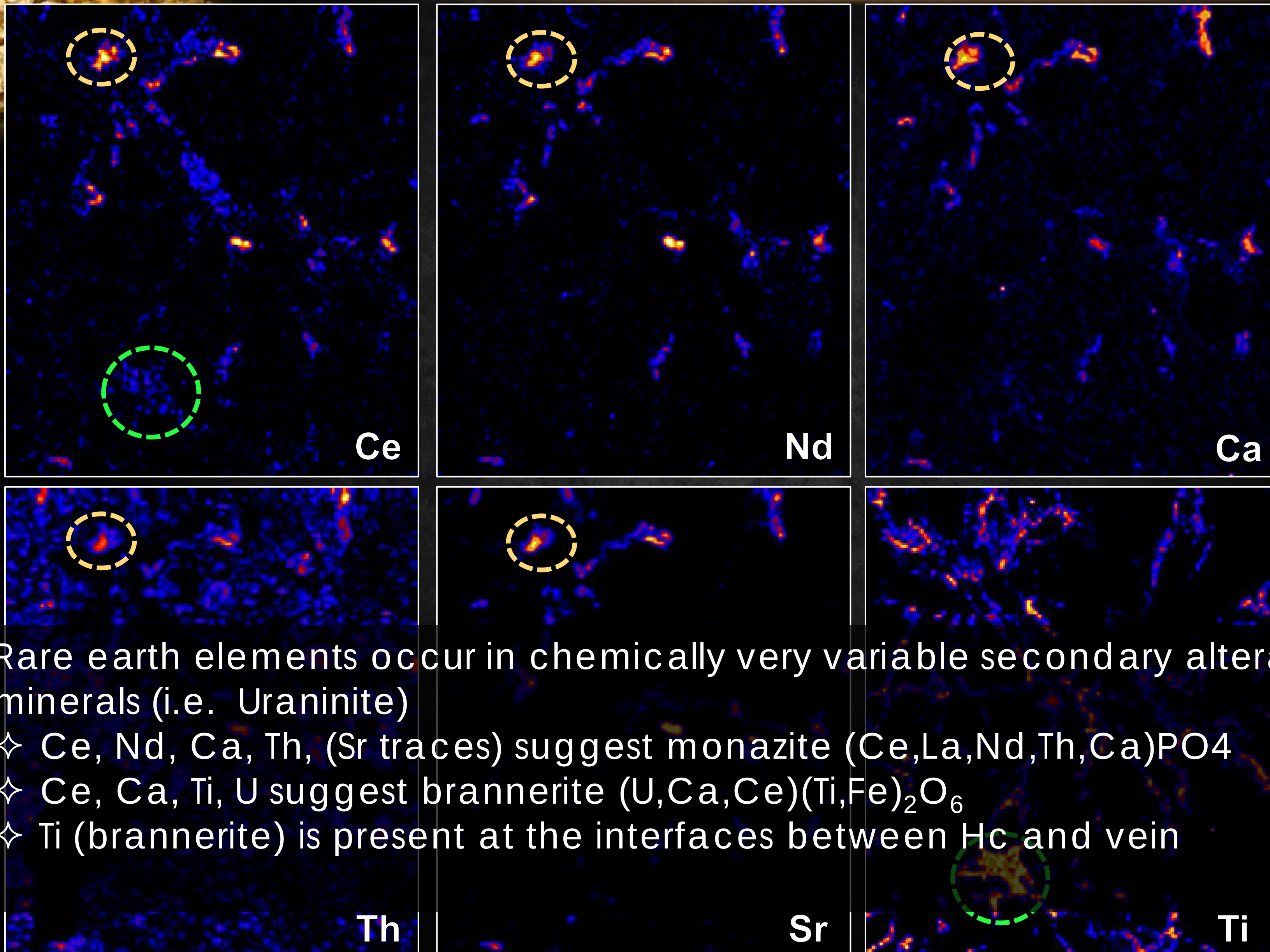

Rare earth elements occur in chemically very variable secondary alteration minerals (i.e. Uraninite)

- ✧ Ce, Nd, Ca, Th, (Sr traces) suggest monazite (Ce,La,Nd,Th,Ca)PO4
- ✧ Ce, Ca, Ti, U suggest brannerite $(U,Ca,Ce)(Ti,Fe)_2O_6$
- ✧ Ti (brannerite) is present at the interfaces between Hc and vein

Rimmings and Veins

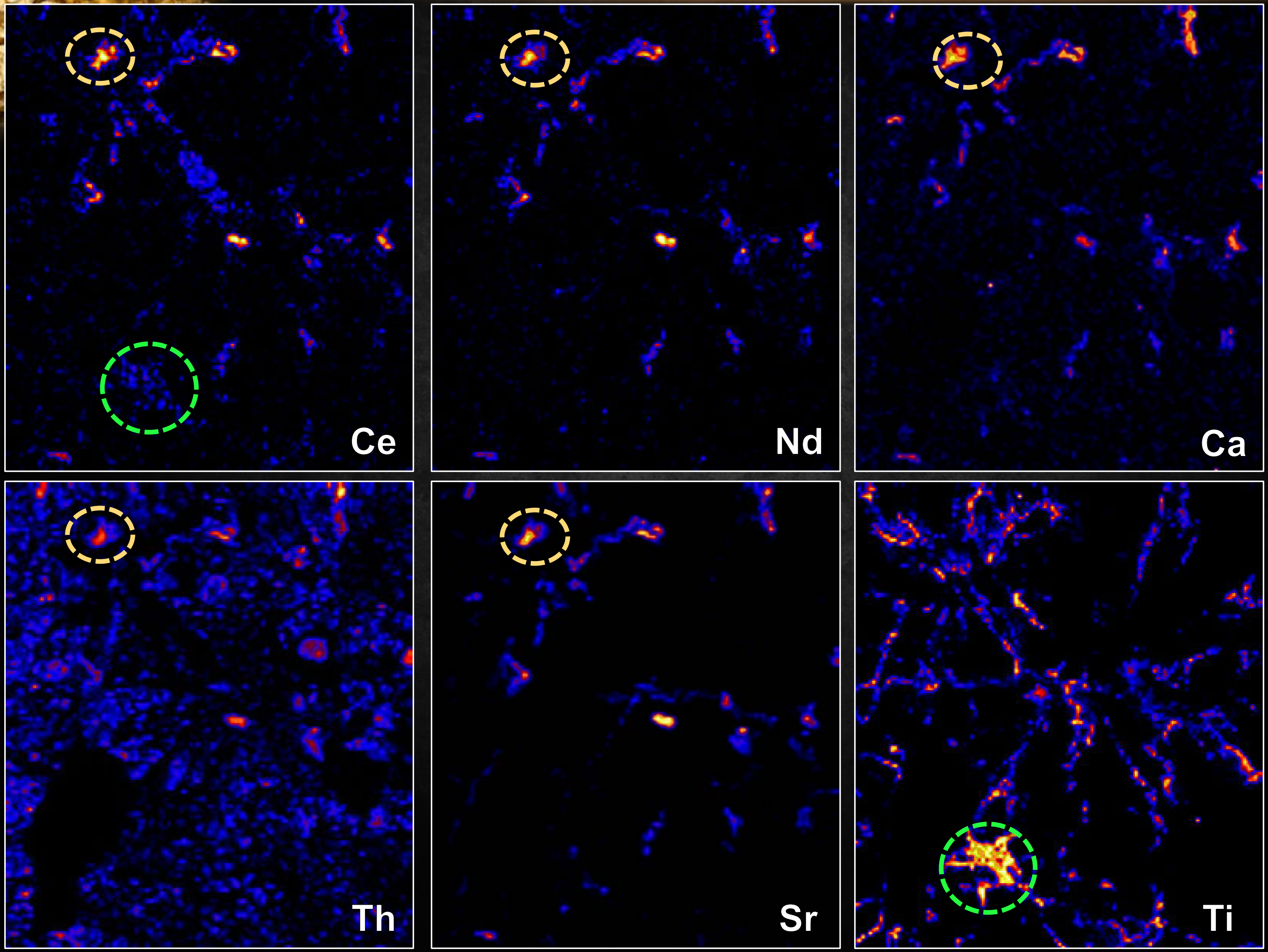

Vein-related Mineralization

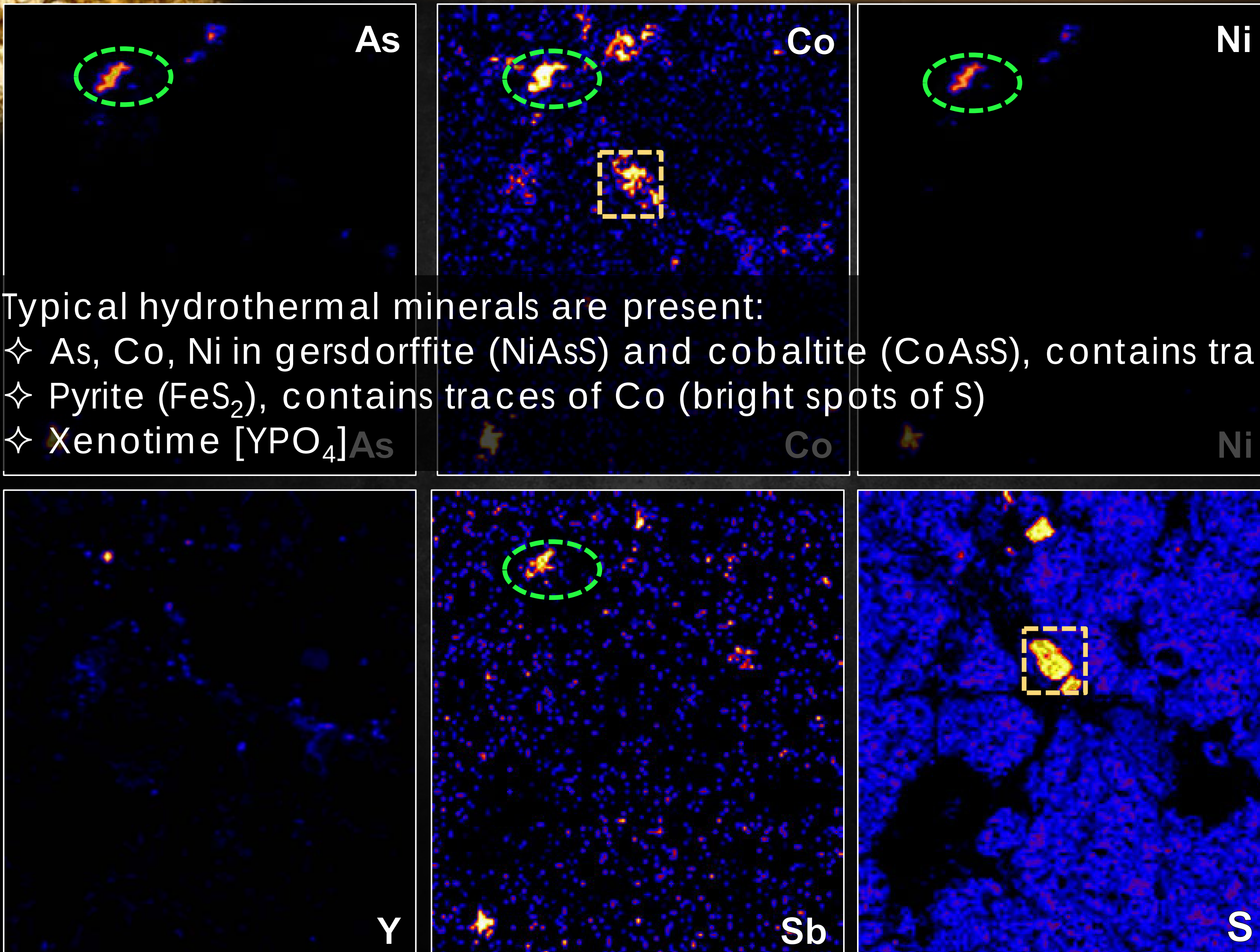

Typical hydrothermal minerals are present:

- ✧ As, Co, Ni in gersdorffite (NiAsS) and cobaltite (CoAsS), contains traces of Sb
- ✧ Pyrite (FeS_2), contains traces of Co (bright spots of S)
- ✧ Xenotime [YPO_4]

Gold and Organic Matter

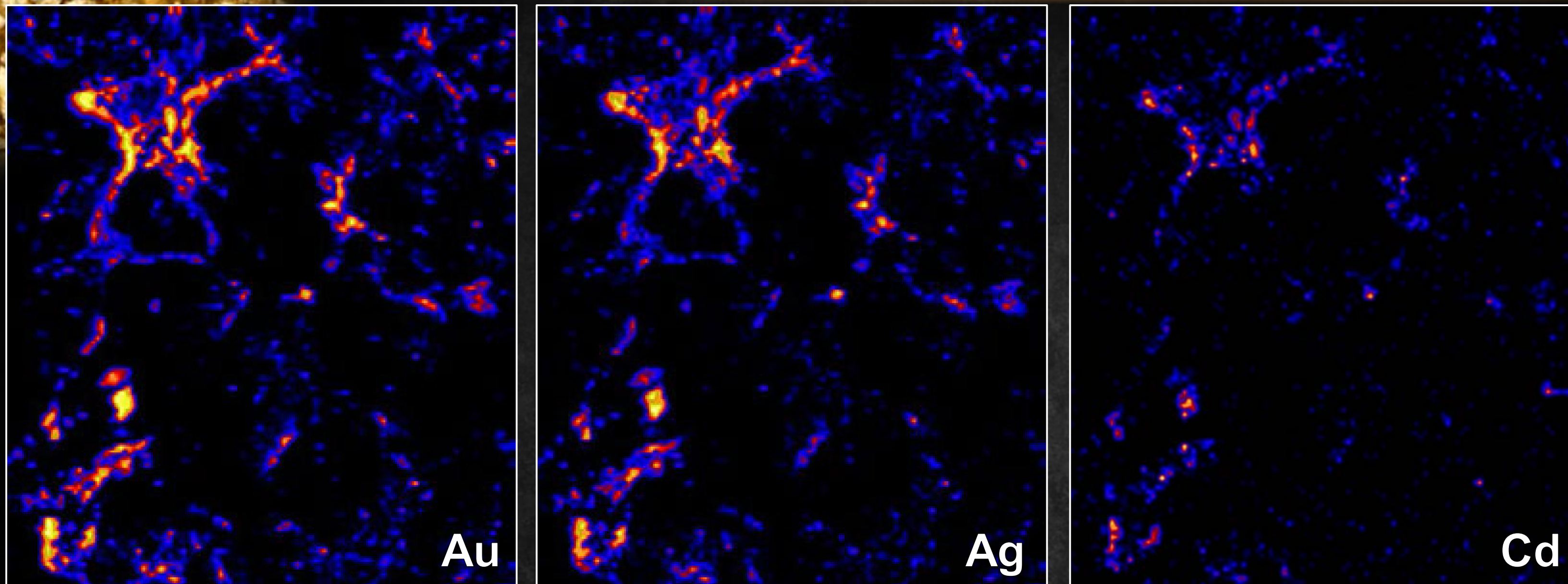

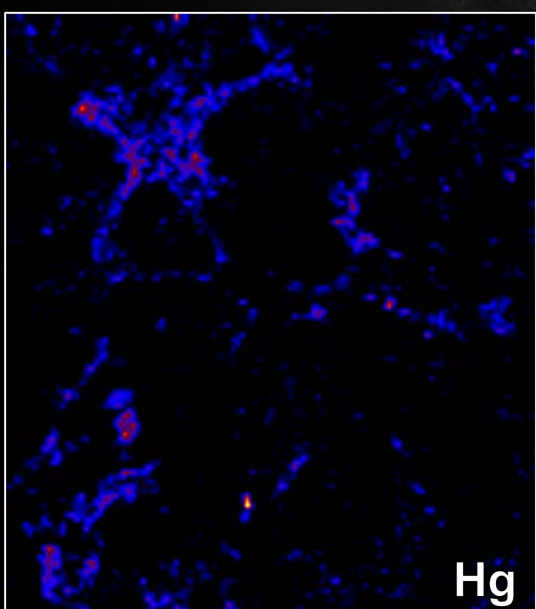

Majority of gold is confined to rimmings around bitumen nodules and is also present in small veinlets

Gold correlates with Ag, and contains Cd and Hg in traces

The style of mineralization and its presence around the nodules suggests that gold precipitated due to reduction from an (hyrothermal) aqueous solution

Proton backscattering (EBS) – how useful it is?

- Information on local concentrations of C, O, H is needed if possible (organic matter is classified on the basis of H/C and O/C ratios)
- It is possible to obtain C, O from EPMA but the results are not reliable
- Is proton backscattering reliable? Can we trust the results?
- Problems: high complexity of spectra, heavy elements cannot be distinguished from fits of EBS spectra
- Heavy elements influence the results for C, O, H

  (H found indirectly as the only missing element)

EBS mapping

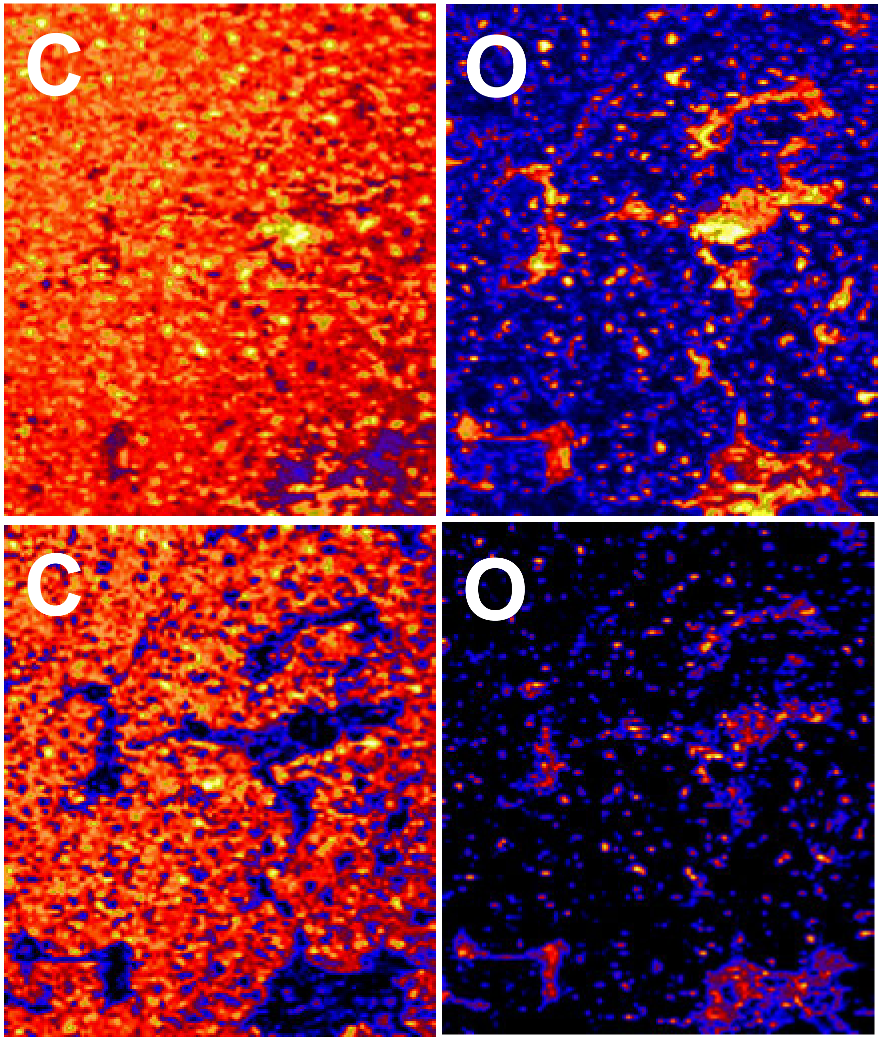

using energy gates

(„C map” is effectively C+O map)

using energy gates with background subtraction (Proper separation of C and O)

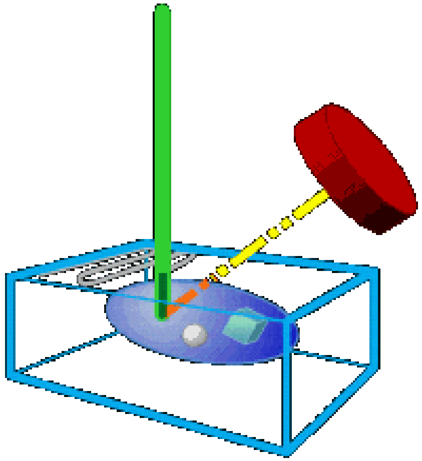

PIXE Analysis of Fluid Inclusions

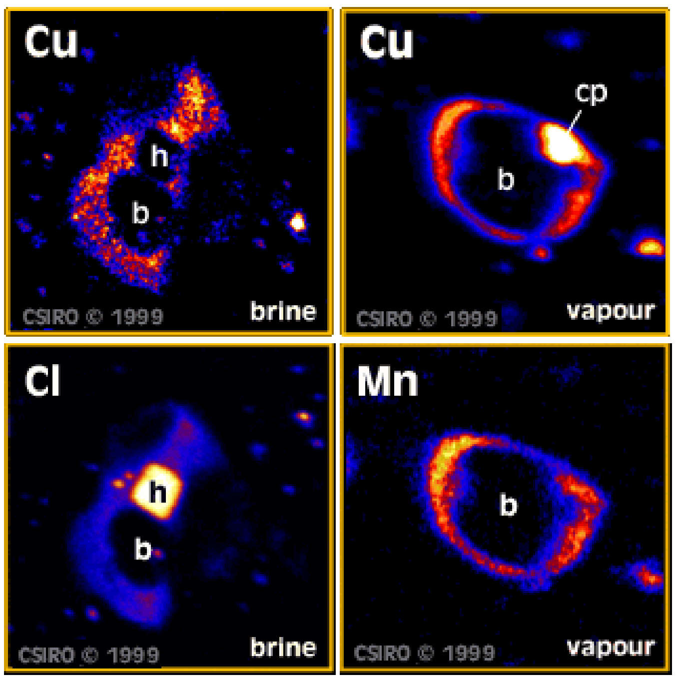

Parameters needed:

Shape (ellipsoidal)
– length, width, thickness

Fluid density
Orientation
Depth

Http://www.syd.dem.csiro.au/hydrothermal/chris

Nuclear Instruments and Methods in Physics Research B 363 (2015) 79–85

Contents lists available at ScienceDirect

Nuclear Instruments and Methods in Physics Research B

journal homepage: www.elsevier.com/locate/nimb

PIXE micro-mapping of minor elements in Hypatia, a diamond bearing carbonaceous stone from the Libyan Desert Glass area, Egypt: Inheritance from a cold molecular cloud?

M.A.G. Andreoli [a,*], W.J. Przybylowicz [b,c], J. Kramers [d], G. Belyanin [d], J. Westraadt [e], M. Bamford [f], J. Mesjasz-Przybylowicz [b], A. Venter [g]

[a] School of Geosciences, University of the Witwatersrand, P.O. Box 3, Wits 2050, South Africa
[b] iThemba LABS, National Research Foundation, P.O. Box 722, Somerset West 7129, South Africa
[c] AGH University of Science and Technology, Faculty of Physics & Applied Computer Science, al. A. Mickiewicza 30, 30-059 Kraków, Poland
[d] Department of Geology, University of Johannesburg, Auckland Park 2006, South Africa
[e] Department of Physics, Nelson Mandela Metropolitan University, Port Elizabeth 6031, South Africa
[f] Evolutionary Studies Institute, University of the Witwatersrand, P.O. Box 3, Wits 2050, South Africa
[g] South African Nuclear Energy Corporation, P.O. Box 582, Pretoria 0001, South Africa

It all started with a black pebble, discovered by Aly Barakat, an Egyptian geologist, in the area of the enigmatic Libyan Desert Glass (LDG), in SW Egypt...

1996

Tut ankh amen's coffin jewel with Libyan Desert Glass

Libyan Desert Glass

Datowanie: wiek utworzenia - 26 mln lat (fission tracks, argon dating)

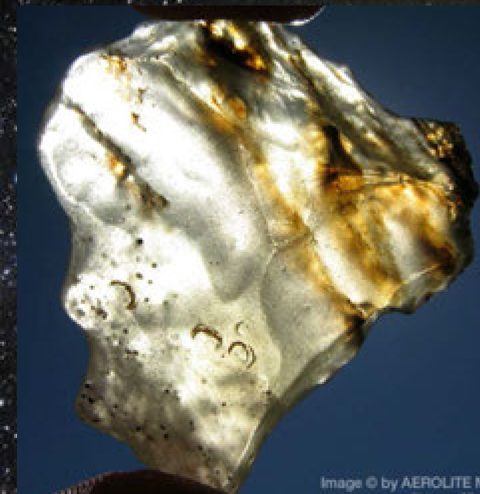

Hypatia – (Photograph by Roberto Appiani)

Beneath the desert varnish, the stone and all its contents are extraordinarily well preserved.

Cechy Hypatii:

C-dominuje, bogata w diamenty

Materiał pozaziemski – na podstawie badań izotopowych gazów szlachetnych
oraz izotopów azotu

Dwa rodzaje matrycy:
Matryca 1 – prawie czysta węglowa
Matryca 2 – zawiera Fe, Ni, O, S w ilościach mierzalnych mikrosondą elektronową (WDS)

Fazy w matrycy 2 (wtrącenia):
(i) Siarczki (Fe, Ni), skupienia sub-mikronowych ziaren w strefach matrycy wzbogaconych w Fe i S
W tych strefach matrycy {atomowe proporcje}
$(Ni+Fe)/P = 1.51 \pm 0.24$ Oraz $Ni/Fe = 0.086 \pm 0.061$

(ii) Ziarna moissanitu (SiC) o wielkości do 5 mikrometrów
[Mossanit został odkryty został przez francuskiego chemika i mineraloga H. Moissana w meteorycie Canyon Diablo w Stanach Zjednoczonych, bardzo rzadki]

(iii) Ziarna fosforku Ni o wielkości do 60 mikrometrów; kryptokrystaliczne lub amorficzne; Skład {proporcje atomowe} (Ni + Fe)/P = 5.6 $\pm$ 1.7 i Ni/Fe = 74 $\pm$ 29
Obie wartości znacznie wyższe niż we wszystkich znanych minerałach, fosforkach Ni

(iv) Rzadkie ziarna (pojedyncze obserwacje) grafitu, metalicznego Al, Fe i Ag oraz fazy Składającej się z Ag, P oraz jodu (I)

W matrycy 2 spektroskopia Ramana wykazuje wyraźne wąskie diamentowe pasmo ($1340\ cm^{-1}$)
W matrycy 1 dominują pasma D i G nieuporządkowanego węgla, oraz wszędzie występuje mało intensywne pasmo diamentowe (to tłumaczy twardość materiału)

Stosunek intensywności D/G = 0.75 $\pm$ 0.09
[wartość podobna do wartości w najstarszej materii węglowej w układzie słonecznym – *Similar to those in the most primitive solar system carbonaceous matter*]

Uważa się że faza diamentowa powstała w wyniku impaktu.

Faza siarczkowa (Fe, Ni) to prawdopodobnie pirotyt, również sugeruje się pochodzenie impaktowe

Moissanit jest związany z fazą fosforku Ni;
Przyjmuje się że są starsze od układu słonecznego

Brak rekrystalizacji fazy fosforku Ni sugeruje że Hypatia nie była poddana termalnemu metamorfizmowi, zgodnie z charakterystyką pasm D-G Ramana

Brak materii krzemowej odróżnia Hypatię od cząstek pyłu międzygwiezdnego oraz od znanego materiału z komet.

Ta cecha, oraz „wymieszanie" matryc, może świadczyć o wysokiej niejednorodności we wczesnej mgławicy słonecznej

Wcześniejsza teza o pochodzeniu **(Kramers et al. 2013):**

- **Pozostałość jądra komety która mogła rozerwać się i eksplodować w atmosferze tworząc Libyan Desert Glass' (LDG)**

została kategorycznie odrzucona przez **Reimolda and Koeberla (2014)** którzy stwierdzili:

‚There is no conection between the diamond-bearing rock fragment and the LDG except that they occur in the same region'

Wobec tego teraz stwierdzono:
‚A lack of silicate matter sets the stone apart from interplanetary dust particles and known cometary material. This, along with the dual intermingled matrices Internal to it, could indicate a high degree of heterogeneity in the early solar nebula'

Dalsze badania:

In-situ analizy izotopów stabilnych w matrycy węglowej

Analizy izotopów C, Si i Ni w moissanicie i fosforkach Ni

Powinny ustalić wynik debaty co do pochodzenia materii tworzącej Hypatię

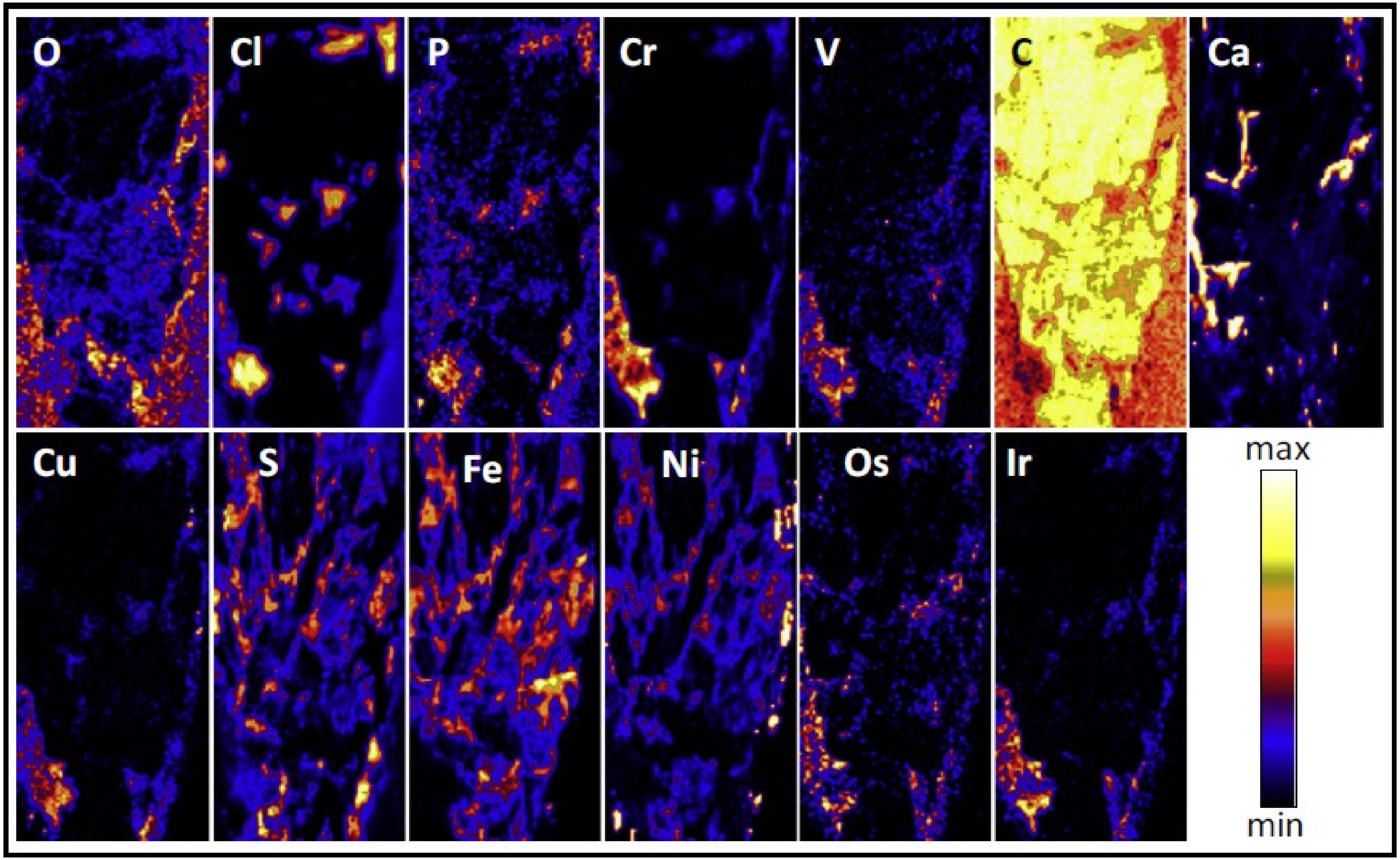

Fig. 2. PIXE elemental maps of selected elements from the sample *Hypatia*//*Mick Rebak B*/*III*/*Region 00* obtained using GeoPIXE and the Dynamic Analysis method. Qualitative maps of C and O (reported in counts) were obtained by EBS method using energy "gates" with background subtraction. Top: lithophile elements; bottom: chalcophile elements (left grouping) and siderophile elements (right grouping). Scan size 782 μm × 1668 μm.

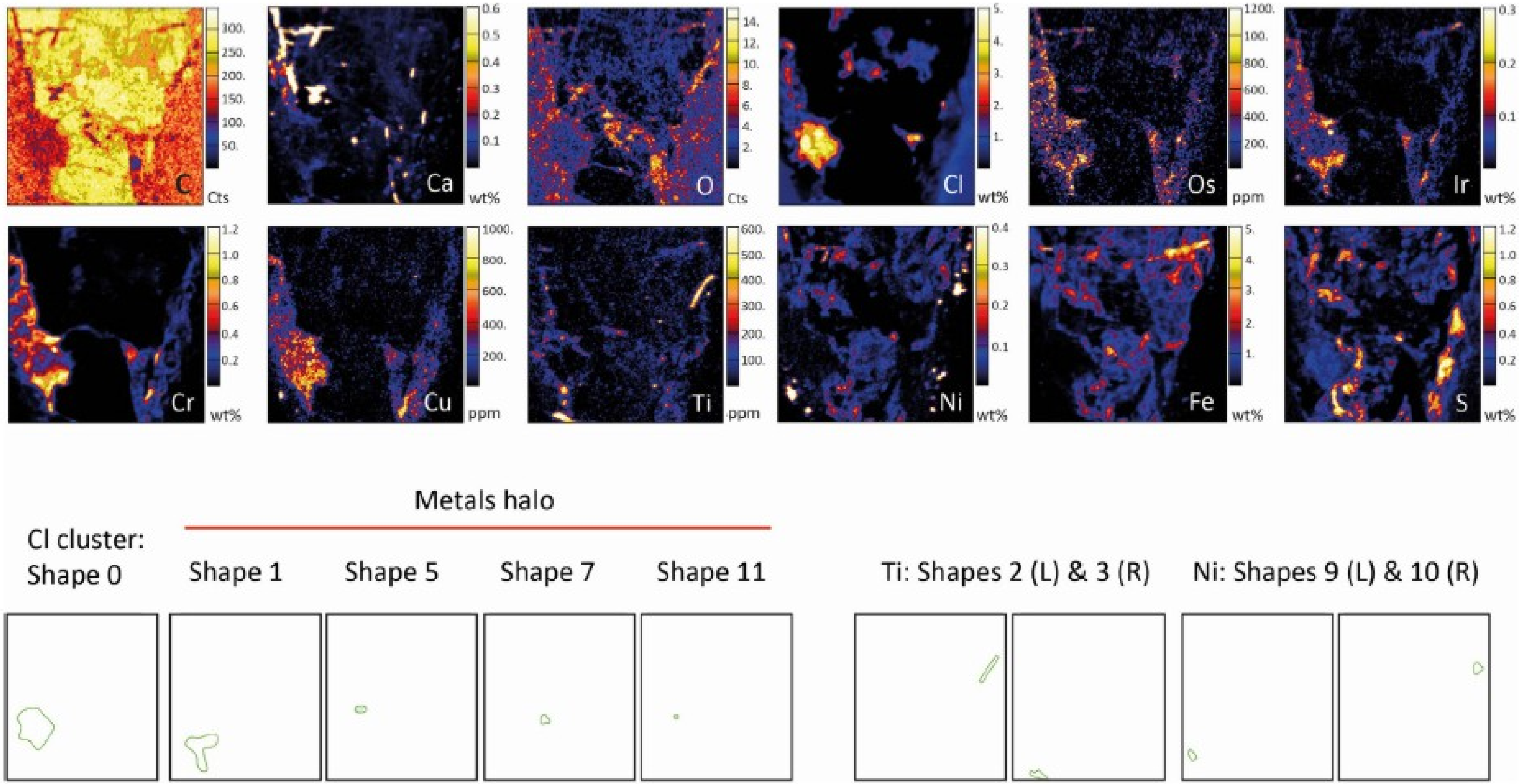

Fig. 3. PIXE quantitative elemental maps of selected elements from the sample *Hypatia//Mick Rebak B/III/Region 5*, obtained using GeoPIXE and the Dynamic Analysis method. Qualitative maps of C and O (reported in counts) were obtained by EBS method using energy "gates" with background subtraction. Scan size 750 μm × 750 μm. Results from selected shapes are reported in Table 1.

Table 1
PIXE analyses of Cl-, PGM, and metals-rich shapes in *Hypatia*//*Mick Rebak B*/*III* (see Fig. 3). Concentrations reported in mg/kg.

Region	5								
Shape	0	1	5	7	11	2	3	9	10
Comment	Cl core	Metals halo around Cl core				Ti-rich Shapes		Ni-rich Shapes	
Elements									
Si	2550 ± 170	4450 ± 260	10,310 ± 530	17,200 ± 700	2320 ± 670	500 ± 65	7620 ± 390	19,800 + 1200	2680 ± 280
Ti	56 ± 2	90 ± 3	110 ± 14	<14	76 ± 19	370 ± 9	460 ± 11	<12	86 ± 7
Al	<560	<610	4950 ± 1190	19,120 ± 1260	<4400	<530	<1150	<1600	<1060
Fe	780 ± 23	2240 ± 44	2280 ± 100	24,260 ± 390	710 ± 43	550 ± 19	260 ± 11	343 + 25	950 ± 40
Mn	65 ± 29	127 ± 49	150 ± 63	<20	310 ± 75	340 ± 20	17 ± 11	<17	6380 ± 73
Ca	480 ± 6	550 ± 14	770 ± 16	360 ± 17	450 ± 24	147 ± 6	640 ± 17	93 + 9	173 ± 8
K	200 ± 9	194 ± 7	320 ± 13	84 ± 12	210 ± 20	100 ± 10	230 ± 10	<17	40 ± 7
P	520 ± 100	280 ± 41	280 ± 60	<92	570 ± 120	<28	150 ± 56	1370 + 140	<60
Cl	30,840 ± 240	13,150 ± 180	14,000 ± 220	<33	29,200 ± 240	247 ± 9	5370 ± 64	3760 + 100	930 ± 33
S	1380 ± 120	1550 ± 66	1290 ± 70	3830 ± 71	1210 ± 75	200 ± 15	1650 ± 42	626 + 36	490 ± 33
V	90 ± 8	88 ± 10	130 ± 30	28 ± 8	790 ± 38	n.d.	n.d.	n.d.	<11
Cr	5090 ± 65	6700 ± 80	9820 ± 110	88 ± 10	11,310 ± 190	930 ± 17	640 ± 20	254 + 17	840 ± 20
Ni	110 ± 8	249 ± 16	113 ± 37	875 ± 32	<70	900 ± 270	145 ± 11	56,100 + 590	6460 ± 90
Cu	310 ± 18	450 ± 21	460 ± 42	<33	n.d.	50 ± 10	41 ± 10	n.d.	n.d.
Zn	58 ± 8	112 ± 11	135 ± 24	<35	n.d.	<18	<20	n.d.	n.d.
Sr	71 ± 9	50 ± 12	<150	<160	n.d.	n.d.	n.d.	n.d.	n.d.
Mo	330 ± 32	410 ± 44	<400	<430	n.d.	<220	n.d.	n.d.	n.d.
Os	190 ± 27	310 ± 28	580 ± 78	<90	n.d.	100 ± 25	<50	n.d.	n.d.
Ir	780 ± 43	1170 ± 53	1650 ± 130	<90	4640 ± 300	170 ± 32	<50	n.d.	n.d.

N.d.: not detected.

Biology and environment; medicine

unique combination of techniques
related to <u>specimen preparation</u> and <u>microanalysis</u>
at ONE research centre
gave us international acclaim as one of the few best laboratories

In addition:
Capability of microanalyses of biological materials in frozen-hydrated (the closest to natural) state from 2004

The first such facility in the world, a definite highlight

Leica EM CFC-Cryo-workstation

- Cryofixation
- Cryopreparation
- Observation

- Plunge Freezing/Immersion Cryofixation
- Ice Embedding/Bare Grid Technique
- Metal Mirror Freezing/Impact Cryofixation
- UV-Polymerisation,
- Progressive Lowering of Temperature, Freeze Substitution

Leica EM CFD Cryosorption Freeze Dryer

Automatic freeze drying of bulk specimens and cryosections at temperatures above -140°C in a clean vacuum provided by a cryosorption pump.

Low temperature embedding with UV lamp.

From: van der Ent et al. New Phytologist (Tansley Review) vol.218 Issue 2 (2018) 432-452.

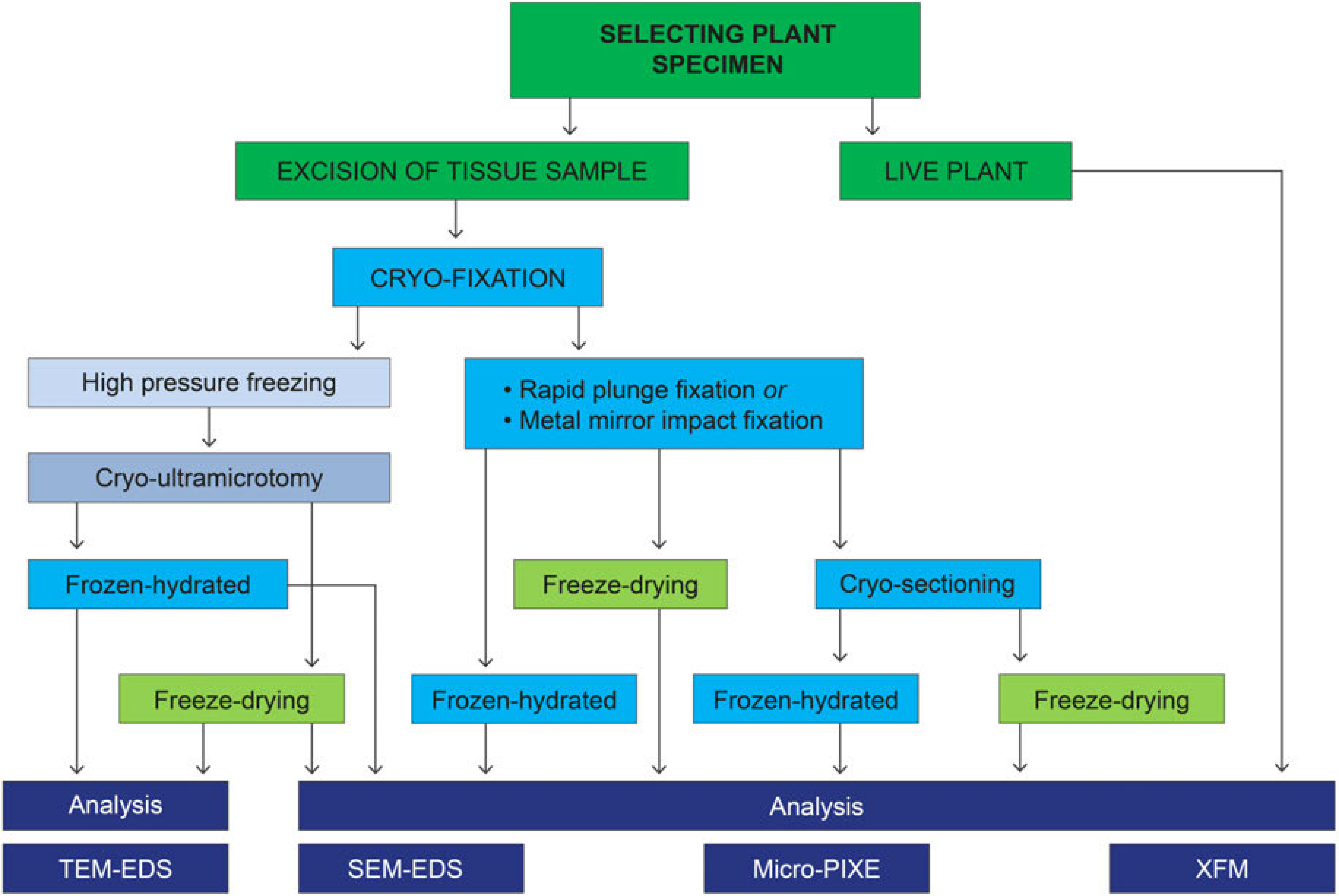

Slow freezing – formation of ice crystals

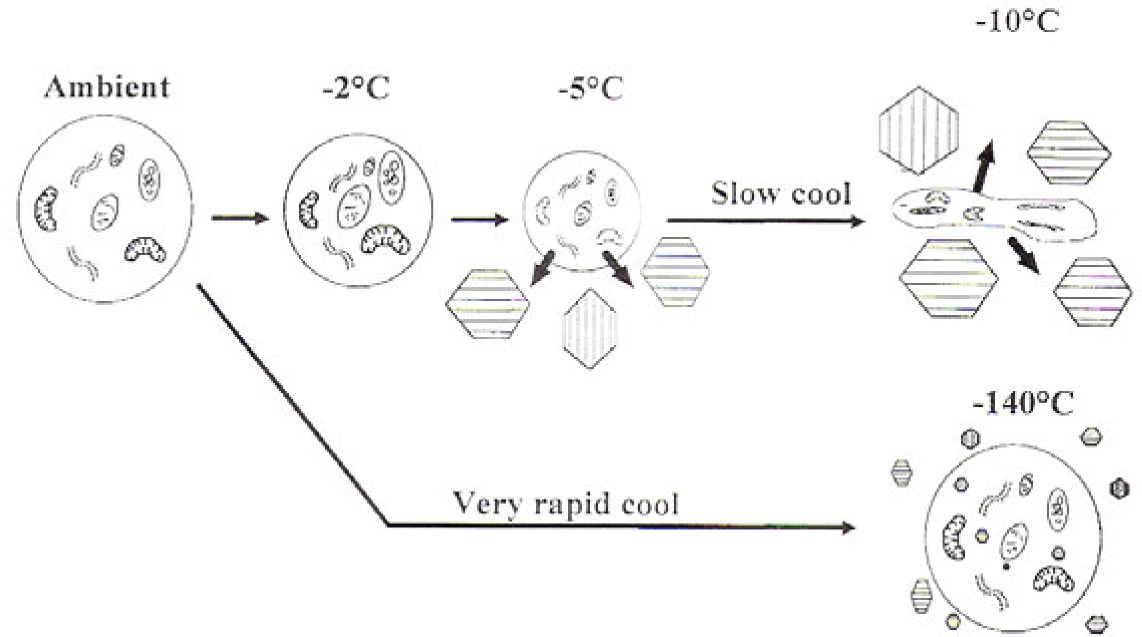

From: Llabador and Moretto, Nuclear Microprobes in the Life Sciences, World Scientific 1996

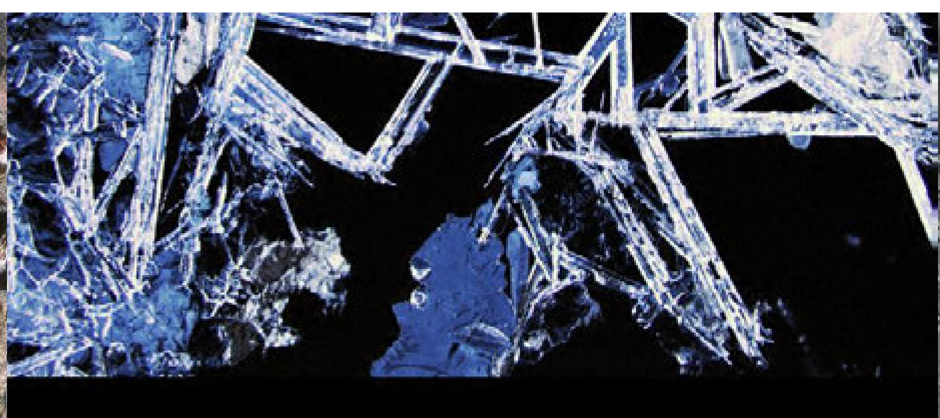

Cryo-micro-PIXE

Temperature ~100K; biological frozen-hydrated samples of any thickness, automated filling of liquid nitrogen

First in the world, achieved at minimum cost
Now another system in Slovenia

2004

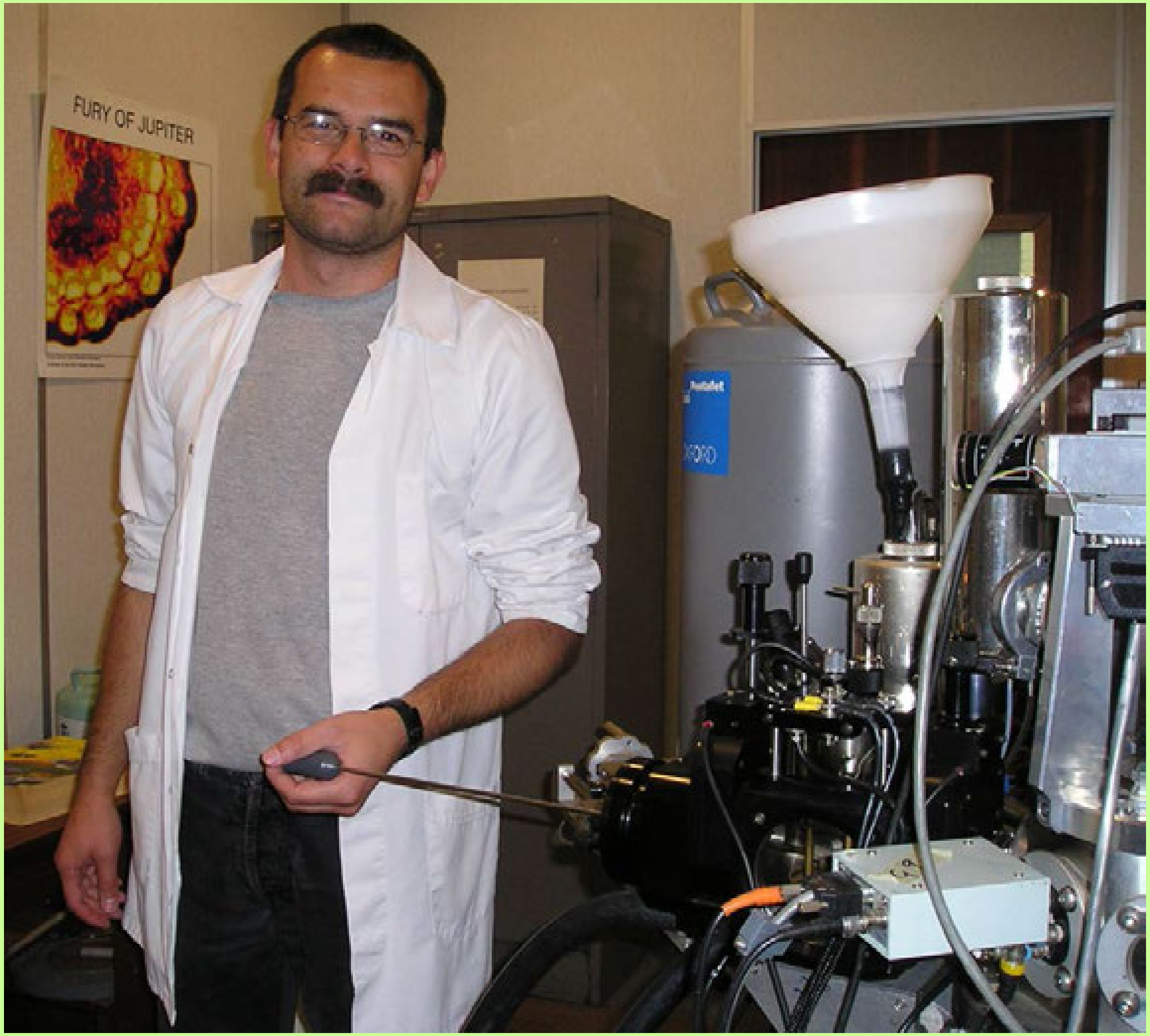

Dr Grzegorz Tylko operates the cryotransfer system at a nuclear microprobe of iThemba LABS.

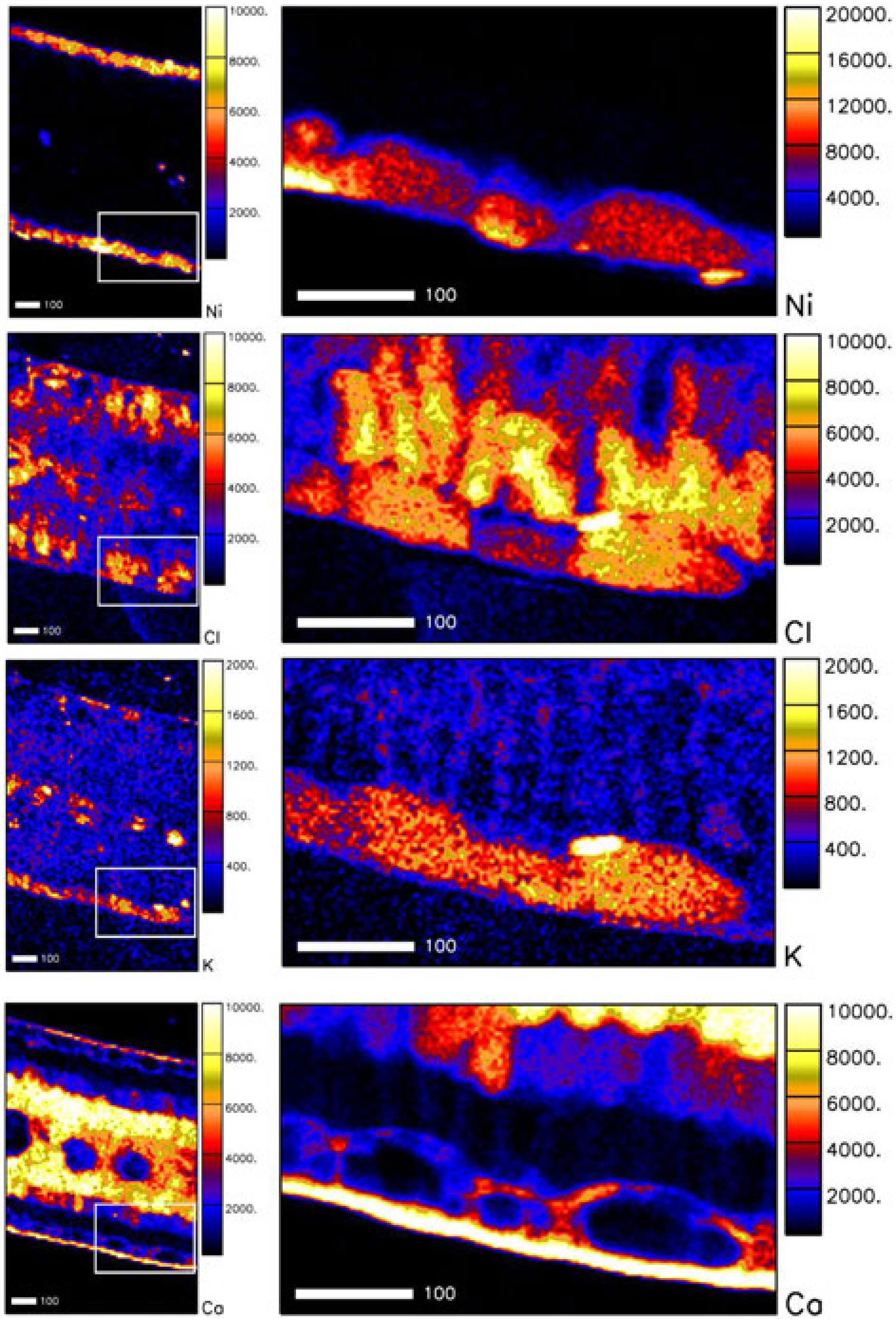

PIXE quantitative elemental maps of the leaf cross-section of *Senecio coronatus* analysed in frozen hydrated state.

All results are shown in μg g^{-1}.
Accumulated charge was 0.5 μC.
Scale bar is 100 μm.

van der Ent et al. X-ray elemental mapping techniques for elucidating the ecophysiology of hyperaccumulator plants. New Phytologist (Tansley Review) vol.218 Issue 2 (2018) 432-452. DOI:10.1111/nph.14810.
IF=7.33

Matrix evaluation (composition, areal density)

Our strength – complementary techniques are available

Particle (proton) Backscattering spectrometry (BS)
or
Scanning Transmission Ion Microscopy (STIM)

Particle Backscattering spectrometry (BS)

- specimen thickness (areal density)
- matrix composition = concentration of major elements in biological tissue

(C, O, N and indirectly H)

Done simultaneously with PIXE

Gives MEAN AREAL DENSITY

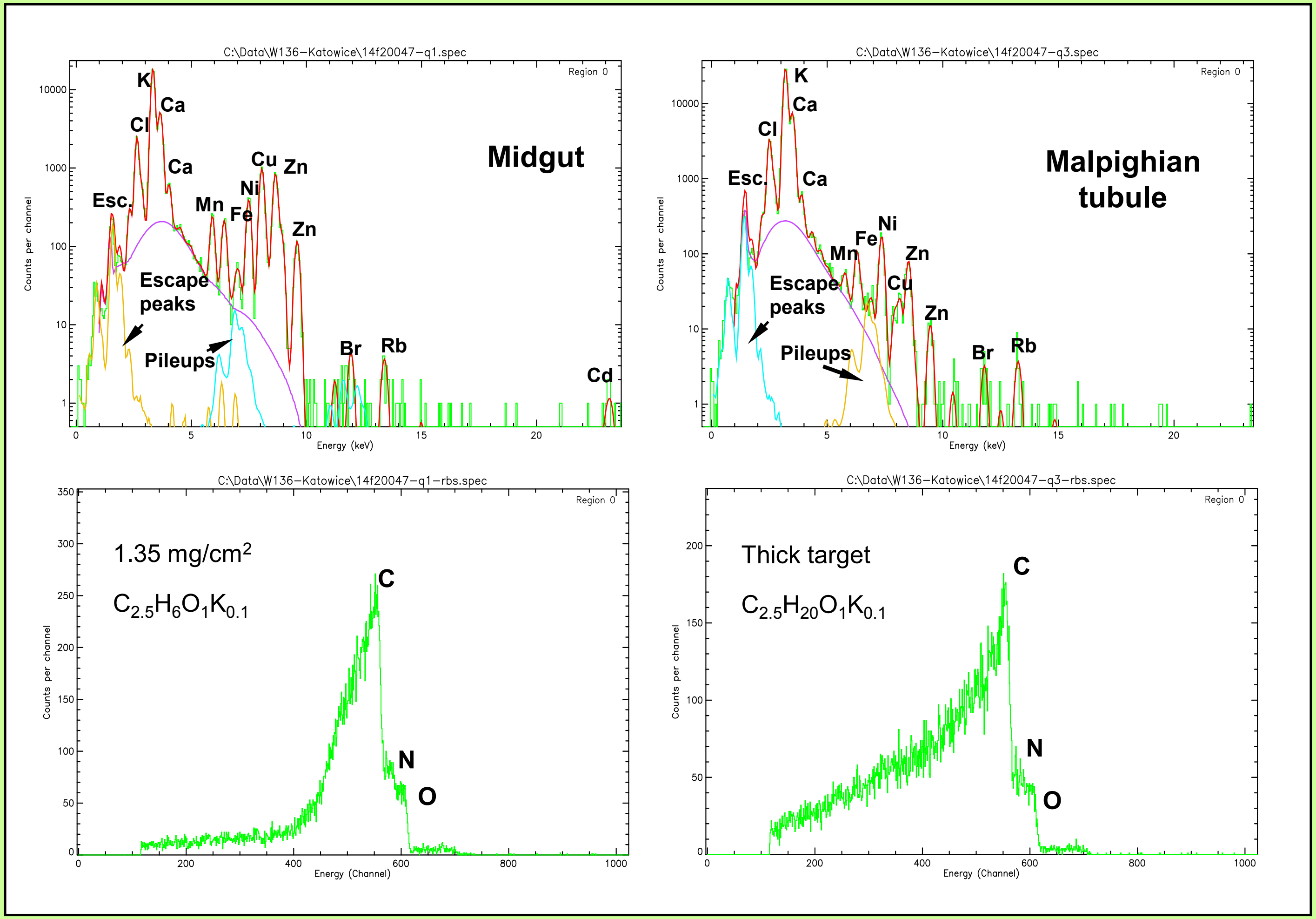

PIXE (top) and BS (bottom) spectra from regions selected on elemental maps. Note local differences in specimen thickness and ratios of major matrix components.

Specimens from various biological projects

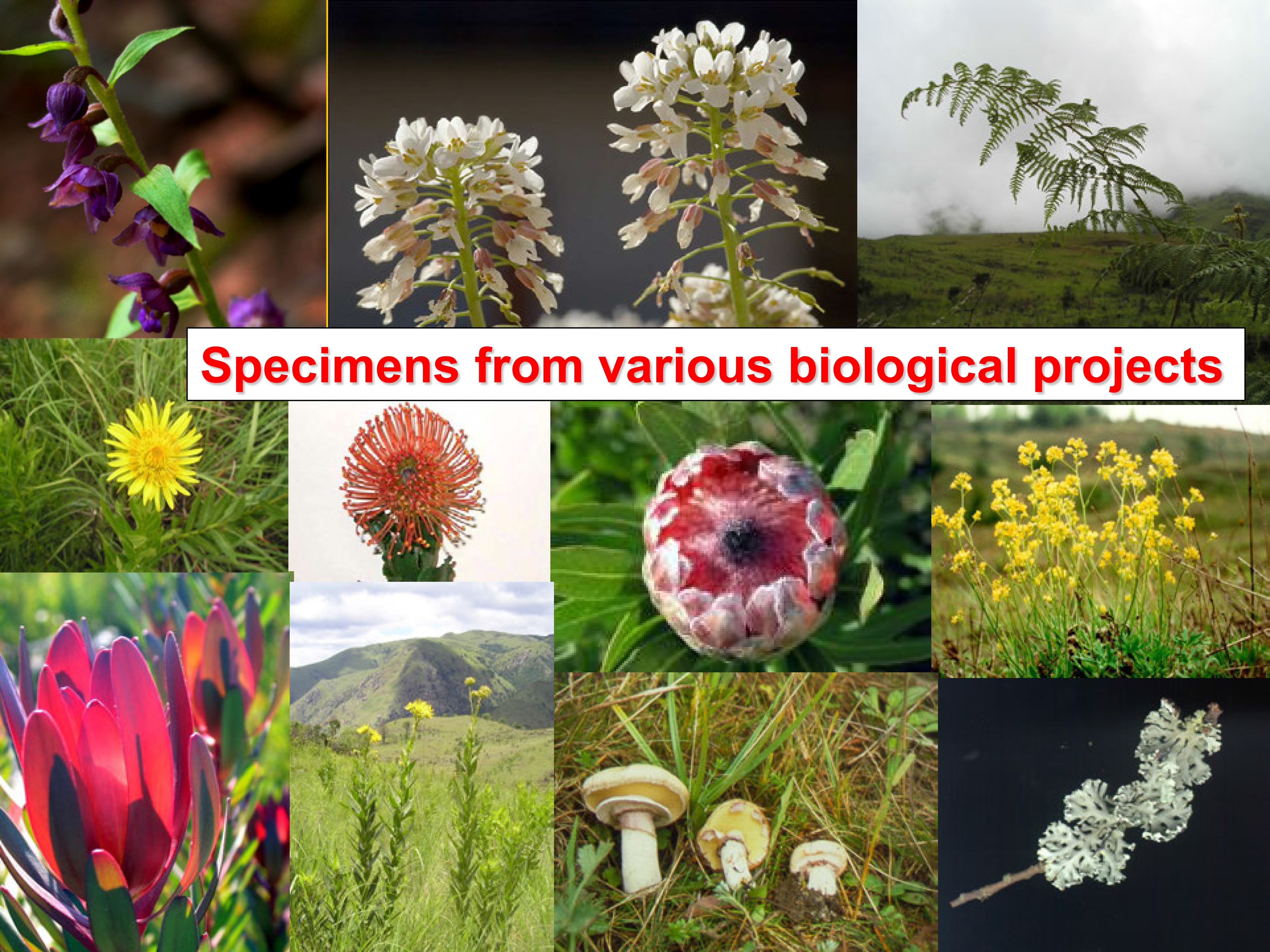

PLANTS:

- **Macronutrients : C, H, O, N, K, Ca, Mg, P and S above 0.1%**
- **Micronutrients: B, Cl, Cu, Fe, Mn, Mo, Ni and Zn < 100 mg/kg dry weight).**

Essential 17 elements known to be required by all higher plants

- **Beneficial: Si, Na, Co, Se**
- **Candidates for essential or beneficial elements: Cr, V, Ti**

ANIMALS:

- **additional essential trace elements As, B, Br, Cd, Cr, Pb, Li, Mo, Se, Si, Sn, V**

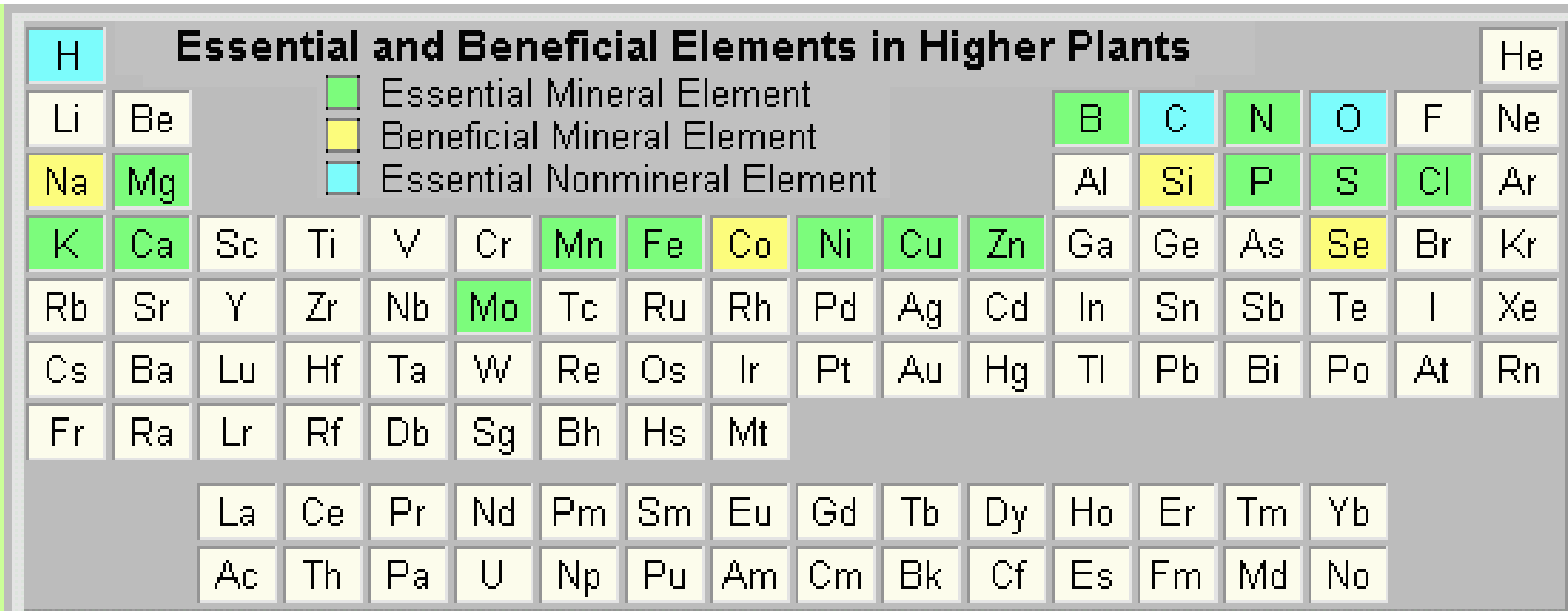

Where micro-PIXE is applied?

BASIC AND APPLIED LIFE SCIENCES

- Elemental transport and accumulation
- Micro-nutrient uptake and their function in metabolism
- Studies on the function of trace elements
- Elemental deficiency and toxicity
- Environmental pollution
- Ionomics and metallomics

ECOPHYSIOLOGY, ECOTOXICOLOGY, MEDICINE, AGRICULTURE

Hyperaccumulation in plants

Certain species accumulate metals to concentrations several orders of magnitude higher than those found in other species on the same site

(above toxicity level for most plants)

Elements reported to be hyperaccumulated:

Al, As, Cd, Co, Cu, Mn, Ni, Pb, Se, Zn

Shoots show metal enrichment in comparison with roots (usually the opposite)

METAL HYPERACCUMULATING PLANTS

After: van der Ent et al. Plant Soil 2013, **362**: 319–334.

Metal	Concentration criterion (% in leaf dry matter)	No. of taxa	No. of families
Antimony	>0.1	2	2
Arsenic	>0.1	5	1
Cadmium	>0.01	2	1
Cobalt	>0.03	30	11
Copper	>0.03	32	15
Chromium	>0.03	?	?
Lead	>0.1	14	7
Manganese	>1.0	12	5
Nickel	>0.1	450	38
Selenium	>0.01	20	7
Thallium	>0.01	2	1
Zinc	>0.3	12	5

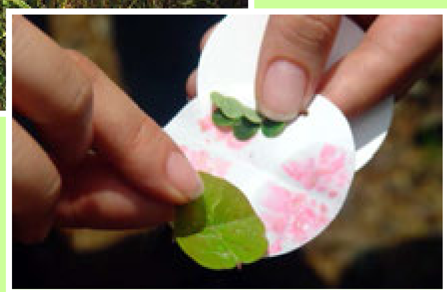

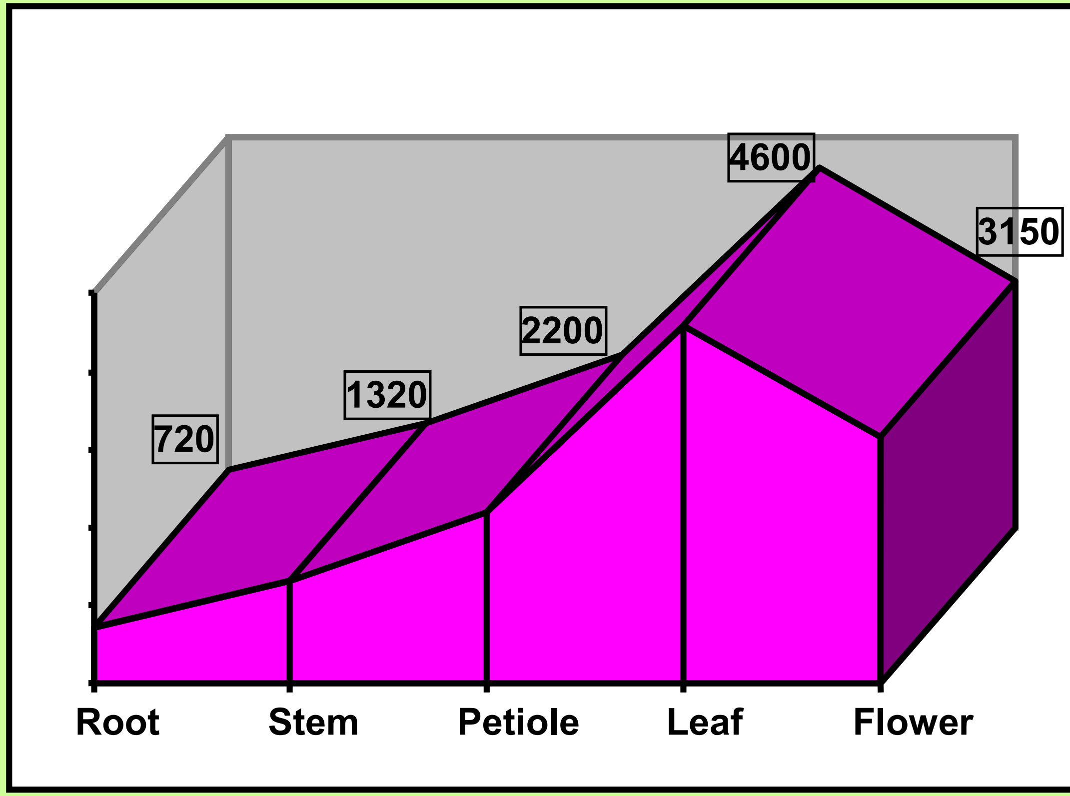

Average Ni concentrations (µg/g dry weight) in *Senecio anomalochrous* analysed by ICP-AES

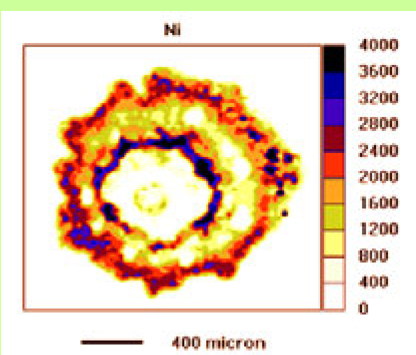

Root

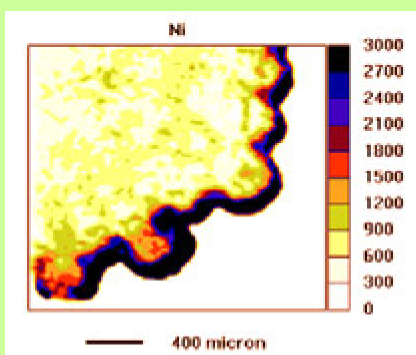

Stem

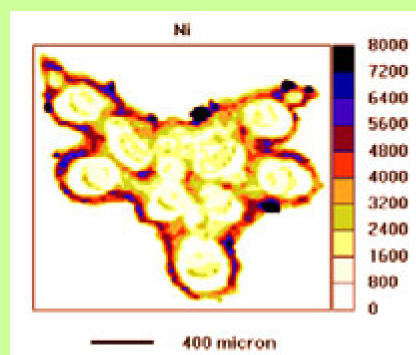

Petiole

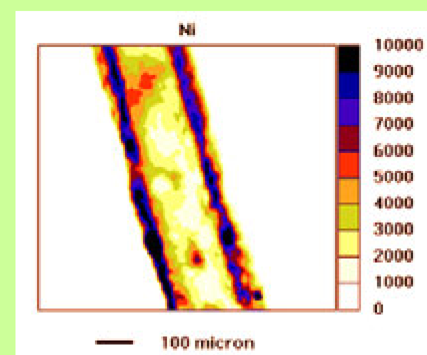

Leaf

Plant-insect herbivore interaction

Chrysolina pardalina

It has been proved that this beetle is able to complete its full life cycle for several generations feeding exclusively on *Berkheya coddii* leaves

The elemental maps for S, K, Ca, Mn, Fe, Ni, Cu and Zn of the midgut cells and Malpighian tubules in *Chrysolina pardalina*

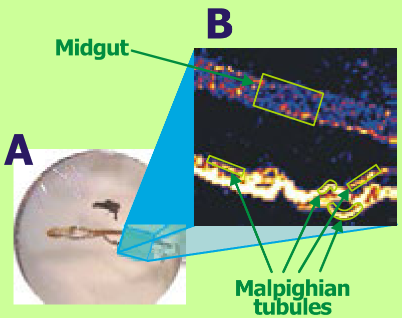

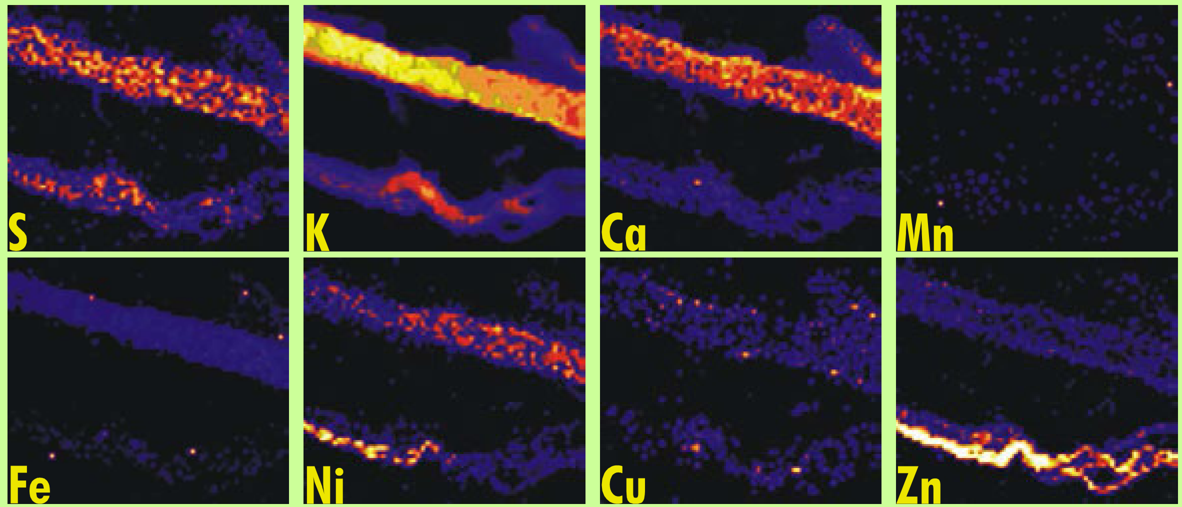

C – male

C – female

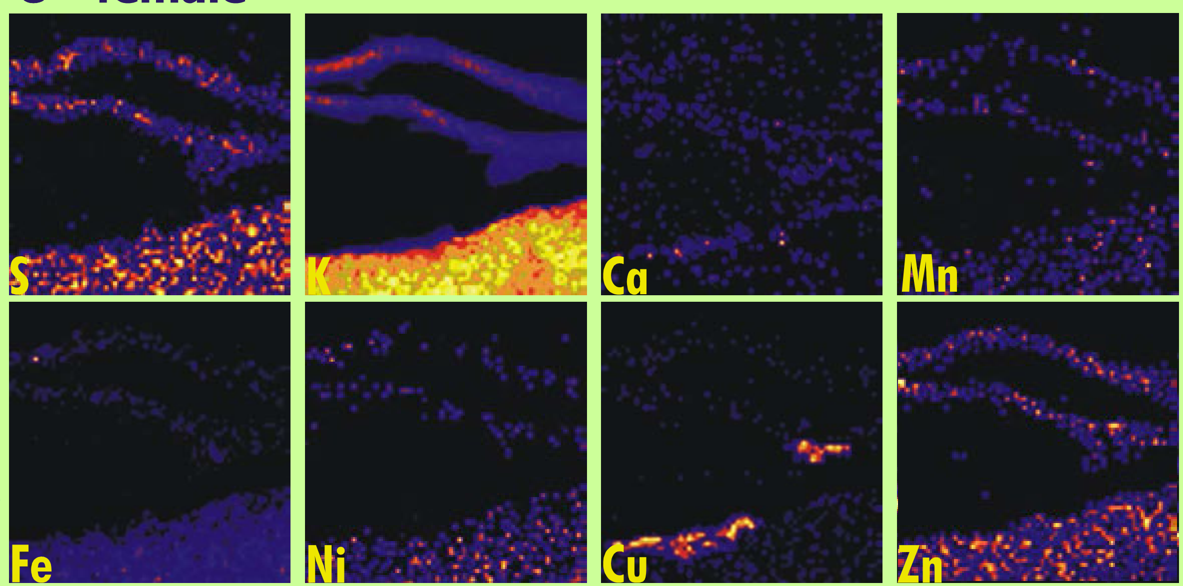

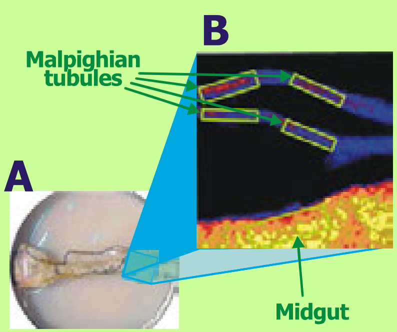

Bioaccumulation Factor (BAF) values for various elements

BAF = concentration in tissues of *Ch. pardalina*/concentration of metals in food

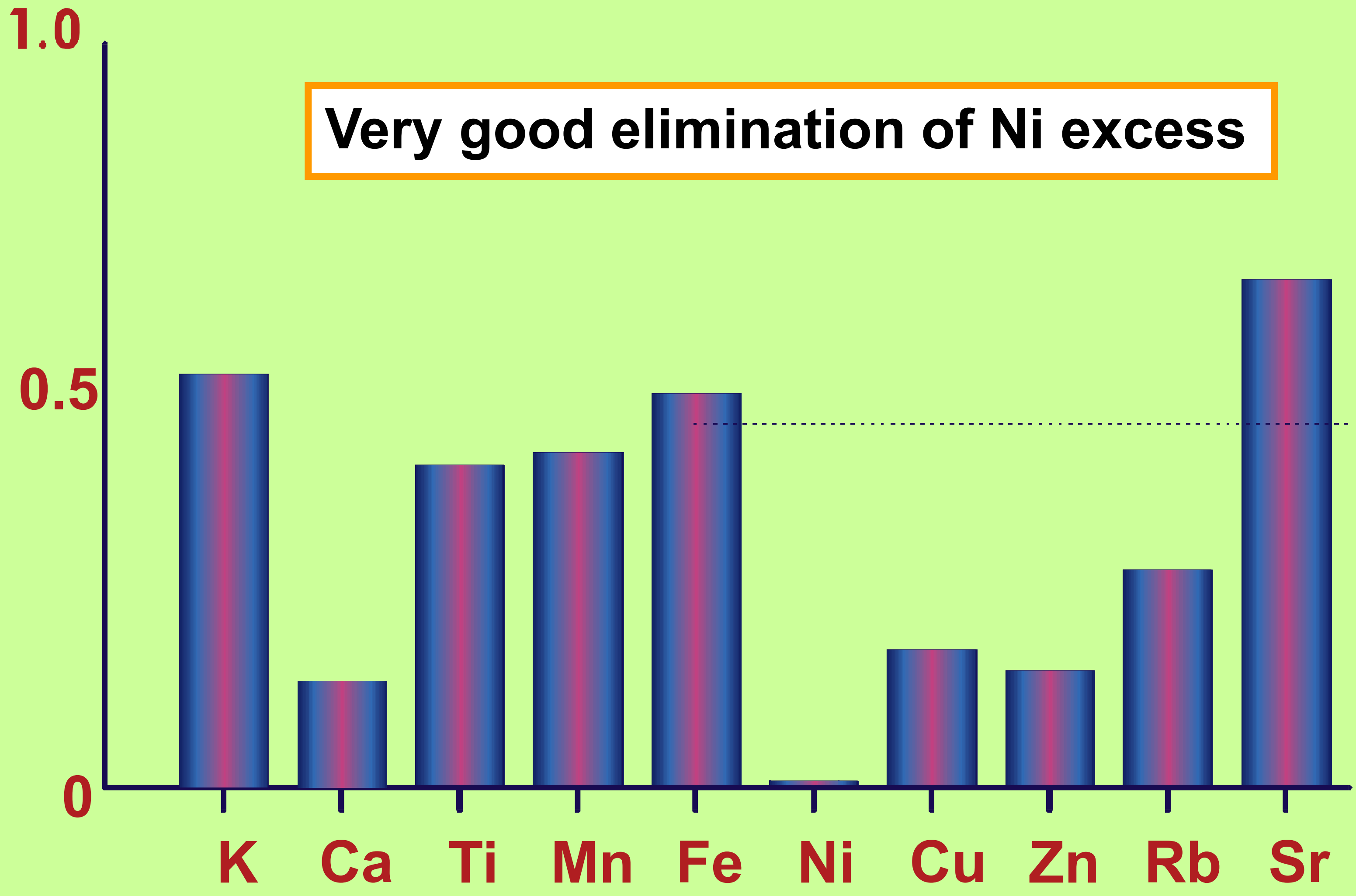

Rinorea bengalensis
(Violaceae)
Ni – hyperaccumulating tree

Borneo, Malaysia

Very high nickel concentration (ICP-OES):

Nickel (% dry weight) in:	Phloem	Leaves
Phyllanthus balgooyi	17 (sap)	0.86
Phyllanthus securinegoides	1.08 (tissue)	2.325
Rinorea bengalensis	1.28 (tissue)	2.26

More information is needed to understand how these hyperaccumulators take up and store nickel; what are the relations between nickel and other elements

ROOTS

Ni mainly concentrated in the phloem

in all three species

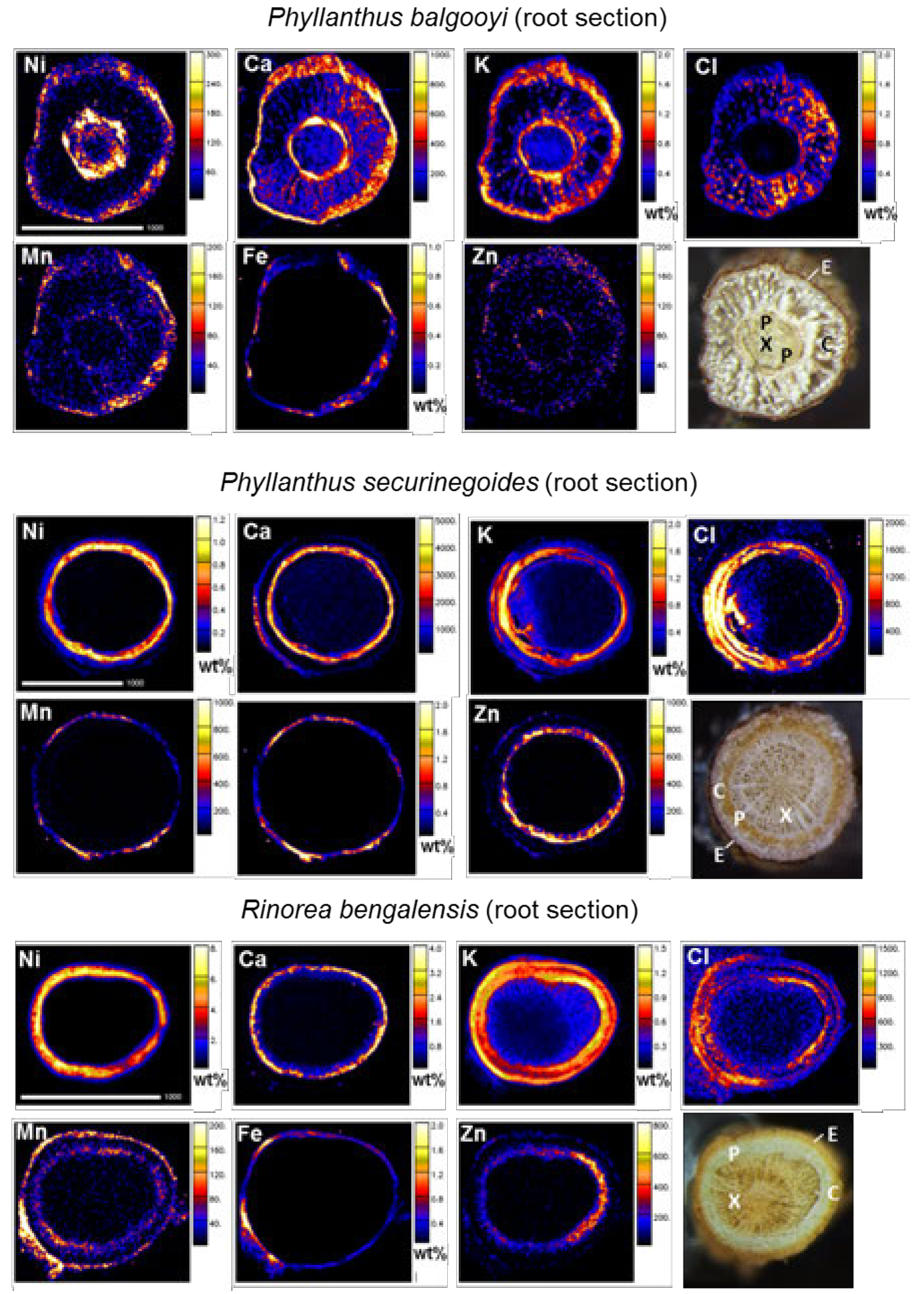

STEMS

Ni mainly concentrated in the phloem

in all three species

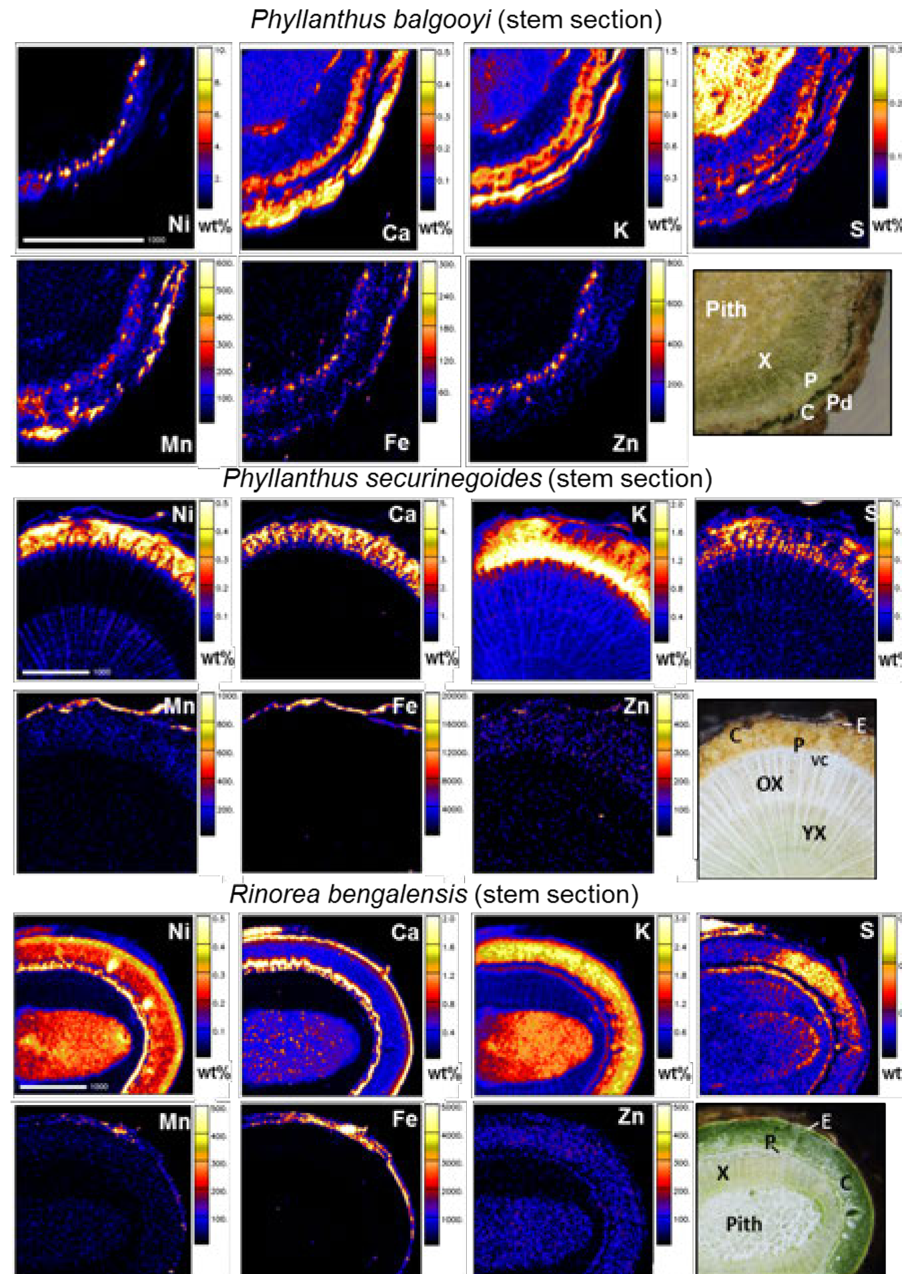

LEAVES – differences between species

Highest Ni concentration in the phloem

Phyllanthus balgooyi (leaf section)

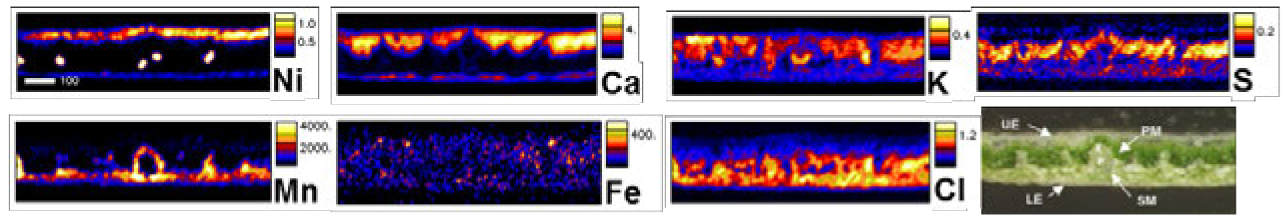

Highest Ni concentration in the epidermis

Phyllanthus securinegoides (leaf section)

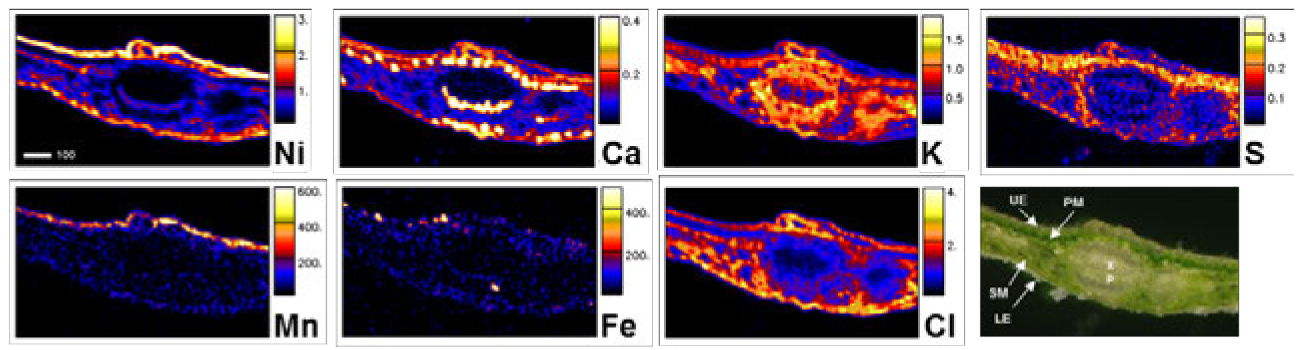

Highest Ni concentration in the epidermis and the spongy mesophyll

Rinorea bengalensis (leaf section)

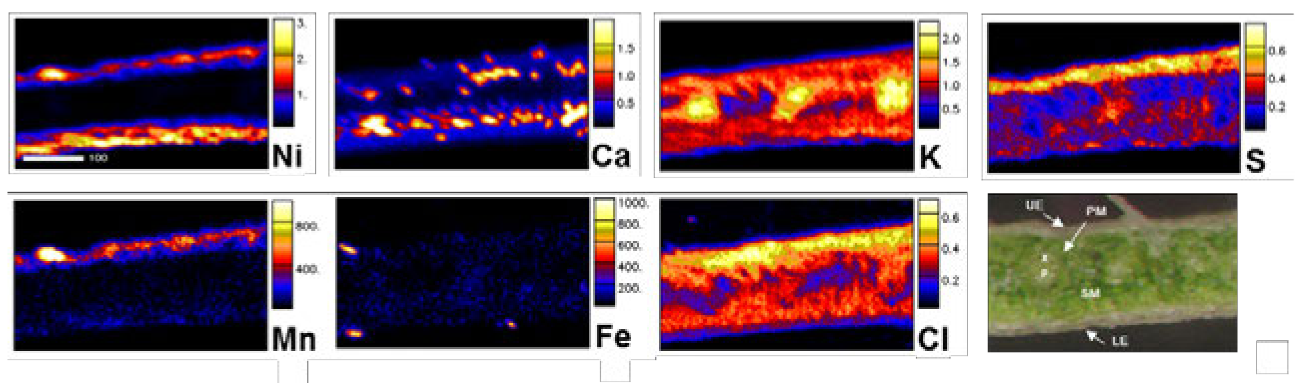

PROTEA FARMING
Phosphorus toxicity – a problem for Protea farming on previously agricultural land

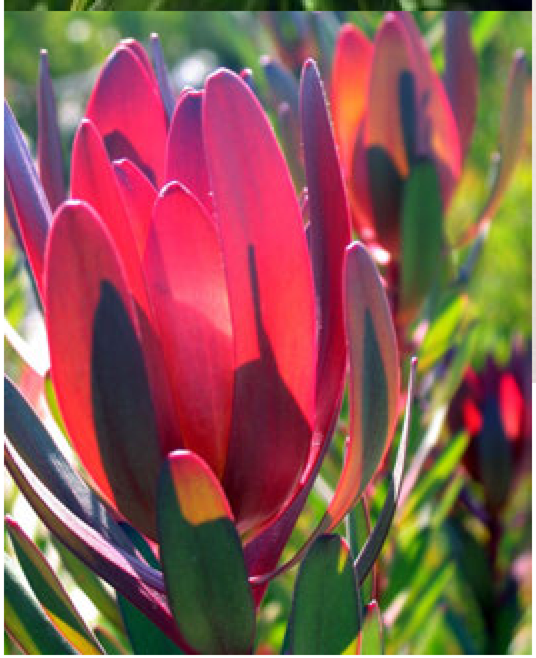

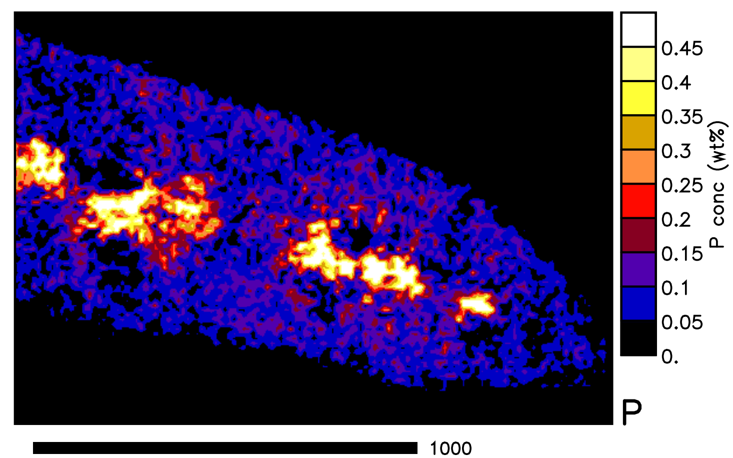

H.-J. Hawkins, H. Hettasch, L. Louw, C. O'Brian, J. Mesjasz-Przybylowicz, W.Przybylowicz, M.D. Cramer. Phosphorus toxicity in the Proteaceae: a problem in post-agricultural lands. Scientia Horticulturae, 117 (2008), 357-365.

PROTEA FARMING

Phosphorus toxicity – a problem on previously agricultural land

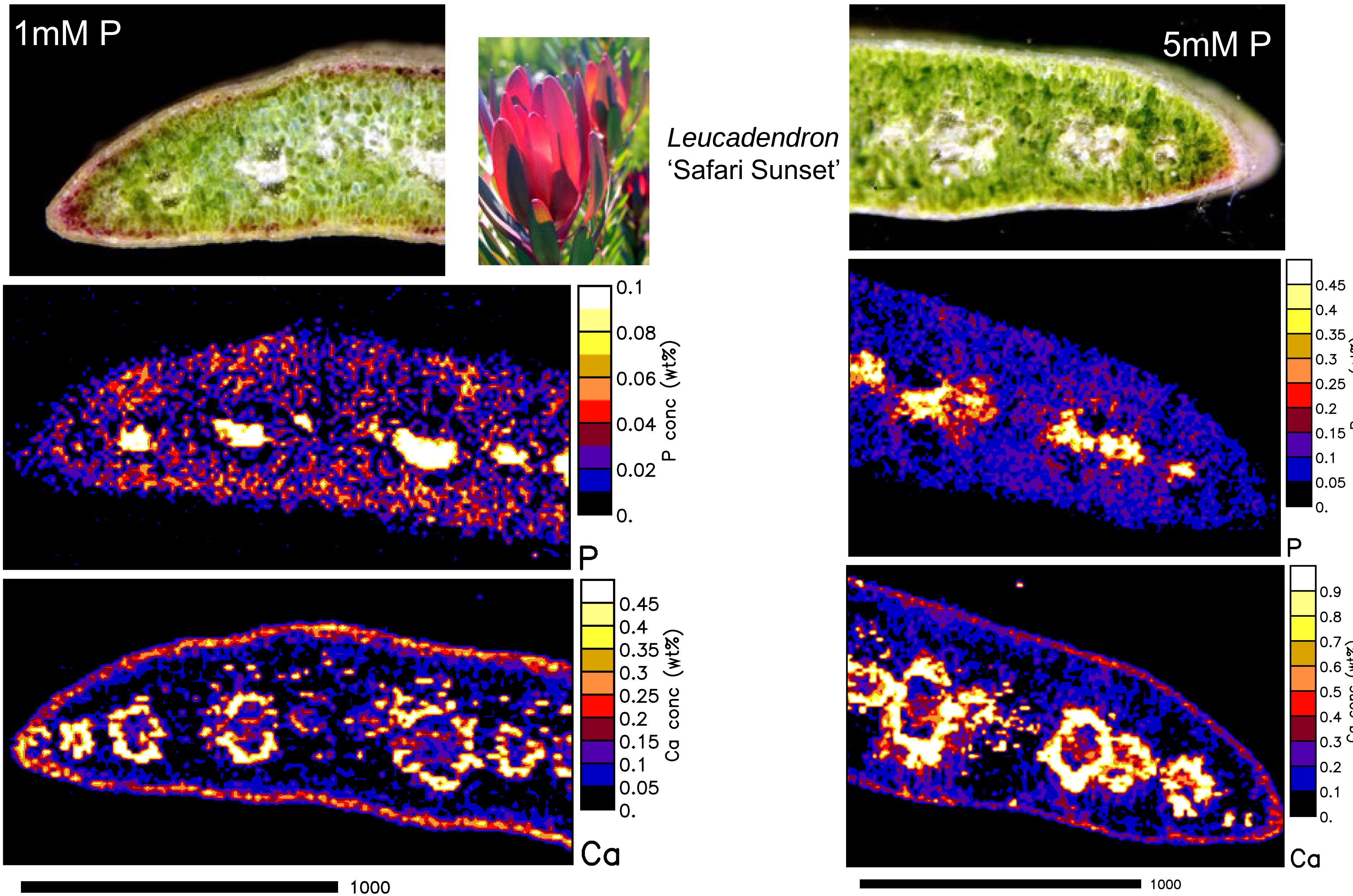

Plant resistance to pathogen infection

Hypersensitive response (HR) - a rapid, localised death of cells associated with the restriction of pathogen growth.
A resistant genotype of a wild plant (*Lagenaria sphaerica*, Cucurbitaceae) inoculated with fungal pathogen (*Sphaerotheca fuliginea*)

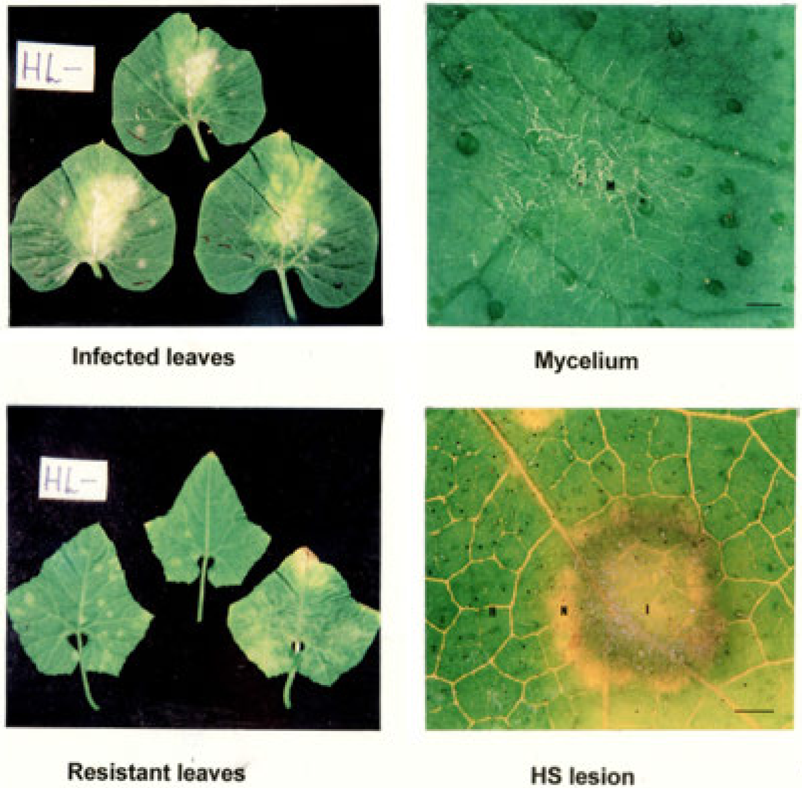

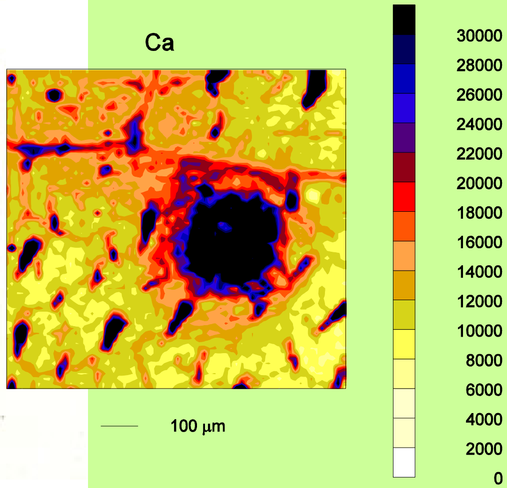

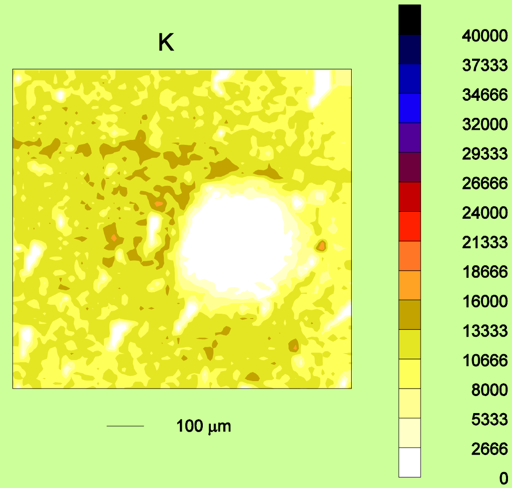

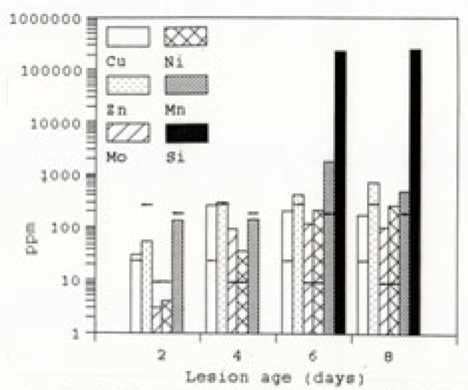

Fig. 2. Metal and Si accumulation during lesion development. Solid lines represent toxicity values[1-3].

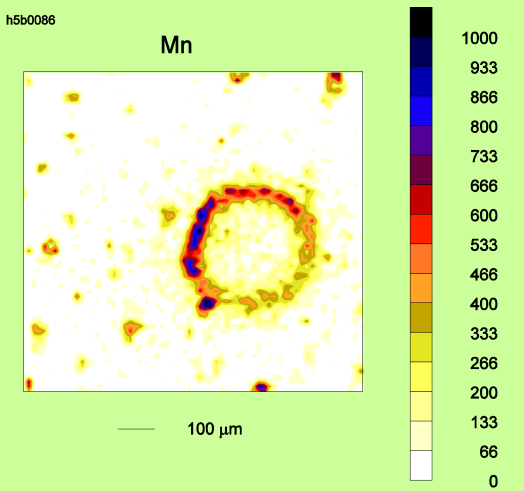

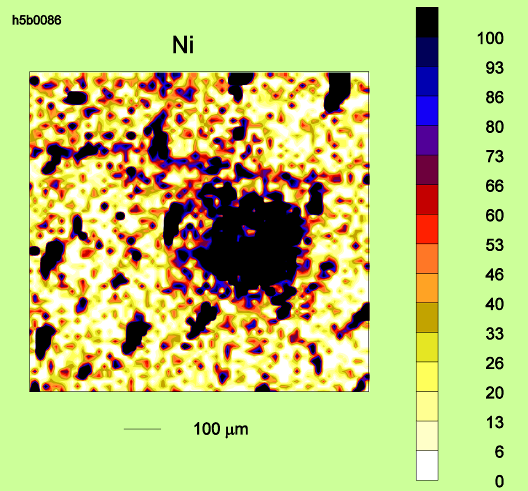

I.M. Weiersbye-Witkowski, W.J. Przybyłowicz, C.J. Straker, J. Mesjasz-Przybyłowicz, Nucl. Instr. and MethB 130 (1997) 388.

Nutrient biofortification of a staple food - micro-PIXE and biotechnology

Part of broader studies which aim at reducing malnutrition in developing countries

Synergy: molecular biology – micro-PIXE

Study revealed the accumulation sites of micro- and macronutrients in important crop legumes

This information is crucial for future studies of the molecular mechanisms responsible for the micronutrients' accumulation in legume seeds

Cvitanich *et al. BMC Plant Biology* 2010, **10**:26
http://www.biomedcentral.com/1471-2229/10/26

BMC Plant Biology

RESEARCH ARTICLE Open Access

Iron and ferritin accumulate in separate cellular locations in *Phaseolus* seeds

Cristina Cvitanich[1*], Wojciech J Przybyłowicz[2,3], Dorian F Urbanski[1], Anna M Jurkiewicz[1], Jolanta Mesjasz-Przybyłowicz[2], Matthew W Blair[4], Carolina Astudillo[4], Erik Ø Jensen[1], Jens Stougaard[1]

Abstract

Background: Iron is an important micronutrient for all living organisms. Almost 25% of the world population is affected by iron deficiency, a leading cause of anemia. In plants, iron deficiency leads to chlorosis and reduced yield. Both animals and plants may suffer from iron deficiency when their diet or environment lacks bioavailable iron. A sustainable way to reduce iron malnutrition in humans is to develop staple crops with increased content of bioavailable iron. Knowledge of where and how iron accumulates in seeds of crop plants will increase the understanding of plant iron metabolism and will assist in the production of staples with increased bioavailable

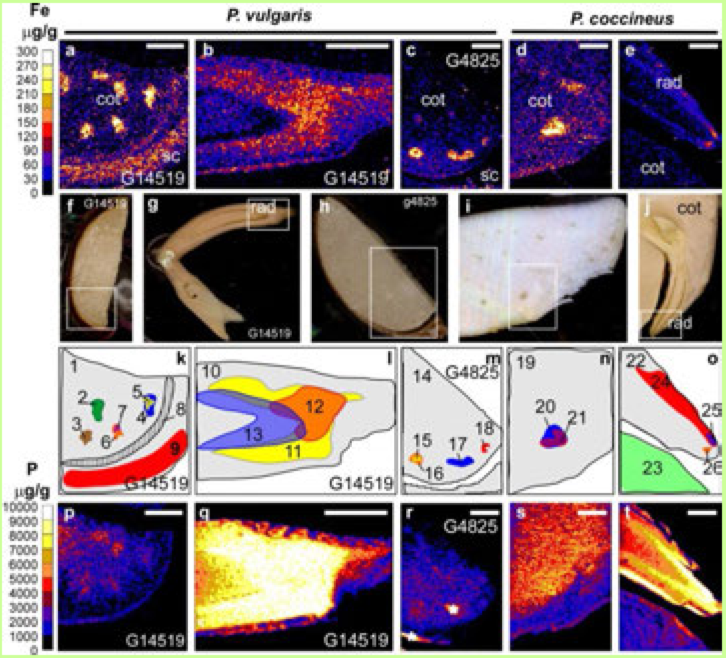

Micro-PIXE quantitative elemental maps of iron (a-e) and phosphorus (p-t). in mature seeds from *Phaseolus vulgaris* and *P. coccineus* (f-o show the analyzed tissue, the scanned area is marked with an open square). Scale bars: 0.5 mm.

14 Maj 2013 Pożar około 3-ciej nad ranem, dewastacja połowy budynku

14 Maj 2013

14 Maj 2013


21 Grudzień 2016


Listopad 2017


HVE Tandetron T-Shape Accelerators		**Model 4130**
Terminal Voltage	**MV**	3MV
Terminal voltage range	**MV**	0.2 – 3MV
Terminal Voltage ripple		
Standard system	Vpp	200
With de ripple kit	Vpp	30
Terminal voltage stability		
GVM	± V	300
Slit stabilization	± V	30
X-ray level	**µSv/hr**	< 2

Ion source, H^- and D^-
Multicusp

Model SO120

direct negative extraction

Energy spread	10 eV
Beam current H^-	700 µA
Beam current D^-	500 µA

Ion source, He
Multicusp

Model SO130

positive extraction

Energy spread	10 eV
Beam current He^-	30 µA
Typical He^- current	75 µA

science & technology
Department:
Science and Technology
REPUBLIC OF SOUTH AFRICA

NRF National Research Foundation
iThemba LABS Laboratory for Accelerator Based Sciences

NEGATIVE SPUTTER ION SOURCE

Model 860A and 860C

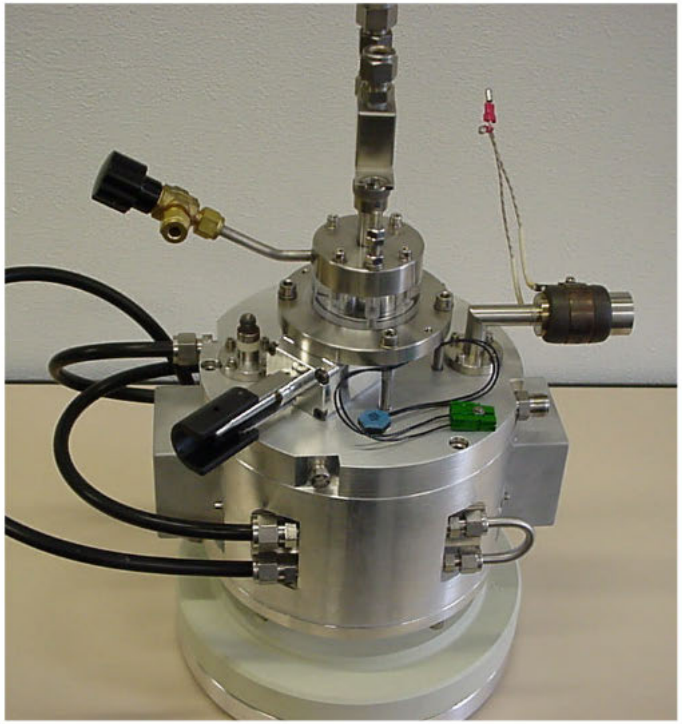

Features

- Easy operation and maintenance
- High intensity ion beams of almost all elements in the periodic table
- Beam currents up to 150 μA
- Low beam emittance
- Easy cesium reservoir loading
- Lifetime cesium charge > 1000 hours
- Easy (ex)change of source materials

$^{11}B^-$	10 μA
$^{12}C^-$	100 μA
$^{16}O^-$	100 μA
$^{28}Si^-$	100 μA
$^{31}P^-$	30 μA
$^{58}Ni^-$	30 μA
$^{63}Cu^-$	20 μA
$^{75}As^-$	15 μA
$^{197}Au^-$	80 μA

Synchrotron X-ray / MeV ion Beam Complementarity

Nuclear Microprobe Ion-beam Techniques

- Light element analysis (F, Na, Li, Be, B …) using nuclear reactions.
- H analysis, imaging and profiling (p recoil).
- Diffusion depth profiling (resolution to <10 nm) using RBS; (to 0.5 Å using high resolution RBS).
- Energy loss imaging (STIM), tomography (transmitted beam).

PIXE - SXRF Synergy

- Fluorescence microscopy (PIXE, SXRF).
- Imaging at <μm resolution.
- Non-destructive.
- Quantitative, Standardless.
- Deep penetration:

  ~80 μm - 3 MeV protons.
  ~mm - 15 keV photons.

Synchrotron X-ray Microprobe Techniques

- Tune photon E for selective SXRF sensitivity.
- Chemical state sensitivity and local atomic structure (EXAFS, XANES).
- Crystal structure (μXRD).
- Phase, absorption contrast, tomography (transmitted beam).

Personal remarks:

Since 1994 I was involved in 364 experimental sessions, typically of the order of 1 week each.

I am a co-author of 117 refereed publications related to research with the use of this microprobe, 70 conference proceedings and about 320 conference presentations.

Most of this reported work was done in collaboration with scientists and students from local South African universities, as well as visitors from African countries and overseas visitors.

Very effective collaborations with few teams of Polish scientists (Jagiellonian University, University of Silesia, Institute of Botany PAN)

Contacts made in the microprobe room often lasted very long, and many of those who came to perform experiments I can consider my good friends.

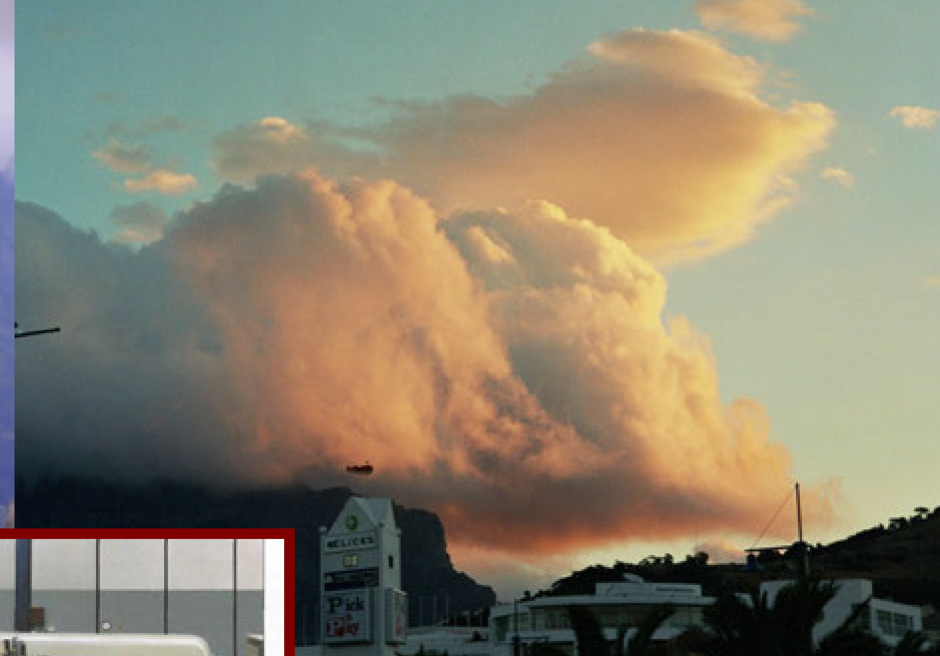

Dziękuję za uwagę! Mam coś na „bis”

Collaboration Procedures

In order to make use of the facilities at the Materials Research Department of iThemba LABS, a researcher must first submit a **written project proposal**. The proposal must clearly state the aims of the experiment, what techniques are required, how the samples are prepared, previous work completed, the time scale anticipated for work at the MRD and the person who will be responsible for the work (see **appendix A** for details). The project is then discussed with MRD researchers and facility time is allocated. **A "run report" (1 page maximum) is required after each usage of the equipment.**

Research falls into one of the following three categories. Each has its own implications regarding intellectual property right (IP) and funding.

1) Researchers are from an academic, non-profit making institute or university without financial support for the project. If the project is accepted, the work is done with full access to data by iThemba LABS. All papers, reports, conference presentations are done on a full co-authorship basis. If the results are used as part of M.Sc. or Ph.D. thesis, the title of the thesis and the name of supervisor(s) should be included in the project description. If the thesis relies substantially on results obtained at iThemba LABS, co-supervision by a scientist from iThemba LABS may be required. **No financial cost is incurred**. **Contribution to iThemba Annual Report is mandatory before the end of March each year.**